Graduate School of
Systemic Neurosciences
LMU Munich

Neural circuit mechanisms underlying modulation of food consumption and reward by the central amygdala

Dissertation der Graduate School of Systemic Neurosciences der

Ludwig-Maximilians-Universität München

Amelia M. Douglass

Submitted on 26th June 2017

SIGILL: UNIVERSI TAT: LUDOVIC: MAXIM:

Thesis Supervisor: Prof. Rüdiger Klein

Second Reviewer: Prof. Magdalena Götz

Third Reviewer: Prof. Philip Tovote

Date of Defense: 8th November 2017

SIGILL: UNIVERSI TAT: LUDOVIC: MAXIM:

Abstract

Food intake and appetite-related behaviours are important for survival of an organism. The acquisition and consumption of food is regulated by a complex network of neural circuits. The central nucleus of the amygdala (CeA) is an important brain region in which emotionally-relevant salient environmental stimuli are integrated and which orchestrates behavioural responses to those stimuli. To-date, the CeA has been most rigorously studied in the context of aversive behaviours including fear and anxiety. However, despite considerable evidence for the CeA as a modulator of appetitive behaviour, the CeA neural players and associated circuits that underlie these behaviours are poorly understood. Here, I have identified a population of CeA neurons that express the serotonin receptor Htr2a. Activity of these cells promotes food consumption in the absence of homeostatic deficit, and functionally antagonize CeA protein-kinase Cδ (PKCδ)-expressing neurons that reduce food intake. Importantly, activity of CeA^{Htr2a} neurons promotes increased food consumption but not food-seeking behaviour. This was corroborated by *in vivo* calcium (Ca^{2+}) imaging experiments, which showed that these neurons are active during eating but not food seeking. Additional experiments revealed that activity of CeA^{Htr2a} neurons is positively reinforcing, suggesting that activity of the neurons sustains ongoing eating behaviour. Finally, this positive reinforcement signal appears to modulate the positively rewarding properties of food such that activity of CeA^{Htr2a} neurons promotes ongoing food consumption. At the neural circuit level, efferent projections from CeA^{Htr2a} neurons to the parabrachial nucleus (PBN) promote food consumption and positive reinforcement. Together,

my findings reveal a role for the CeA in positively regulating food consumption and provide insight into the underlying mechanisms and associated neural circuits. This work is an important advance in the understanding of the function of the CeA and may have important implications in human health and appetite and emotion-related conditions.

Contents

Chapter 1

Introduction

1.1 Neural control of feeding and reward

1.1.1 Energy homeostasis

Energy homeostasis is achieved by an exquisite communication system between the body and the brain that maintains energy expenditure and intake at an equilibrium. Circulating hormones and nutrient signals inform the brain of the levels of body fat and current nutritive state in order to influence food intake such that stored energy reserves remain stable. Deficits in the body's ability to properly detect and report changes in nutritive state can lead to disorders of energy homeostasis that manifest as obesity, diabetes or anorexia and bulimia[1]. Many of these disorders have a genetic basis where mutations in genes that act in pathways that control food intake are affected[2–4]. However, food intake is also subject to external modulation where food palatability and availability can promote consumption even when caloric needs are met[5]. Conversely, stress, anxiety and sickness can also negatively modulate food intake even in the presence of homeostatic need. Neural circuits that control feeding are informed of the state of the body's long-term adiposity stores by two major circulating homones leptin and in-

sulin, which are present in the blood in proportion to the body's fat stores[6,7]. Leptin is secreted from adipocytes and by acting on neurons, most notably in the hypothalamus and hindbrain, decreases food intake and body weight[8–10]. Insulin, a pancreatic hormone, has a similar function to leptin, albeit with much less potency[11]. Deficiencies in leptin and insulin signaling lead to hyperphagia in both laboratory animals and humans, demonstrating the importance of these signals for maintaining body weight over a long time scale[10,12,13]. Food intake is also modulated by short-term factors that inform the brain about the state of the body in response to an ongoing meal. Ghrelin, a gastric hormone, stimulates feeding by acting on hypothalamic neurons[14,15]. Satiety signals from the gastrointestinal tract including cholecystokinin (CCK) and glucagon-like-peptide 1 (GLP1) are secreted in response to a meal[16,17]. Components of ingested nutrients including amino acids as well as the physical feeling of satiety due to gastric distension also contribute to meal cessation[18,19]. Satiety signals reach the brain from the gastrointestinal tract by vagal nerve fibres that project to the nucleus of the solitary tract (NTS) in the hindbrain[20]. Long-term fat storage is maintained through interactions between long- and short-acting signals in the hypothalamus and hindbrain[21].

1.1.2 Neural control of homeostatic feeding

Studies examining the neural control of homeostatic feeding behaviour have predominantly focused on two antagonistic cell types in the arcuate nucleus of the ventral hypothalamus. Neurons that co-express agouti-related protein, GABA and neuropeptide Y (NPY) (henceforth, AgRP neurons) are activated by energy deficit and potently stimulate food intake, food seeking behaviour and motivation to work for food[22–24]. In contrast, pro-opiomelanocortin-expressing neurons (POMC neurons) are activated by energy surfeit and their activity leads to eating cessation and weightloss[25,26]. Circulating hormones that reflect the levels of stored energy act directly on these neurons. AgRP neurons are inhibited by the adiposity signal leptin and activated by ghrelin, while the opposite is the case for POMC neurons[27,28]. Hunger was originally

thought to be controlled by circulating hormones that increase the activity of AgRP neurons and inhibit POMC neurons. As a result, the animal seeks and consumes food until satiety hormones and the physical feeling of fullness negatively regulated food intake. However, recent studies where the activity of AgRP and POMC neurons was recorded *in vivo* in mice revealed that the activity of these neurons is strongly modulated by the sensory detection of food and by food cues[25,29,30]. More specifically, the activity of AgRP neurons was drastically reduced compared to in the hungry state while POMC neuron activity increased even before the animal had commenced eating. These studies suggest that modulation of AgRP and POMC neuron activity occurs prior to food consumption rather than post-ingestively. This profound finding has been postulated to reflect an anticipatory response to an ongoing meal that serves to modulate the effects of hormone and nutrient changes that act over a longer time scale[31,32]. It may also be the case that AgRP neurons do not directly promote food intake but transmit a sustained hunger signal that gaits the activity of downstream neurons that directly influence feeding[31]. These findings remain to be reconciled with the classical model of adiposity and hormone-regulated feeding, but it is clear that AgRP and POMC neurons are integral components of homeostatic feeding.

The neural circuits by which AgRP neurons exert potent effects on food consumption has been dissected using optogenetic strategies where the pre-synaptic terminals of these neurons in specific projection fields were individually stimulated. These studies revealed that activation of AgRP terminals in the paraventricular hypothalamus (PVH), lateral hypothalamus (LH) and bed nucleus of the stria terminalis (BNST) were sufficient to recapitulate the effect of cell body stimulation, while projections to the paraventricular thalamus (PVT) moderately increased food intake[23,34] (Figure 1.1). Other studies have revealed that AgRP neurons are also critically important for gaiting malaise signals that if left unchecked, lead to death by anorexia. Postnatal ablation of AgRP neurons in mice leads to death by starvation which was initially attributed to

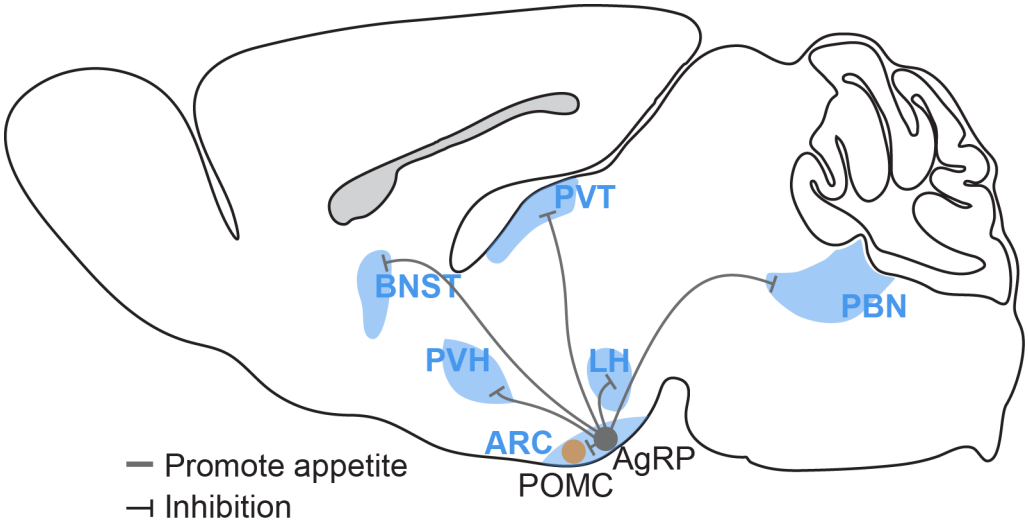

Figure 1.1: Scheme of arcuate nucleus-associated circuits that promote food consumption. Inhibitory afferents from arcuate AgRP neurons targeting PVH, LH and BNST strongly drive food intake as does activation of AgRP cell bodies. AgRP inputs to the PBN gait the activity of visceral malaise-promoting neurons to prevent starvation by anorexia. AgRP neurons also inhibits satiety-promoting arcuate POMC neurons thereby promoting food consumption under caloric deficit. Abbreviations: AgRP- Agouti-related peptide; PVH- Paraventricular hypothalamus; LH- lateral hypothalamus; BNST- bed nucleus of the stria terminalus; PBN- Parabrachial nucleus; POMC- , pro-opiomelanocortin. Adapted from:[33]

the function of these neurons as actuators of voracious feeding[35]. However, it was shown that efferent projections of AgRP neurons to the parabrachial nucleus (PBN), rather than eliciting an increase in food consumption, are responsible for gating the malaise-promoting activity of the PBN (Figure 1.1). The PBN is a hindbrain region that processes gustatory and malaise signals and is important for the cessation of appetite during sickness and after ingestion of toxic compounds[36,37]. AgRP-mediated inhibition of the PBN has been shown to be a critical gate of PBN activity, preventing uncontrolled feeding cessation by malaise signals and controlling the interaction between homeostatic and malaise feeding circuits[38]. The role of the PBN and associated circuits in promoting feeding suppression under anorexigenic conditions is further reviewed in the section “Modulation of feeding by anorexigenic signals”.

1.1.3 Food reward

Food consumption is not only a reflection of energy state and nutrient requirements. Food palatability or reward value of food strongly influences ingestive behaviour. Food reward is

integral to the homeostatic regulation of energy balance, as palatable, energy-dense foods, when obtained at the same cost as less palatable food, contribute significantly more to energy intake. There are several lines of empirical evidence that demonstrate a tight relationship between food reward and homeostatic energy balance. In humans and laboratory rodent studies, satiety has been shown to diminish perception of food reward value while fasting has the opposite effect[39–41]. In addition, fasting also increases willingness to work for food rewards and food-related cues are more strongly reinforced[42,43] . Furthermore, the strength of response of AgRP and POMC neurons to the sensory detection of food depends on food palatability[25]. This suggests that food reward value strongly factors into the motivated seeking and consumption of food, in addition to food accessibility and internal energy state and satiety signals. The neural circuits that control food reward are involved in processing reward cues and hedonic value of food and promoting motivated food consumption. The most studied of these regions are the mesolimbic dopamine system (the ventral tagmental area (VTA) and nucleus accumbens (NAc)) and the LH. Intriguingly, these reward circuits also underlie the rewarding effects of drugs of addiction, suggesting that maladaptive eating behaviour directed at highly palatable rewarding foods and drug addiction disorders may be governed by similar neural mechanisms[44,45].

Since the 1950s, the LH has been implicated in the control of feeding and reward. Electrical stimulation not only was found to elicit hyperphagia but also animals will strongly self-stimulate their LH neurons, suggesting that this region promotes feeding and reinforcement and reward-seeking behaviours[46,47]. The LH has been shown to form extensive connections with the energy homeostasis and reward systems. Strong inputs onto the LH come from subcortical limbic and reward regions including the BNST, NAc and ventral palladium[48–50] (Figure 1.2). Inhibitory input from the BNST onto glutamatergic LH neurons importantly evokes both feeding on calorie-dense foods and self-stimulation behaviours[49] while inhibition of GABAergic LH neurons by neurons in the NAc shell suppresses palatable food intake[51] (Figure 1.2). Interaction

with the energy homeostasis system of the hypothalamus including inputs from the AgRP neurons of the arcuate nucleus and projections to PVH neurons both evoke food consumption[34,52] (Figure 1.2). Innervation of the VTA by the LH has also been shown to elicit food intake and reinforcement behaviour through disinhibition of dopamine release in the NAc[53–55] (Figure 1.2). Additionally, projections to the PBN and arcuate nucleus are also postulated to control feeding behaviour[56] (Figure 1.2). Together these data support a role for the LH as an integrator of energy state signals with reward-based food consumption.

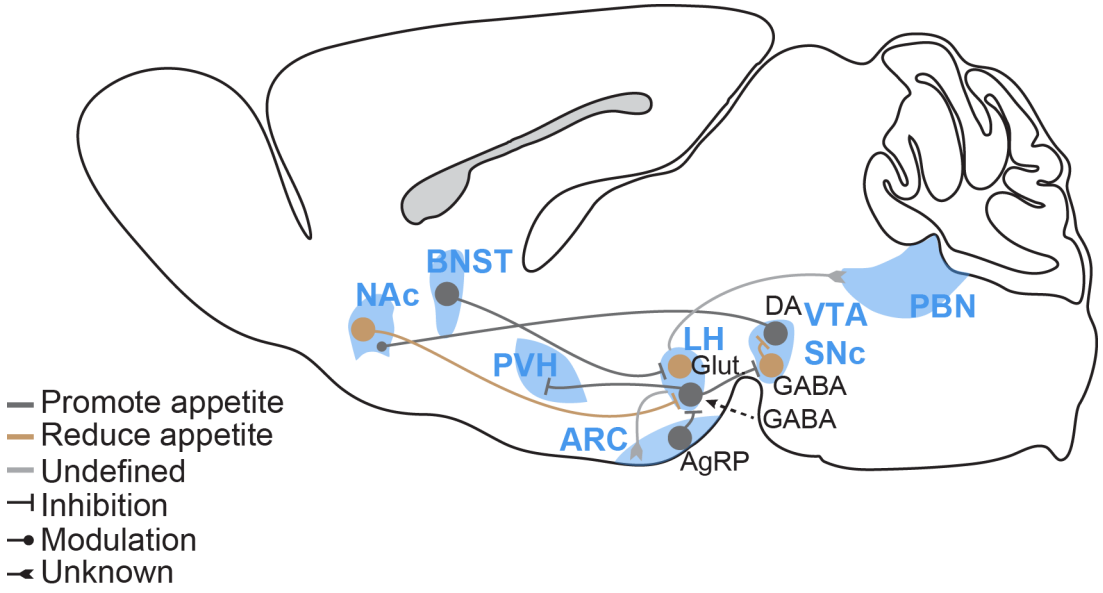

Figure 1.2: Scheme of neural circuits that modulate food reward to influence food intake. GABAergic LH neurons promote food intake, potentially through inputs to the PVH as well as through inhibition of GABAergic VTA neurons, which leads to disinhibition of DA release in the VTA, modulating food reward. Activity of GABAergic LH neurons is modulated by inhibition from the NAc and by homoestatic input from arcuate AgRP neurons. Food intake is also modulated by glutamatergic LH neurons which are inhibited by BNST input to promote food consumption. Additional outputs of the LH to the PBN and arcuate nucleus are postulated as additional pathways for control of feeding. Abbreviations: LH- lateral hypothalamus; PVH- paraventricular hypothalamus; VTA- ventral tagmental area; DA- dopamine; NAc- Nucleus accumbens; BNST- Bed nucleus of the stria terminalis; PBN- parabrachial nucleus. Adapted from:[33,56]

Mesolimbic dopamine neurons in the VTA and substantia nigra (SN) that project to the NAc have an important function in motivated behaviours. Dopamine intrinsically promotes reward and reinforcement behaviour as laboratory animals will self-stimulate their VTA neurons for dopamine release[57,58]. Release of dopamine promotes goal-directed behaviours includ-

ing food seeking and consumption and further, enhances salience of reward-predictive stimuli as well the rewarding properties of food[55,59–61]. Dopamine has been postulated to control appetitive behaviour by designating reward-predictive cues with increased salience (incentive salience)[62].A second theory suggests that dopamine encodes reward-prediction error which acts as a teaching signal based on the difference between a reward prediction and reward outcome[63,64]. Regardless of the specific underpinnings of dopamine function in reward, it is clear that the mesolimbic reward system along with the LH are key players in mediating motivated food seeking and reinforcement.

1.1.4 Modulation of feeding by anorexigenic signals

In addition to being influenced by the rewarding properties of food, the energy homeostasis system is subject to modulation under circumstances where the survival of the animal is jeopardized. In such cases, maintenance of bodily energy stores becomes of secondary importance, and food intake is inhibited until the threat has passed. Anorexigenic conditions include illness, the presence of a predator and ingestion of toxic compounds. The neural circuitry controlling emergency cessation of feeding has been known for some years, however a more recent circuit-mapping based approach has allowed a more thorough dissection of the neural mechanisms that interact with homeostatic feeding circuits to mediate these effects.

Gustatory and visceral malaise signals reach the brain from the periphery by the vagus nerve and arrive in the medulla region of the brain at the NTS. Gastrointestinal signals also reach the NTS directly via the area postrema (AP) which has a permeable blood-brain barrier. From here, signals are conveyed onto the PBN, a diverse region with known roles in appetite, taste, pain and thermosensation. PBN neurons project onto the ventral posterior lateral thalamic nucleus (VPL) and the CeA from where signals reach the insular cortex[65] (Figure 1.3). Recently, the neural pathway from the PBN to the CeA was interrogated in mice in detail and was found to mediate the anorexigenic effect of several malaise-inducing com-

pounds. Neurons within the external lateral PBN that express calcitonin gene-related peptide (CGRP) are activated by lithium chloride (LiCl) and lipopolysaccharide (LPS), which when administered by intraperitoneal injection to mice mimic the appetite-suppressant effects of toxic food and bacterial infections respectively[37]. Artificial activation of these neurons evokes acute feeding suppression while conversely, inhibition of these neurons increases food intake under anorexigenic conditions. Together, these data demonstrate a role for these neurons in emergency cessation of feeding. Importantly, silencing of PBN^{CGRP} neurons was found to rescue anorexia-induced starvation as a result of AgRP neuron ablation[37]. This demonstrated that this emergency feeding circuit is under the tonic control of neurons that sense and maintain energy balance and that internal energy state and external signals interact to ensure that feeding occurs under appropriate conditions.

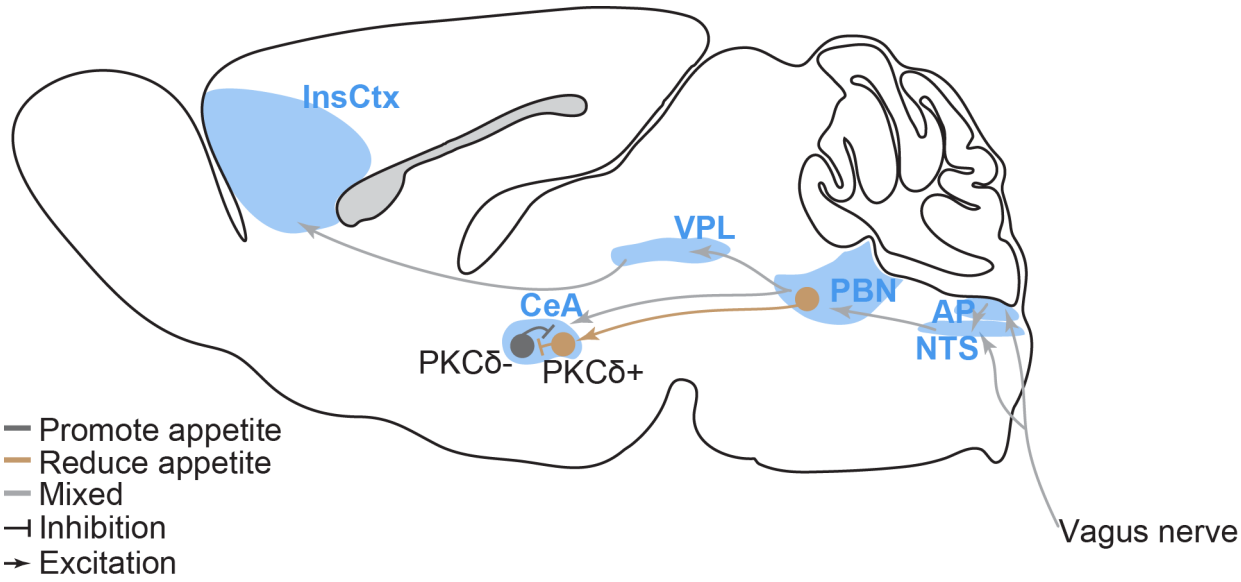

Figure 1.3: Scheme of neural circuits that modulate food intake under anorexigeneic conditions. Viseral and gustatory signals are relayed from the periphery to the brain via the vagus nerve into the AP and NTS which then converge on the PBN. These signals are relayed to the forebrain via the VLP which arrives in the InsCtx or via the CeA. In the CeA, visceral malaise, satiety and unpalatability signals from the PBN excite CeAPKCδ+ neurons which, through local inhibition of CeAPKCδ- neurons, supress feeding. Abbreviations: AP- Area Postrema; NTS- Nucleus of the solitary tract; PBN- Parabrachial nucleus; VLP- ventral posterior lateral thalamic nucleus; InsCtx- Insular cortex; CeA- Central amygdala. Adapted from:[33,65]

In a second study in mice, the effects of PBN^{CGRP} neurons were proposed to be mediated, in

part, through their afferents onto GABAergic neurons of the CeA that express PKCδ. $CeA^{PKC\delta}$ neurons are activated by LiCl and the satiety peptide CCK as well as by bitter tastants which mimic unpalatable foods[66]. The artificial activation of these neurons promotes robust feeding suppression, while inhibition also promotes eating under anorexigenic conditions. Given the anatomical connection and functional similarity, it was suggested that activation of $CeA^{PKC\delta}$ neurons by glutamatergic input from PBN^{CGRP} neurons may corroborate the anorexigenic effect of PBN^{CGRP} neuron activation. However, the responsiveness of PBN^{CGRP} and $CeA^{PKC\delta}$ neurons to different compounds suggest that different anorexigenic signals may be relayed from the periphery by divergent pathways. Although $CeA^{PKC\delta}$ neurons strongly inhibit feeding, activation of the major efferent projections to the BNST and lateral PBN failed to recapitulate the effect of somatic stimulation[66]. The CeA is comprised of GABAergic neurons that are highly interconnected, with $CeA^{PKC\delta}$ neurons strongly inhibiting other neurons in this region[67]. Concurrent with *in vivo* artificial $CeA^{PKC\delta}$ neuron activation, intra-CeA infusions of $GABA_A$ antagonist bicuculline blunted the anorexigenic effects, suggesting that $CeA^{PKC\delta}$ neurons suppress feeding through inhibition of other CeA neurons. This observation would suggest that a population of neurons within the CeA promotes food intake (Figure 1.3). However, despite this observation, the identity of the antagonizing CeA population remained unidentified. The notion that neurons within the CeA promote an appetitive behaviour such as food consumption may be surprising, given that this region is strongly implicated in controlling aversion. More specifically, decades of research have described roles for the CeA in fear and anxiety, leading this region to be considered one where negative valence signals are processed. However, seminal studies have in the past revealed clues for bivalence processing within the CeA as well as the amygdaloid complex more broadly.

1.2 The amygdaloid complex

1.2.1 Anatomy and functions of the amygdaloid complex

The amygdala is an evolutionarily conserved complex of nuclei bilaterally situated in the temporal lobe of the brain. The long-standing view of the amygdala as a region strongly involved in aversive behaviours came from lesion studies in primates where such manipulations resulted in reduced aggression, defensive behaviors and learning of fearful stimuli[68–70]. These findings were also recapitulated in human patients with damaged amygdala, where recognition of emotionally salient events and emotions conveyed in human faces was markedly reduced[71,72]. Anatomically, the amygdala comprises different nuclei, the major subregions being: the basolateral complex (BLA), comprising the lateral (LA), the basal (BA) and basomedial (BMA) regions; the central amygdala (CeA), containing lateral (CeL) and medial (CeM) subdivisions; and the medial amygdala (ME) (Figure 1.4 shows the mouse amygdala). The CeA anatomically transitions into another limbic structure, the BNST which together form the central extended amygdala. The BLA contains both excitatory principal neurons and inhibitory interneurons while the CeA predominately comprises GABAergic neurons[73]. Knowledge of the neural circuitry within the amygdaloid complex and connections with other brain regions has predominately come from the study of fear conditioning- a form of emotional associative learning. In this paradigm, an initially neutral stimulus (conditioned stimulus- CS) is repeatedly paired with an aversive unconditioned stimulus (US). Through repeated pairings, the animal forms an association between the two stimuli and upon presentation of the CS alone, displays fear behaviour, characterized by freezing in rodents[74]. The amygdala is a key site of learning and expression of fear behaviour as disrupted function of this region impairs such behaviour. The BLA has been classically considered the site of convergence of sensory information from the cortex and thalamus with the information subsequently relayed to the CeA[75] (Figure 1.4). However, there is consider-

able evidence that sensory information of multiple modalities arrives directly in the CeA and that projection neurons arising from both the CeL and CeM may underlie the function of this region[66,73,76,77] (Figure 1.4).

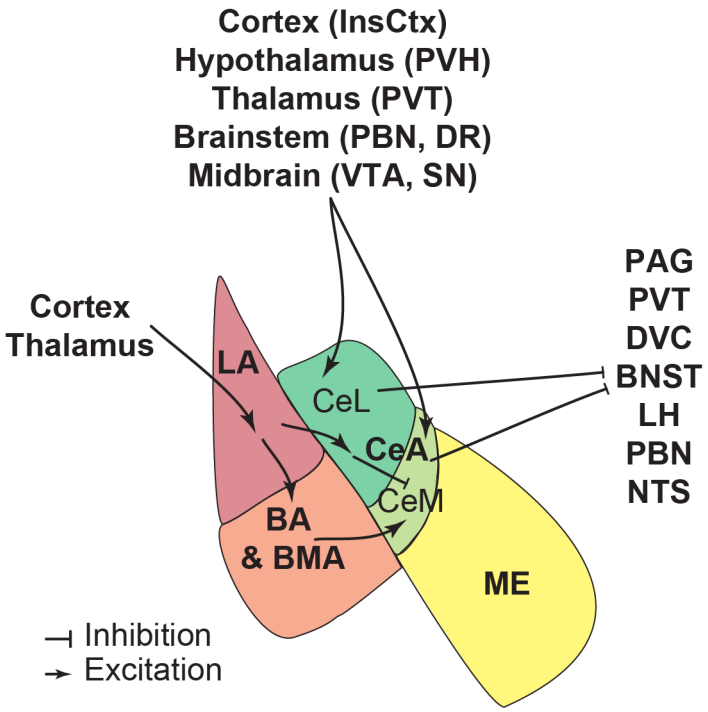

Figure 1.4: Anatomical organization and information flow in the mouse amygdalaloid complex. Abbreviations: LA- Lateral amygdala; BA- Basal amygdala; BMA- basomedial amygdala; CeL- Central lateral amygdala; CeM- Central amygdala; ME- Medial amygdala; InsCtx- Insular cortex; PVH- Paraventricular hypothalamus; DR- Dorsal Raphe, VTA- Ventral tegmental area; SN- Substantia nigra; PAG- Periaqueductal grey; PVT- Paraventricular thalamus; DVC- Dorsal vagal complex; BNST- Bed nucleus of the stria terminalis; LH- Lateral hypothalamus; PBN- Parabrachial nucleus; NTS- Nucleus of the solitary tract. Adapted from:[73,74].

1.2.2 Anatomy of the central amygdala and neuronal subpopulations

The central amygdala is a heterogeneous region, containing multiple molecularly and physiologically distinct GABAergic neuron subpopulations with a high degree of reciprocal connectivity[78–80]. In addition to direct input from the BLA, CeA neurons also receive input from multiple brain areas, including cortex, hypothalamus, brainstem and neuromodulatory regions including the substantia nigra and dorsal raphe (DR)[73] (Figure 1.4). The convergence of sensory inputs in the CeA suggests that this region may act as a hub for the integration of diverse in-

formation sets that inform about the external environment and internal state to orchestrate the appropriate behavioural response. Indeed, long-range projections from both the CeL and CeM target regions that are implicated in defensive behaviours including the periaqueductal grey (PAG), PVT and the dorsal vagal complex (DVC)[77,81,82] (Figure 1.4). Additionally, the CeA also sends projections to the BNST, LH, VTA, PBN and NTS[73] (Figure 1.4), which are implicated in a diverse range of behaviours including anxiety, feeding, reward and gustatory and taste processing. These anatomical studies implicate the CeA in controlling a diverse range of behaviours, however the role of neurons in this region and their projections has been predominately studied in the context of aversive behaviours.

Efforts to understand the function of CeA neurons, intra-CeA information flow and functional output has focused on molecularly-defined subpopulations of neurons in the mouse. Using modern circuit neuroscience tools including chemogenetics and optogenetics, imaging and anatomical tracings, the function of a number of these subpopulations has been defined. Some of the first hints at the functional diversity of CeA neurons arose from an *in vivo* recording study in mice during fear conditioning. This revealed the presence of two subpopulations of CeL neurons that were either excited (CeL_{ON}) or inhibited (CeL_{OFF}) to the CS. CeL_{OFF} neurons were shown to tonically inhibit the CeM and that their inhibition by CeL_{ON} units leads to activation of CeM output neurons and freezing to CS presentation[83] (Figure 1.5). A subsequent study showed that CeL neurons expressing the cellular marker PKCδ likely correspond to the CeL_{OFF} cells as their *in vivo* silencing augments conditioned fear responses[67]. Furthermore, neurons in the CeL that express the neuropeptide somatostatin (SOM) were shown to drive conditioned fear responses and that potentiation of synapses from the LA onto CeA^{SOM} neurons is necessary for fear learning, indicative of a role for these neurons as CeL_{ON} cells[84]. The inhibitory connections of both $CeA^{PKC\delta}$ and CeA^{SOM} neurons onto other neurons in the CeL suggests a local circuit mechanism where activity of one or the other population dominates the behavioural

output depending on the experience of the animal[67,84].

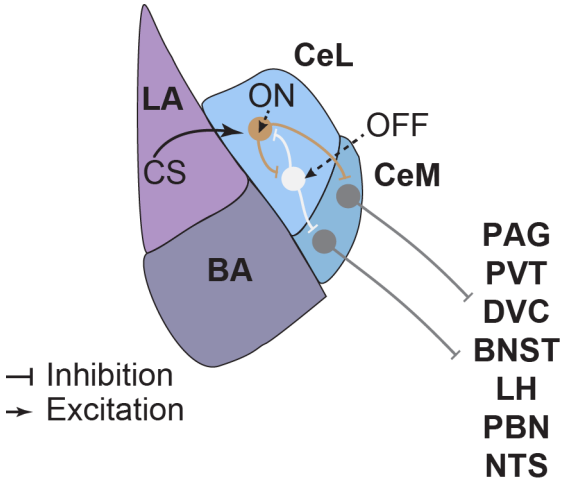

Figure 1.5: Central amygdala microcircuits that control fear behaviour. CS presentation excites LA neurons which relay information into the CeL onto CeLON cells. CeLON cells drive conditioned freezing by inhibition of CeLOFF neurons, leading to dishibition of CeM output neurons that drive the behaviour response. CeLON neurons also directly inhibit the CeM and these neurons may also drive behaviour in specific contexts. Abbreviations: CS- Conditioned stimulus; LA- lateral amygdala; CeL- Central lateral amygdala; CeM- Central medial amygdala. PAG- Periaqueductal grey; PVT- Paraventricular thalamus; DVC- Dorsal vagal complex; BNST- Bed nucleus of the stria terminalis; LH- Lateral hypothalamus; PBN- Parabrachial nucleus; NTS- Nucleus of the solitary tract. Adapted from:[67,73,74].

Activity of CeA$^{PKC\delta}$ neurons has also been shown to control anxiety. Spontaneous activity of CeL$_{OFF}$ cells is heightened following fear conditioning which is correlated with increased generalized fear responses[83,85]. Additionally, activity of CeA$^{PKC\delta}$ neurons is both necessary for and sufficient to evoke anxiety behaviours[85]. The finding that CeA$^{PKC\delta}$ neurons mediate both anxiety and feeding suppression suggests a potential interaction between these effects. However, activation of CeA$^{PKC\delta}$ neurons under conditions that reduce food intake has an anxiolytic effect[66] suggesting that feeding and anxiety behaviour may be differently controlled by CeA$^{PKC\delta}$ neurons under different conditions. Converse to the role of CeA$^{PKC\delta}$ neurons, a subpopulation of PKCδ- CeA neurons that express the serotonin receptor Htr2a were shown to be inhibited by innate fear stimuli while activation of these neurons decreases innate fear responses[86]. Together, these studies demonstrate that the CeA bidirectionally affects fear and anxiety behaviours through distinct neuronal populations.

The studies described above highlight the intensity with which the role of the CeA in aversive behaviours has been investigated at the neuron subpopulation level. This had led to the narrow-sighted view that the CeA is primarily involved in emotional defensive and avoidance behaviours. The following section is a review of behavioural and anatomical evidence for the involvement of the CeA in processing appetitive signals to mediate reward and consummatory behaviours, which suggests that this region promotes diverse behaviours and is not as specialized as initially though.

1.2.3 The role of the CeA in appetitive and consummatory behaviour

The pursuit of reward is an adaptive process that is integral to the survival of an animal. The seeking and consumption of natural reinforcers such as food or water involves motivation to obtain such a reward and learning of reward-predictive cues. The amygdala was first postulated to contribute to reward-related behaviours when the same lesions that attenuated learnt fear responses also blunted responses to reward[70–72]. In addition, to impairing conditioned fear responses, lesions of the CeA have also been shown to abate conditioned appetitive responses[87,88], suggesting a general role for the CeA in emotional learning.

The CeA has been implicated in processing reward associated with alcohol and drugs of addition, though the precise mechanism requires further investigation[89–91]. There is however, considerable evidence for the CeA in motivated reward seeking. A recent study demonstrated that optogenetic activation of the CeA in rats enhanced the pursuit of reward by increasing the reward incentive salience and increasing motivation to work for a sucrose reward[92]. This study revealed that reward enhancement was not generated from a general increase in motivational state and did not extend to consumption of unconditioned rewards, but that only magnified pursuit of an associated external reinforcer was affected. In contrast, another study reported that opioid stimulation in the CeA increased food consumption as well as appetitive behaviour toward a food reward-predictive stimulus[93]. Additionally, it has been shown that animals will self-

administer CeA stimulation, suggesting that under certain conditions CeA activation can trigger an internally reinforcing state[94]. Clearly, a more rigorous interrogation of the CeA and related circuitry is required since CeA manipulations elicit both aversive and appetitive behaviours and the aspects of reward-related behaviour mediated by this region varies between studies. It is plausible that distinct neurons in the CeA respond to appetitive or aversive cues and that processing of different valence signals occurs in a segregated manner. Indeed, this was found to be the case in the BLA, where positive and negative representations are segregated based on projection target[95–97]. Given the cellular heterogeneity in the CeA this may indeed be the case, however the identity of neurons that mediate such polarizing effects remains to be determined.

Aside from behavioural evidence, the position of the CeA as an interface between sensory systems and other limbic and reward-related regions strongly hints at a function in appetitive behaviour. Reciprocal connections between the CeA and midbrain dopaminergic neurons in the SN and VTA has been demonstrated[98–101]. Although CeA-dopaminergic connections have been postulated to be involved in learned appetitive behaviours[102–104], this hypothesis has not be rigorously tested. CeA neurons also project to the LH, an important mediator of motivated and appetitive behaviour via intra-hypothalamic and mesodopaminergic connections[56,105]. Despite the reported links with the brain's reward circuitry, the functional significance of these connections is not clear.

In addition to appetitive and reward-related behaviour, there is also evidence for the involvement of the CeA in consummatory behaviour. However, the direction of the effects reported between studies are not consistent, again highlighting the likely functional heterogeneity of neurons in this region. With respect to food consumption, studies using CeA lesions or electrical stimulations have reported increases or decreases in food intake and body weight[106,107]. Additionally, infusion of neuromodulatory antagonists or agonists into the CeA has been shown to affect overall consumption and food preference based on palatability to varying degrees[108,109].

Given the cellular heterogeneity and high degree of interconnectivity between neurons in this region, it is not surprising that these relatively non-specific methods have yielded inconclusive results and revealed little about the underlying mechanisms. The identification of CeA neurons that express PKCδ which mediate feeding suppression under anorexigenic conditions is a first step to dissecting consummatory behaviour mediated by the CeA in detail. However, the reported effects on appetitive behaviour and food consumption upon CeA manipulations suggest that distinct neuron populations may mediate distinct functions. In recent years, the use of cell-type-specific methods to target, observe and manipulate populations of neurons *in vivo* has allowed a thorough interrogation of the function of specific cell populations in a given behaviour. These approaches are key to resolving the contribution of the CeA to diverse behaviours.

1.3 Targeting, manipulating and observing activity of neural subpopulations *in vivo*

1.3.1 Targeting: Cre mice

The appreciable cellular heterogeneity in the CeA has contributed to the reported conflicting results regarding the precise function of the CeA in different behaviours. A prevailing approach in neuroscience is to target defined neural subpopulations and probe their connectivity within a neural circuit and function in behaviour. However, there is still ongoing debate about the definition of a neural subpopulation. This is because there are many criteria that can be used to classify neurons into a subpopulation. These include: developmental origin, expression of a specific gene, protein, receptor or neurotransmitter, projection target, physiological properties, activity pattern during a given behaviour, morphology and anatomical location within a structure, or a combination of several of these[110–112]. The wide use of these different classification methods has not necessarily led to clearer ideas of what constitutes a neural subpopulation

given that we do not know the complete list of properties a given subgroup of neurons must have in order to be deemed a 'subpopulation'.

One of the most common ways to classify neurons in recent years has been through the use of genetic markers to identify molecularly-defined subpopulations. However, it should be mentioned that this approach does have its limitations as expression of a particular gene in a given cell group does not necessarily correlate with anatomical, physiological or functional characteristics. The prevalent use of genetic methods to target, manipulation and observe neurons *in vivo* has arisen due to the development of genetically engineered mice that express specific transgenes, that when used in combination with a toolbox of viral vectors can be a powerful method to accessing neural populations *in vivo*.

In order to target neural subpopulations *in vivo*, transgenic mice that express the cre-recombinase enzyme are widely used. Cre is a bacteriophage enzyme that can be expressed under a specific promoter or enhancer through multiple approaches including transgenesis or BAC transgenesis, where an exogeneous promoter or enhancer is inserted into the genome to strongly drive a gene of interest[111]. Gene targeting strategies including 'knock-ins' can be used to express any gene of interest under a specific promoter[111]. To target cre-expressing neurons in a region of interest within the brain, genetically engineered adenoassociated viruses (AAVs) can be used to stereotaxically deliver protein-based tools for neural circuit mapping and manipulation into cre-expressing neurons. This system takes advantage of the enzymatic function of cre, which recognises short DNA sequences (lox sites) that flank the cell-targeted tools. Recombination between two sets of lox sites catalysed by cre, allows expression of the tool only in cre-expressing neurons, an ideal method to target neurons in a cell-type specific manner[111]. In neuroscience, viral vectors that carry proteins for neuron morphology visualisation, neural activity manipulation using light or pharmacological agents, or visualization of neural activity are commonly used. Several of these are discussed in the following sections.

1.3.2 Manipulating: Optogenetics

Optogenetics is a revolutionary tool now considered a key technique in circuit neuroscience. Defined populations of neurons are transduced with light-activated microbial opsins, allowing the activity of neurons to be controlled by light in a reversible and temporally and spatially specific manner. To achieve this, mice expressing cre in the neural population of interest are stereotaxically injected with a cre-dependent AAV carrying the actuator opsin into the brain region of interest. Multiple opsin varieties exist to either activate or inhibit neurons. The most common neuron activator is channelrhodopsin-2 (ChR2), a cation channel which is activated by blue light ($\sim$450-490nm). Photon absorption leads to flow of cations into the cell and membrane depolarization[113]. ChR2 can be used to induce high fidelity spiking patterns in neurons, in some way mimicking endogenous neural activity[114].

Two inhibitory opsins, halorhodopsin (NpHR) and archaerhodopsin (Arch) silence neurons by different methods. NpHR is activated by $\sim$590nm yellow light and pumps extracellular chloride ions into the cell[115]. Arch is a proton pump activated by $\sim$560nm light, which when active pumps protons out of the neuron[116]. Activation of both inhibitory opsins leads to a hyperpolarizing current and decreased firing rates in neurons, however both have advantages and limitations. Both the most efficient variants of NpHR and Arch generate large photocurrents, but higher expression of Arch on the cytoplasmic membrane means that overall, more photocurrent is generated. The kinetics and light sensitivity of both opsins are however, comparable[117]. Moreover, NpHR was shown to be more liable to permit postsynaptic spiking after prolonged photoinhibtion than Arch[118].One major advantage of NpHR over Arch comes from pre-synaptic terminal inhibition experiments, where Arch was found to evoke spontaneous neurotransmitter release with sustained activation[119]. Therefore, care must be taken to choose the correct inhibitory opsin depending on the parameters of the experiment. To date, optogenetics has been predominantly applied in two settings. The first is pairing expression of ChR2 in a defined cell

type with recording, using *ex vivo* slice electrophysiology, of putative post-synaptic neurons[120]. This allows precise mapping of circuit wiring diagrams with cell-type specific precision. The second application is *in vivo* manipulation of groups of defined neurons in awake, behaving animals, allowing the sufficiency and necessity of a specific neuronal population in a given behaviour to be explored. In laboratory animals, light is delivered to the brain through optic fibres that are most commonly implanted chronically in the brain above the target structure or, for terminal manipulations, over the presynaptic terminals of a neural projection. The most common light sources are lasers or LEDs which are generally delivered through lightweight optic fibre patch cables. However, wireless systems using LEDs are becoming more prevalent[121].

Use of optogenetics *in vivo* offers advantages over previously used methods such as lesions and electrical stimulations to dissect the role of a given brain region in behaviour. Activity manipulations can be time-locked to a particular event or cue to understand the function of neurons in a subcomponent of behaviour. As well as open-loop experiments, closed-loop manipulations based on prior behaviour of the animal or another parameter are also possible. Optogenetics is particularly powerful when dissecting the role of a brain region containing heterogeneous neural populations as these can be systematically targeted and their roles parsed out. There are however, caveats of this approach, which include but are not limited to: 1) Bulk, synchronized activation of a cell population does not necessarily recapitulate the *in vivo* dynamics of the network nor mimic physiological neurotransmitter/neuropeptide release patterns. 2) Transient neuronal activity manipulations may have off-target effects on the function of downstream-circuits. 3) Uneven light penetration means that cells closer to the implanted fibre will be differently affected than those further away. 4) Local heating of the tissue, which can have consequences on neural physiology[122–125].

1.3.3 Manipulating: Chemogenetics

Chemogenetics is another technique that has been implemented in the control of neural activity during behaviour. This approach uses engineered proteins that are activated by otherwise biologically inert ligands to activate or inhibit neuronal activity. The classes of proteins modified for chemogenetic approaches include ion channels, enzymes, G-protein coupled receptors (GPCRs) and kinases (reviewed in[126]). The most widely used tools in neuroscience are modified GPCRs called Designer Receptors Exclusively Activated by Designer Drugs (DREADDs). These are human muscarinic receptors that, through engineering, were rendered insensitive to the native ligand acetylcholine and instead activated by the biologically inert small molecule chlozapine-N-oxide (CNO). CNO can be delivered orally or via intraperitoneal injection to the DREADD-expressing animal. The most common DREADD used to activate neurons is the hM3Dq variant which activates the Gαq signalling pathway upon CNO binding, leading to depolarization and burst firing of neurons[127]. The DREADD variant for neuron inhibition is hM4Di which leads to hyperpolarization through Gαi-mediated activation of inwardly-rectifying potassium channels that leads to an influx of potassium ions into the cell[128]. Proteins used for chemogenetics are delivered in the same way as optogenetic actuators, via cre-dependent AAVs, offering cell-type specific control of neuronal activity in order to understand the function of specific cell populations in heterogeneous brain regions.

The main advantage of DREADDs over optogenetic approaches is that the CNO-mediated effects are long lasting and allow behavioural monitoring for hours[127]. Additionally, the broad diffusion of CNO allows activity modulation of a spatially diffuse neuronal population with similar efficacy. Further, compared to optogenetic strategies, the technology is easier to implement. The main disadvantage of chemogenetics is that it lacks precise temporal control of neural activity and so is not ideal for dissecting the function of neurons in response to a cue or behavioural event.

1.3.4 Manipulating: Cell ablations

Long before the advent of temporally and spatially precise methods like chemogenetics and optogenetics, scientists have investigated the contribution of specific cells to behaviour using neuron ablation techniques. The most common of these are the neurotoxin ibotenic acid and the use of high frequency electrical currents to induce targeted ablations. The main difference is that ibotenic acid specifically targets neurons while electrical lesions damage both cells and fibres of passage[129]. Both these techniques have been used to investigate the involvement of the CeA in different behaviours[130,131], however the outcome of these techniques is difficult to interpret when targeting regions that contain heterogeneous intermingled cell populations. Additionally it is also difficult to control the extent of the lesion site and control for damage to fibres that pass through the targeted region[129]. These challenges have been overcome by the use of genetically-targetable virally-delivered tools that when used in conjunction with cre mice, allow for precise ablation of defined cell types within a spatial region of interest. AAV-mediated delivery of the diphtheria toxin A subunit (dtA)[132] or apoptosis-inducing caspase[133] into cre-expressing neurons are now commonly used methods to target a specific neural population of interest and to ablate these neurons in adult animals. These tools therefore, allow the requirement of genetically-defined neurons in behaviour to be investigated.

1.3.5 Observing: *in vivo* Ca^{2+} imaging

An important consideration in circuit neuroscience is that while neural activity manipulations provide evidence for the functional role of a given group of neurons, they give no insight into the endogenous activity of neurons during behaviour. Furthermore, these methods do not allow an appreciation of functional heterogeneity within a neural population. In order to address these caveats, electrophysiological recordings or imaging of neural activity is used in behaving animals to allow a more comprehensive understanding of neural circuit function. *in vivo* imaging has

become prevalent following the advent of genetically-encoded calcium (Ca^{2+}) indicators such as GCaMPs which bind to Ca^{2+}[134,135]. During increased neuronal activity, the Ca^{2+} concentration inside the cell transiently rises. This can be measured by increased fluorescent signal release by the GCaMP indicator. Thus, GCaMP fluorescence fluctuations can be used as a proxy for changes in neuronal activity.

Compared to *in vivo* electrophysiology recordings, Ca^{2+} imaging offers several advantages. Firstly, sampling of larger numbers of neurons and resolution of their spatial distribution is permitted. Additionally, both dense or sparsely distributed cells as well as sub-cellular compartments can be imaged, while electrophysiological recordings capture a much smaller sample of neurons, with little information about their anatomical location. Conversely, Ca^{2+} imaging suffers from poorer temporal resolution than electrophysiological recordings. Ca^{2+} transients do not precisely correlate with voltage changes across the cell membrane, as intracellular changes in Ca^{2+} are dependent on voltage changes[136]. Thus, unlike *in vivo* recordings, Ca^{2+} imaging does not allow an accurate estimation of neural spike timing. The relationship between the action potential and Ca^{2+} signal depends on the properties of the indicator including the kinetics and Ca^{2+} binding properties[137]. Variants of the most advanced and currently widely used Ca^{2+} indicator, GCaMP6, allow fairly accurate spike-time resolution depending on the sensitivity and kinetics of the particular variant[138]. This also depends on the spiking pattern and Ca^{2+} handling properties of the neuron type, with the properties of excitatory neurons permitting a better approximation to the underlying voltage changes than interneurons[139]. It is important to also note that Ca^{2+} imaging does not allow appreciable detection of hyperpolarations or sub-threshold events.

One of the challenges of implementing Ca^{2+} imaging is that biological tissue has light scattering properties. This has been circumvented by the advent of two-photon microscopy, which can be used to image up to $\sim$600μm below the tissue surface by using low-energy photons,

allowing spatially focused excitation and optical sectioning. This decreases background signal and increases the resolution[140,141]. However, this requires the animal to be head-fixed under a conventional microscope objective and in this manner only allows imaging of superficial brain structures during a limited range of behaviours. To circumvent these limitations, alternative technologies have been recently development to allow imaging of deeper brain structures in freely-moving animals.

Fibre photometry, where an optical fibre is implanted above the target structure, is used to measure the fluorescent signal changes that occur in a population of GCaMP-expressing neurons[142]. Animals are tethered to an optic fibre bundle, which permits relatively free movement. However, the main caveat of this technique is that it lacks single cell resolution as bulk fluorescence changes are measured. Thus, this approach is suited for imaging homogenous neuron populations or to measure Ca^{2+} changes in the pre-synaptic projection field[143]. The challenge of imaging deep brain structures at single cell resolution has been circumvented by the use of microendoscopic lenses, which comprise two GRIN (gradient-refractive-index) lenses with a relay lens in-between that allows access to deep structures. GRIN lenses have optical properties that guide and focus light and when implanted above a target structure, relay the Ca^{2+} fluorescent signal from the target tissue[144]. The fluorescent dynamics are captured using an integrated head-mounted microscope that is light-weight enough to permit free movement of the animal. The major advantage of this approach over fibre photometry is that it affords single cell resolution imaging and provides spatial information. However, the tissue damage incurred by the implanted lenses, which range from 0.5mm-1mm in diameter, may have adverse effects on the neural network under investigation[145]. Additionally, since this approach uses single-photon imaging, optical sectioning is not possible, which decreases the resolution due to collection of out-of-focus light. However, with post-processing, single cell bodies can be isolated for analysis[145]. Despite the drawbacks, use of GRIN lenses in conjunction with miniaturised mi-

croscopes allows monitoring of activity of large numbers of neurons with single cell resolution in previously inaccessible brain regions. GRIN lenses are also now being used in conjunction with two-photon imaging, allowing a better resolution of the neurons of interest[146]. Overall, the use of neuronal activity imaging techniques are an important step forward in understanding the function of neural circuits in behaviour.

Chapter 2

Thesis objectives

The overwhelming perception that the amygdaloid complex principally controls aversive behaviours such as fear and anxiety is short-sighted given the wealth of studies documenting this region in controlling reward and appetitive behaviour. The so-called output amygdala region, the CeA, contains many populations of molecularly-defined neuron types, rendering it a very heterogeneous region. This is a likely explanation for the lack of clarity in defining the function of the CeA in appetitive and reward-related behaviours. Given the availability of tools to genetically-target, manipulate and observe defined populations of neurons *in vivo*, the aim of my thesis was to investigate the CeA circuits that control appetitive behaviour in a cell-type specific manner.

My starting point was the report that $CeA^{PKC\delta}$ neurons mediate feeding suppression under specific conditions, and that the likely mechanism is through local inhibition of $CeA^{PKC\delta-}$ neurons[66]. This suggested, first, that $CeA^{PKC\delta-}$ neurons promote feeding and secondly, since food intake can be considered the results of an appetitive or positive valence signal, that $CeA^{PKC\delta-}$ neurons may be involved in reward seeking behaviour. To test these hypotheses, I focused on two molecularly-defined populations of CeA neurons: 1) CeA^{SOM} neurons, that functionally antagonise $CeA^{PKC\delta}$ neurons in fear behaviour, 13% of which reportedly express PKCδ[84] . 2)

CeA^{Htr2a} neurons, which overlap with CeA^{SOM} neurons, but not with $PKC\delta$[86].

To probe the function of these neurons in feeding behaviour, I used *in vivo* chemogenetic, optogenetic and targeted cell-ablation methods in cre-expressing mice in combination with assays to determine food intake in different conditions. I found that indeed defined populations of $CeA^{PKC\delta-}$ neurons functionally oppose those that express $PKC\delta$. However, there were differences between the CeA^{SOM} and CeA^{Htr2a} neurons, with CeA^{Htr2a} neurons mediating the strongest effect.

Next, since food intake can reflect different internal states and the influence of environmental factors, including hunger and hedonia influences[5] I sought to determine the aspect of feeding that CeA^{Htr2a} neurons control. To do so, I placed the results of neural activity manipulation experiments in context by monitoring the endogenous activity of the CeA^{Htr2a} neurons during food consumption using *in vivo* Ca^{2+} imaging with single cell resolution using a head-mounted miniscope. These findings revealed a role for CeA^{Htr2a} neurons in the consummatory aspect of food consumption.

Finally, the consumption of food is strongly influenced by its intrinsically rewarding properties[147]. The finding that CeA^{Htr2a} neurons promote food intake and are active during consumption suggested a role of these neurons in processing the rewarding properties of food rather than hunger. I determined that CeA^{Htr2a} neurons intrinsically promote reward seeking using closed-loop self-stimulation experiments. Further, I found that activity of CeA^{Htr2a} neurons modulates food's intrinsically rewarding properties to influence consumption. Thus, these neurons appear to promote food consumption by positively reinforcing ongoing eating behaviour. Together, these findings reveal a role for a defined subpopulation of CeA neurons in promoting food consumption and reward seeking, demonstrating that within the same brain regions, neighbouring populations of neurons perform antagonistic functions. More broadly, these results add to the current understanding of how appetitive signals are routed through the brain

and implicate the CeA as a candidate in the study of maladaptive feeding-related behaviours.

Chapter 3

Materials and Methods

3.1 Animals

The *Htr2a-cre* BAC transgenic line (STOCK Tg[*Htr2a-cre*] KM208Gsat/Mmucd) was imported from the Mutant Mouse Regional Resource Center. *PKCδ-cre* (Tg(Prkcd-glc-1/CFP,-Cre)EH124Gsat) BAC mice were obtained from the Gensat Database and *SOM-IRES-cre* (SSTtm2.1(cre)Zjh/J) mice were purchased from The Jackson Laboratory. Td-Tomato (B6.Cg-Gt(ROSA) 26Sortm9(CAG- tdTomato)Hze/J)[148] and Rosa26R[149] mouse lines have been previously described.

Mice used for all experiments were between 1-4 months old. For immunostaining and electrophysiology, both male and female mice were used. Male mice were used for behaviour experiments, except for the Ca^{2+} imaging, where females were used. All mice that underwent surgery procedures for behaviour experiments were singly housed on a 12hr light-dark cycle with *ad libitum* food and water access unless food or water deprivation was required for experiments. All feeding relevant behaviour experiments were conducted in the early part of the light period (8am-1pm).

3.2 Viral constructs

The following AAVs were purchased for the University of North Carolina Chapel Hill Gene Therapy Center Vector Core: AAV8-hSyn-DIO-hM3D(Gq)-mCherry, AAV8- hSyn -DIO-mCherry, AAV5-Ef1a-DIO-ChR2-eYFP, AAV5-Ef1a-DIO-eYFP, AAV5-flex-mCherry-dtA, AAV5-ef1a-DIO-npHR3.0-mCherry. The AAV2/9-Ef1a-DIO-GCaMP6s-eYFP virus was produced at University of Pennsylvania Vector Core.

3.3 Stereotaxic surgeries

3.3.1 Virus injections

Mice were anesthetized for surgery with isoflourane and placed on a heating pad on a stereotaxic frame (Kopf Instruments). Throughout the surgery isolfourane as maintained at (1.5-2%). A systemic (Carprofen 5 mg / kg bodyweight) was administered.

Mice for optogenetic and chemogenetic experiments received a bilateral injection of 0.3µl of virus in the CeA through a 0.2mm hole drilled in the skull at the following coordinates from bregma: - 1.22mm anteroposterior, $\pm$2.8mm lateral. Virus was injected at the same coordinates 4.72mm ventral from bregma. Mice for *in vivo* optogenetic experiments received a bilateral implantation of optic fibres (200µm core, 0.22 NA, 1.25mm ferrule (Thor labs)) above the CeA (-4.2mm ventral) or PBN (-5.1mm anteroposterior, $\pm$1.7mm lateral, -3.0mm ventral). Implants were secured with cyanoacrylic glue and dental acrylic was used to cover the exposed skull (Paladur). For all other animals, the incision was closed with sutures.

Mice for *in vivo* Ca^{2+} imaging experiments were injected unilaterally in the left CeA using the same coordinates as above. 0.3µl AAV-GCaMP6s of virus was used.

3.3.2 GRIN lens implantation

One week after the virus surgery, mice were again anesthetized and placed in the stereotaxic frame. A 0.8mm hole was drilled at the same coordinates where the virus was injected. The hole as cleared of bone and coagulated blood and a sterile 20G need as lowered into the brain to clear a path for the lens to a depth of -4.5mm from the cortical surface. The GRIN lens (GLP-0673; diameter: 0.6mm, length: $\sim$7.3mm Inscopix) was lowered into brain and secured at -4.35mm from the cortical surface. The lens was glued in place with UV-curable glue (Loctite 4305). A 2cm metal headbar that extended 1.5cm beyond the back of the mouse's head as fixed to the skull adjacent to the lens using dental cement which was also used to cover exposed skull (Paladur). The headbar assisted with mounting of the miniature microscope. The top of the lens was covered with a small pies of Parafilm and covered with silicone adhesive (Kwik-cast).

3.4 Behaviour

3.4.1 Feeding experiments

Mice for all experiments were habituated to the behaviour context for 2x daily 10 minute sessions prior to the experiment. Testing was conducting at the beginning of the light cycle with *ad libitum* food access (CeA^{Htr2a}::hM3D and CeA^{SOM}::hM3D) or after 24 hours food deprivation ($CeA^{PKC\delta}$::hM3D and CeA^{Htr2a}::dtA and anorexigenic drug and bitter food tests). The experiments were conducted in a 50cm x 25cm plastic arena inside a soundproof chamber containing houselights and cameras to record the sessions (TSE Multiconditioning System). The behaviour arena contained two plastic cups in opposite corners, one with a pre-weighed food pellet. Experiments were conducted over 40 minute sessions and the remaining food was weight after 20, 30 or 40 minutes depending on the experiment. The session was video recorded and

feeding behavior was scored manually.

Mice for DREADD experiments received CNO (2mg/kg diluted in saline) or saline by intraperitoneal injection (IP) 20 minutes prior to the start of experiments and allowed to recover in their homecage. The following drugs were dissolved in saline and administed IP 20 minutes prior to the experiments: LiCl (150mg/kg) (Sigma), LPS (0.1mg/kg) (Sigma).

Food pellets for bitter food experiments were soaked in 10mM quinine (Sigma) solution in distilled water for 10 minutes and air dried overnight. Clay pellets for experiments comparing consumption of food and clay pellets were prepared by preparing a paste of kaolin (aluminium silicate hydroxide, Sigma) with 1% gum arabic (Sigma) in distilled water. The paste was shaped to resemble food pellets and air dried overnight. The mice were familiarized to the clay pellets in the home cage for three days prior to the experiment.

Mice for optognetic experiments were bilaterally tethered to optic fibre patch cables (Doric Lenses or Thorlabs) via a mating sleeve (Thorlabs). The mice were habituated to this process and the behaviour context for 3x 15 minute daily sessions prior to the experiment. The patch cables were connected via a rotary joint (Doric Lenses) to a 473nm (CNI lasers) or 561nm (Cobolt) lasers. Photoactivation experiments were conducted with 10-15mW 10ms, 473nm light pulses at 5, 10 or 20Hz. Photoinhibition experiments were conducted with constant 561nm 10mW light. Lasers were controlled by Bonsai[150] and Arduino microcontrollers (www.arduino.cc). Prior to the experiment, mice were tethered to the patch cables and allowed to recover in the behaviour arena for 5 minutes. For photostimulation experiments, mice with *ad libitum* food access received 20 minutes laser ON and 20 minutes laser OFF. For photoinhibition experiments, food deprived mice received 10 minutes laser ON and 10 minutes laser OFF. The food remaining at the end of each epoch was weighed. The session was video recorded and feeding behavior during the photostimulation epochs was scored manually.

For *in vivo* validation of hM3D and ChR2 tools, the mice were subjected to either IP injection

of CNO (2mg/kg) injection and perfused two hours later (CeA^{Htr2a}:: hM3D and mcherry controls) or 20 minutes 20Hz, 10mW photostimulation and perfused one hour later (CeA^{Htr2a}:: ChR2 and eYFP controls).

3.4.2 Taste sensitivity

CeA^{Htr2a}::hM3D, CeA^{SOM}::hM3D mice and mCherry controls were deprived of water overnight. The mice were trained in 5x daily 1 hour sessions to drink distilled water from a two-bottle custom licometer[151]. Mice were allowed *ad libitum* access to water in their homecage for 1 hour. On the 6th day, mice received an IP injection of CNO (2mg/kg diluted in saline) 20 minutes prior to the experiment. The mice were tested for their preference to drink 1mM Quinine (in distilled water) (Sigma) solution over distilled water. Preference ratio:

$$\frac{\text{Number of 1mM Quinine solution licks}}{\text{Number of Quinine solution licks} + \text{Number of } H_2O \text{ licks}}$$

Licks were timestamped with Arduino microcontrollers and analysed with a custom written Python script.

3.4.3 Open field

CeA^{Htr2a}::hM3D, CeA^{Htr2a}::dtA mice and controls were allowed to explore a novel custom plexiglas arena (50 x 50 x 25cm). The location of the animals were tracked for 15 minutes. Number of entries to the centre of the arena (a 25 x 25cm square), velocity and distance travelled were calculated using Ethovision XT 11 (Noldus). CeA^{Htr2a}::hM3D and control mice were injected IP with CNO (2mg/kg diluted in saline) 20 minutes prior to the experiment.

3.4.4 Real-time place preference

Mice for all experiments were allowed to freely explore a custom plexiglas two-chambered arena (50 x 25 x 25cm). The photostimulated/inhibited compartment was randomly assigned. ChR2-expressing mice and controls received 5, 10 or 20Hz 473nm photostimulation in one compartment. NpHR-expressing mice and controls received constant 561nm light in one compartment. The location of the animal was tracked using Bonsai[150] and the laser was triggered with Arduino microcontrollers (www.arduino.cc). The experiments were conducted over 20 minutes with the percent time spent in the photostimulated/inhibited side of the chamber, distance travelled and velocity assessed in the last 15 minutes using Ethovision XT 11 (Noldus).

3.4.5 Intracranial self-stimulation

Prior to the experiments all mice were food restricted overnight. The experiment was conducted over 2x daily 1 hours sessions and took place in a custom chamber equipped with a custom two-port nosepoke system (modified from https://bitbucket.org/takam/behavioural-hardware), with LEDs above each nosepoke and a piezo speaker (Conrad). One port was randomly designated the active port. Both inactive and active ports were baited with food treats to encourage exploration on Day 1. Nosepokes in the active port were coupled to an intracranial light train (473nm, 10-15mW, 60 x 20Hz pulses). Nosepokes in the inactive port had no consequence. Pokes in both ports elicited illumination of a reinforcing LED (1 second) above the respective port and either a 1kHz or 1.5kHz tone (1 second). Nosepoke time stamps were collected via Bonsai[150] and Arduino microcontrollers (www.arduino.cc) and Day 2 data was analysed using a custom written Python script.

3.4.6 Progressive ratio 2 task

CeA^{Htr2a}::hM3D and mCherry mice were maintained at 85-90% free-feeding weight by administering a once daily food pellet of 2.5-3.5g. Mice were trained to nosepoke for food pellets in a custom two-port nosepoke system (as for Intracranial self-stimulation). In the first phase of training, the designated active port led to delivery of a single 20mg food pellet (TSE Systems) from a pellet dispenser (Noldus) into a food magazine on a fixed ratio 1 schedule (FR1; 1 active poke = 1 pellet). Pokes were reinforced by a LED which was illuminated below the respective port (3 seconds) and either a 1kHz or 1.5kHz tone (3 seconds). Nosepoke time stamps were collected via Bonsai[150] and Arduino microcontrollers (www.arduino.cc). Once mice could discriminate between the active and inactive ports on a FR1 schedule by at least 3:1 for three consecutive sessions, mice were subjected to three FR5 sessions (FR5: 5 active pokes = 1 pellet). Following this were four sessions where pellets were delivered on a progressive ratio 2 schedule (each successive pellet requires two additional nosepokes responses eg. 1, 3, 5, 7 etc). PR2 performance of the mice was tested after *ad libitum* food access. Mice received an IP injection of CNO (2mg/kg diluted in saline) or saline 20 minutes prior to the session. The order of the CNO and saline sessions were counterbalanced. The metrics of motivation to obtain food pellets were the number of active nosepokes and the breakpoint (highest number of consecutive nosepokes made to obtain a food pellet).

3.4.7 Palatable reward consumption

CeA^{Htr2a}::NpHR and mCherry mice were maintained at 85-90% free-feeding weight by administering a once daily food pellet of 2.5-3.5g. Mice tethered to optic fibre patch cables were allowed to consume a palatable reward solution (Fresubin, 2kcal/ml) from a metal licometer (as for Taste sensitivity). The mice were trained for daily 30 minute sessions until their licking performance was stable. This was when the number of licks per session over three consecutive

days varied by $<\pm$10% from the first of the three days. Mice were then tested for Fresubin consumption after *ad libitum* food access during a 20 minute session with constant photoinhibition (561nm, 10mW). Licks were recorded and analysed as for Taste sensitivity.

3.4.8 Conditioned flavour preference

CeA^{Htr2a}::ChR2 mice were allowed to freely consumed two differently flavoured non-caloric gels in their homecage overnight. Gels: (0.3% grape or cherry sugar-free Kool-Aid (Kraft), 1% Agar (Sigma), 0.15% saccharin (Sigma) in dH_2O). Baseline flavour preferences was determined as the average of two sessions, conducted as follows: Mice were tethered to optic-fibre patch cables and habituated in an empty plexiglas cage for 30 minutes. 0.3g of both gels were introduced to the cage and the gel that remained was weighed after 15 minutes. Conditioning occurred over two-daily sessions, conducted 4 hours apart, for four days total. The order of the sessions was inverted each day. Conditioning 1: mice were allowed to consume 0.3g of the less-preferred flavour concurrent with 25 minutes 473nm intracranial light pulses (10-15mW, 20Hz). The photostimulation was initiated 5 minutes after the gel as introduced to the cage. Conditioning 2: mice were allowed to consume 0.3g of the more-preferred flavour over a 30 minute session in the absence of photostimulation. The day following the last conditioning session, conditioned flavour preference was tested. Preference was calculated as the average from the two sessions where mice were presented with 0.3g of both flavours for 15 minutes.

3.5 *in vivo* Ca^{2+} imaging

Two weeks after the lens implantation surgery, the mice were checked for GCaMP6s fluorescence. The mice were headfixed using the skull-affixed metal headbar to clamp the animal in place while it ran on a spinning wheel. The top of the lens was cleaned using acetone and 70% ethanol using lens paper (Leica). The miniature microscope (Inscopix) with a baseplate

(BLP-2, Inscopix) in place as positioned above the lens using a custom clamp. The position of the microscope was adjusted to a suitable field-of-view so that GCaMP6s fluorescence and neural dynamics were observable. One an ideal field-of-view was established, the mice were anesthetized in the same position with isoflurane and the baseplate was cemented in place (Vertise Flow). A baseplate cap (BCP-2, Inscopix) was left in place and secured with a hex key (Inscopix) until imaging experiments.

Two groups of CeA^{Htr2a}::GCaMP6s mice were used for the free feeding (4 mice) and FR1 (3 mice) experiments. The miniscope was secured into the baseplate using the hex key while the mice were headfixed and running on the wheel. Mice for the free feeding experiment were habituated to head-fixation and carrying a dummy miniscope to acclimate to the weight for 3 x 15 minute daily sessions prior to the experiment. These mice were food deprived overnight before imaging. Food restricted mice for the FR1 experiment (85-90% free-feeding body weight) were trained to nosepoke for 20mg food pellets on a FR1 schedule (same experimental setup as for Progressive ratio 2 task). Training sessions were conducted with a dummy miniscope in place until the mice could discriminate between the active and inactive nosepokes by at least 3:1 over three consecutive sessions. On the day of the imaging session, miniscope-mounted mice were allowed to acclimate in their homecage for 10 minutes.

For both imaging experiments, images from the miniscope were obtained in compressed TIFF format at 20Hz using the Inscopix nVista HD V2 software. LED power was set to 40-60% (04-0.6mW) and the analogue gain was set at 1-2. Mouse behaviour was video recorded with overhead and side-mounted cameras. The nVista software and behaviour cameras were triggered and synchronized using Bonsai Bonsai[150] and Arduino microcontrollers (www.arduino.cc). Food contact, eating start and stop events were manually scored after the session.

3.6 Ca^{2+} imaging data analysis

Compressed time-lapse imaging of Ca^{2+} activity was filtered using a low-pass fast fourier transform filter, applied to each frame using ImageJ (NIH). This was done in order to reduce neuropil contamination of the signal. Mosaic software (v1.1.3; Inscopix) was used for motion correction, and principal and individual component analysis to identify individual cells and to extract raw fluorescence traces. Each Ca^{2+} trace and cell mask was manually validated to ensure that each arose from an individual cell. Duplicated and overlapping cell masks were removed.

$\delta F/F_0$ was calculated as $(F-F_0)/F_0$, where F_0 is the lowest 5% of the fluorescence of each Ca^{2+} activity trace[29]. Normalized $\delta F/F_0$was used to transform the range of $\delta F/F_0$ to [0 1] by the equation:

$$\frac{\frac{\Delta F}{F_0} - min(\frac{\Delta F}{F_0})}{max(\frac{\Delta F}{F_0}) - min(\frac{\Delta F}{F_0})}$$

For the free-feeding experiment where the first eating bout was considered, the first 20 second was compared to the 20 seconds preceding the bout was analysed. The cells were classified according to changes in activity with all eating bouts longer than 20 seconds in the experiment considered. Average Ca^{2+} activity during the bout was compared to the average activity in the preceding non-eating bout. For the FR1 imaging experiments, the area under the curve was calculated during the event and compared to a baseline period of the same length prior to the event onset. Wilcoxon rank-sum tests were used to statically compare activity during the eating (F_{eating}) and non-eating ($F_{non\text{-}eating}$) bouts. A preference index as calculated for each cell as follows:

$$\frac{(F_{eating} - F_{baseline})}{(F_{eating} + F_{baseline})}$$

Cells with statistically significant changes in activity were considered responsive neurons and those with a positive preference index were classified as activated during eating while those with a negative preference index were classified as inhibited during eating. Analyses were performed using custom written Matlab and Python scripts.

3.7 Histology

Following the conclusion of experiments mice were perfused. The mice were anesthetized with ketamine/xylazine (100 mg/kg, 16 mg/kg respectively) and transcardially perfused with phosphase-buffered saline (PBS) and then 4% paraformaldehyde (PFA) (w/v) in PBS. Brains were removed from the skull as post-fixed overnight at 4°C in 4% PFA overnight before cryopreservation in 15% and then 30% sucrose in PBS at 4°C. Brains were embedded in O.C.T (Fisher Scientific) and cut with a cryostat (Leica) into 50µm floating sections in PBS.

3.8 Immunohistochemistry

Brain sections were washed in 1X PBS 0.5% TritonX-100 followed by blocking at room temperature for two hours in 1% bovine serum albumin (BSA) diluted in 1X PBS 0.1% TritonX-100 and then incubated in primary antibody at 4°C overnight. Primary antibodies: rabbit anti-cfos (1:1000) (Santa Cruz); mouse anti-PKCδ (1:100) (610398, BD Biosciences), chicken anti-LacZ (1:200) (ab9361, Abcam), rabbit anti-SOM (1:1000) (T-4103, Peninsula Laboratories International). After primary antibody exposure, the sections were washes in 1X PBS 0.1% TritonX-100 (3x 15 minutes) and were incubated in secondary antibody at for 2 hours at room temperature. Secondary antibodies: Alexa Fluor donkey anti-rabbit/mouse/chicken488/Cy3/647, (1:500) (Jackson). After 3x15 minutes 1X PBS 0.1% TritonX-100 washes, sections were incubated in DAPI and coverslipped (Dako).

3.9 Microscopy

Confocal Z-stack images were obtained using a Leica SP8 microscope equipped with a 20X/0.75 IMM objective. Epifluorescent images were acquired using an upright microscope (Zeiss) and 5X/0.15 or 10X/0.3 objectives (Zeiss). The brightness and contrast function and median and mean filteres in ImageJ (NIH) were used to minimally adjust the images and to reduce noise. All quantifications from brain sections were performed from bregma -1.22 to -1.58mm (n=3 sections per mouse, n= 3 mice). For colocalization of Htr2a;βgal overlap with PKCδ or SOM immunostaining, ImageJ was used to manually count the cells. For cfos detection, cfos positive cells were quantified from immunostaining on brain sections using ImageJ. For quantification of *Htr2a-cre::tdTomato* neurons that remained in *Htr2a-cre::dtA* mice, mCherry (infected but unablated) expressing neurons were distinguished from tdTomato neurons using an upright epifluorescent microscope (Zeiss). Brain sections from mice from behavioural and imaging experiments were examined using an upright epifluorescent microscope (Zeiss) for validation of virus expression and/or optic fibre placement. Those mice in which either the virus expression or optic fibre was not appropriately located were excluded from analysis.

3.10 Slice electrophysiology

The mice were deeply anesthetized by intraperitoneal injection of Ketamine/Xylazine mixture (100 mg/kg and 10 mg/kg body weight, respectively) and transcardially perfused with ice-cold protective artificial cerebrospinal fluid (aCSF) containing: 92 mM N-methyl-D-glucamine (NMDG), 2.5 mM KCl, 1.25 mM NaH2PO4, 30 mM $NaHCO_3$,20 mM HEPES, 25 mM glucose, 2 mM thiourea, 5 mM Na-ascorbate, 3 mM Na-pyruvate, 0.5 mM $CaCl_2{\cdot}7H_2O$ and 10 mM $MgSO_4{\cdot}7H_2O$. Coronal brain sections of 250μm thickness were cut with a vibratome (Leica, VT1000S) in ice-cold protective aCSF. Slices were recovered for 15 minutes at 32 °C in regu-

lar aCSF containing 126 mM NaCl, 1.6 mM KCl, 1.2 mM NaH2PO4, 1.2 mM $MgCl_2$, 2.4 mM $CaCl_2$, 18 mM $NaHCO_3$, 11 mM glucose, oxygenated with carbogen. Slices were then kept at 25 °C until recording.

Slices were visualized using fluorescent microscope equipped with IR-DIC optics (Olympus BX51). All electrophysiological recordings were performed in a chamber constantly superfused with corbogenated regular aCSF at 30-32 °C. Whole-cell voltage, current-clamp or cell-attached recordings were performed with a MultiClamp 700B amplifier and Digidata 1550 (Molecular Devices).

The patch pipette with a resistance of 4-6 MΩwas filled with intracellular recording solution. The intracellular solution for current clamp contained: 130 mM K-Gluconate, 10 mM KCl, 2 mM $MgCl_2$, 10 mM HEPES, 2 mM Na-ATP, 0.2 mM Na_2GTP, 0.2% neurobiotin, pH7.35 and 290mOsm. The intracellular solution for voltage clamp recordings contained 125 mM CsCl, 5 mM NaCl, 10 mM HEPES, 0.6 mM EGTA, 4 mM Mg-ATP, 0.3 mM Na_2GTP, 10 mM lidocaineN-ethyl bromide (QX-314), pH 7.2 and 290mOsm. For confirmation of hM3Dq function in CeA^{Htr2a} neurons, 1 μM of CNO diluted in aCSF was used. The holding potential for voltage clamp recordings was -70 mV, if not indicated differently.

For ChR2-assisted circuit mapping in brain slices a multi-LED array system (CoolLED) connected to the epifluorescence port of the Olympus BX51 microscope was used. 1-2 ms light pulses at λ = 470 nm ranging from 1 to 10 mW·mm-2 was delivered to trigger action potentials in presynaptic cell.

3.11 Statistics

For behavior experiments, littermates animals were randomly assigned to the experimental group and were identified by unique identification number. Pairwise comparisons were calculated by un-paired or paired two-tailed t-tests and multiple group data comparisons were cal-

culated by one-way or two-way ANOVA with Bonferroni post-hoc test. Normality was assessed using Shapiro-Wilk tests. In the case where normality tests failed, Mann-Whitney or Wilcoxon rank-sum tests were used. Statistical analysis were performed using Graphpad Prism 6.0, Matlab or Python. Significance levels are indicated as follows: * $p<0.05$, ** $p<0.01$, *** $p<0.001$, **** $p<0.0001$.

Chapter 4

Results

4.1 Genetic identification of CeA$^{PKC\delta-}$ neurons

To determine the role of molecularly-defined CeA neuron populations in promoting food intake and reward-related behaviours, we focused on two populations of CeA neurons: somatostatin -expressing (CeA^{SOM}) and serotonin receptor 2A-expressing (CeA^{Htr2a}) neurons. Previously, it was reported that CeA^{SOM} and CeA^{Htr2a} neurons are chiefly PKCδ-[84,86]. To determine the overlap between the two populations, *Htr2a-cre* mice were crossed to a ROSALacZ reporter line. Subsequent immunostaining of brain sections from these mice to visualize the *Htr2a-cre* population (βgalactosidase) and SOM, revealed that although CeA^{SOM} and CeA^{Htr2a} neurons are expressed in an overlapping region, Htr2a was restricted to more medial parts of the CeL and throughout the CeM, while SOM was expressed throughout the CeL and to a lesser extent in the CeM than Htr2a (Figure 4.1a). In the CeL, approximately 50% of CeA^{Htr2a} neurons express SOM, which was lower than previously reported[86] (Figure 4.1a). Given the poor quality of the SOM staining and the lack of methods to visualize the expression of Htr2a+ neurons in *SOM-cre*;LacZ animals, the overlap of these two markers with respect to the CeA^{SOM} population was not possible to determine. Next, the overlap in expression of each marker with PKCδ

was determined by immunohistochemistry for PKCδ on brain sections derived from LacZ reporter mice. Similar to a prior report, a small degree of overlap between SOM and PKCδ[84] was found (Figure 4.1b, d), while <1% CeA^{Htr2a} neurons were found to express PKCδ, lower than was previously reported[86] (Figure 4.1b, d). Together these data demonstrate that CeA^{SOM} and CeA^{Htr2a} neurons constitute partially overlapping populations of primarily PKCδ- neurons.

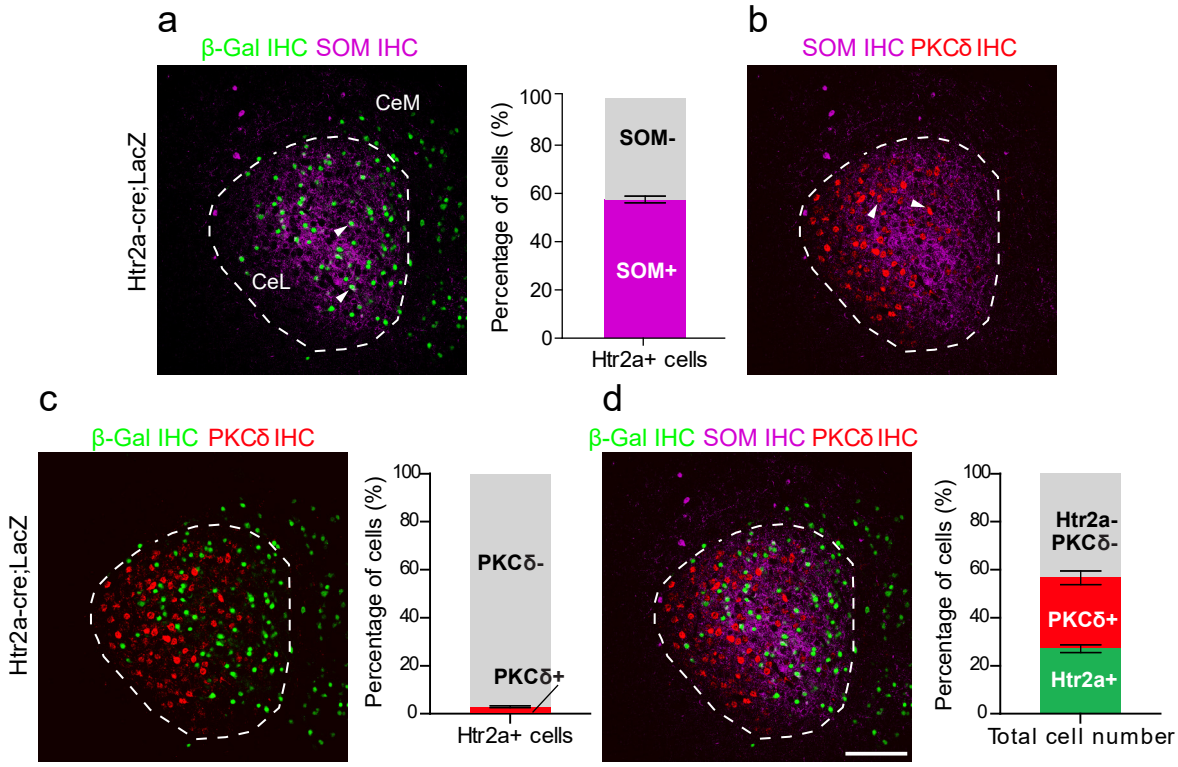

Figure 4.1: Expression pattern of CeA molecularly defined neuron populations. **a)** Expression in the CeA of Htr2a+ neurons marked by βgal and SOM+ neurons. Approximately 50% of CeA^{Htr2a} neurons also co-express SOM (n = 3 brain sections/3 mice). **b)** Expression in the CeA of SOM+ and PKCδ+ neurons (n = 3 brain sections/3 mice). **c)** Expression in the CeA of Htr2a+ neurons marked by βgal and PKCδ+ neurons. Very little overlap exists between the CeA^{Htr2a} and CeA^{PKCδ} populations (n = 3 brain sections/3 mice). **d)** Distribution of CeA neurons that express Htr2a, SOM and PKCδ+. The distinct populations expressing PKCδ or Htr2a each comprise approximately 25% of the total CeA neuron population (n = 3 brain sections/3 mice).

CeL, central lateral amygdala; CeM, central medial amygdala. Scale bar = 100μm. Bar plots indicate mean ±SEM.

4.2 CeA^{Htr2a} neurons are sufficient for food intake

4.2.1 Validation of chemogenetic tools

Given that CeA^{SOM} and CeA^{Htr2a} neurons constitute largely PKCδ- CeA neuron populations, I next asked whether they functionally oppose CeA$^{PKC\delta}$ neurons to promote food intake. I first used a chemogenetic approach in order to investigate the effect of artificial neuron activation over the long timescale afforded by this technique. Here, Cre-dependent AAVs expressing the activating DREADD hM3Dq-mCherry were stereotaxically injected bilaterally into the CeA of *Htr2a-cre* or *SOM-cre* expressing mice (Figure 4.2a). In both cases, expression of hM3Dq-mCherry was expressed throughout the CeA, mainly localised to the neural processes rather than cell bodies (*Htr2a-cre* as an example in Figure 4.2b). In acute brain slices from hM3Dq-mCherry expressing *Htr2a-cre* mice, application of the otherwise biologically inert DREADD ligand Clozapine-N-oxide (CNO) to the slice induced robust firing of the cell, which was suppressed when the CNO was washed off the slice (Figure 4.2c). I confirmed that *in vivo* activation of the DREADD by intraperitoneal injection (IP) (2mg/kg) injection of CNO resulted in robust expression of the neuronal activity marker cfos in DREADD-expressing *Htr2a-cre* mice but not in control animals that express only mCherry (Figure 4.2d,e).

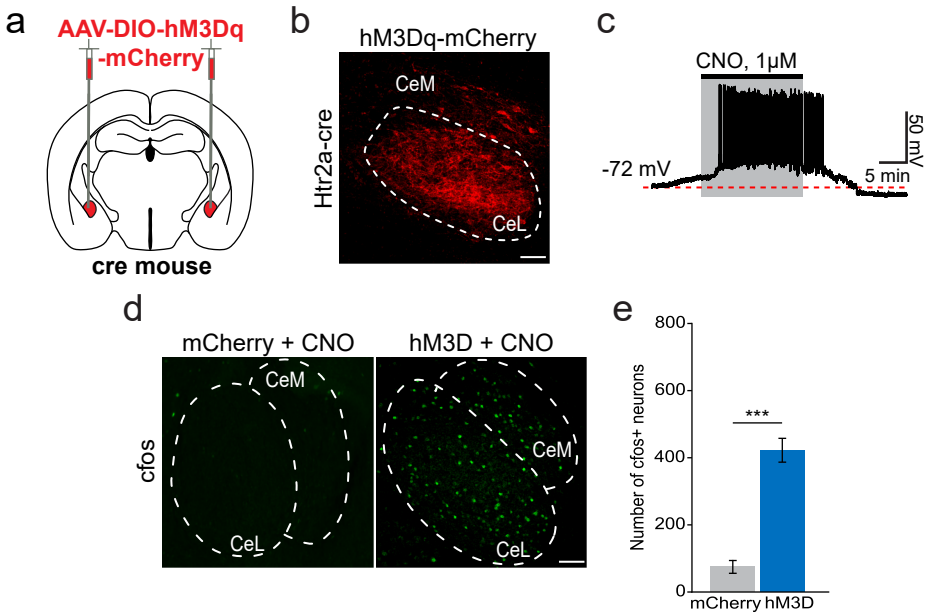

Figure 4.2: Validation of the activating DREADD hM3Dq. a) Scheme depicting transduction of cre-dependent AAV-hM3Dq-mCherry bilaterally into the CeA of *Htr2a-cre* mice by stereotaxic injection. **b)** Representative image of hM3Dq-mCherry expression in the CeA of an *Htr2a-cre* mouse. **c)** Whole-cell current clamp recording of a hM3Dq-mCherry expressing cell in an *ex vivo* brain slice. Firing of the cell was induced when 1 µM CNO was washed into the slice bath (shaded area) which shortly returned to baseline when the CNO was washed out. **d)** Representative images of the CeA from mice expressing mCherry in the CeA (Left) or hM3Dq-mCherry (Right) immunostained for cfos (the cfos channel only is shown) after IP injection of CNO (2 mg/kg). **e)** Quantification of the number of cfos positive neurons in the CeA after IP injection of CNO. Cfos express is strongly induced only in hM3Dq-mCherry expressing mice (n= 3 brain sections/3 mice).

CeL, central lateral amygdala; CeM, central medial amygdala. Scale bar = 100 µm. Bar plots indicate mean ±SEM. Two-tailed unpaired t-test. *** $p<0.001$.

4.2.2 Chemogenetic activation of CeA^{Htr2a} neurons promotes feeding in fed mice

To determine the effect of activating CeA^{Htr2a} and CeA^{SOM} neurons on food intake, I expressed hM3Dq-mCherry or mCherry in the CeA of cre-expressing mice (Figure 4.3a). The mice were then run through a free-feeding assay where they had free access to a pre-weighed food pellet for 40 minutes (Figure 4.3b). The mice received an IP injection of CNO or Saline 20 minutes prior to the start of the assay (Figure 4.3c). Each mouse underwent the experiment twice, with CNO and Saline delivered three days apart in a counterbalanced order. At the end of the food intake test period, the remaining food was weighed (Figure 4.3c). I first confirmed the previously published findings that activation of CeA$^{PKC\delta}$ neurons drastically reduces food intake in mice that have been fasted for 24 hours prior to the experiment (Figure 4.3d). I then investigated whether activation of the two populations of CeA$^{PKC\delta-}$ neurons have the opposite effect- that is to promote food intake. I assessed the effect of this manipulation in *ad lib* fed animals at the beginning of the light cycle when food intake is typically low. Using this approach, I found that DREADD-mediated activation of CeA^{SOM} neurons did not alter the amount of food consumed by CeA^{SOM}::hM3Dq CNO-treated animals when compared to control groups (Figure 4.3e).

Conversely, I found that acute activation of CeA^{Htr2a} neurons led to a significant increase in food consumed (Figure 4.4a, b). Subsequent analysis of video recorded feeding sessions where mice were treated with CNO revealed that this effect was due to an increase in the time that CeA^{Htr2a}::hM3Dq mice spent eating, as the total duration was increased compared to the controls (Figure 4.4c). The average duration of the bouts (Figure 4.4d) and number of bouts were not significantly increased (Figure 4.4e).

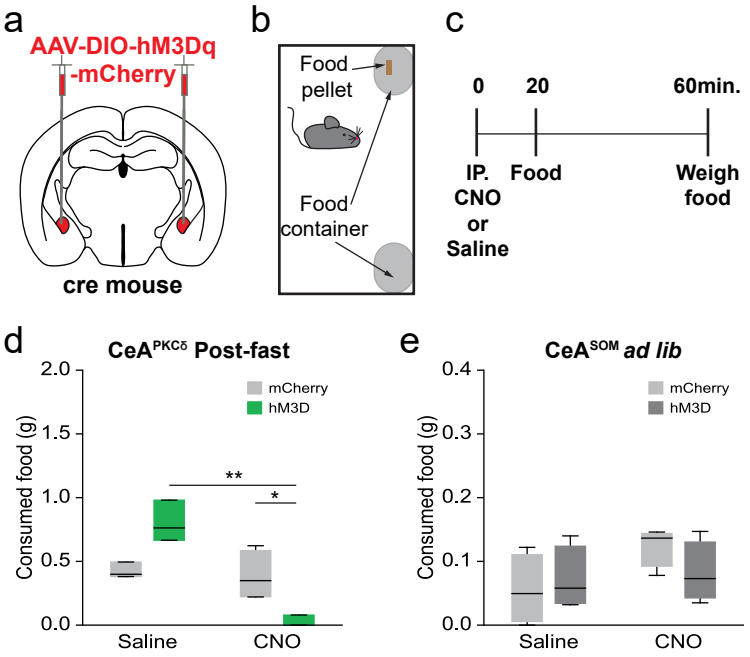

Figure 4.3: Chemogenetic activation of genetically-defined CeA neural subpopulations. **a)** Scheme depicting transduction of cre-dependent AAV-hM3Dq-mCherry bilaterally into the CeA of cre mice by stereotaxic injection. **b)** Scheme depicting behaviour setup. Mice were free to explore an arena in which two plastic food cups were located, with one containing a pre-weighed food pellet. **c)** Experimental timeline. Mice in (d) were food deprived for 24hrs prior to the experiment. Mice in (e) were satiated at the time of the experiment. **d)** Chemogenetic activation of $CeA^{PKC\delta}$ neurons by IP injection of CNO into $CeA^{PKC\delta}$::hM3Dq mice suppressed food consumption in food deprived mice compared to consumption when the same mice were injected with saline and compared to CNO-treated $CeA^{PKC\delta}$::mCherry mice. (n= 6 mCherry, n= 6 hM3Dq). **e)** Chemogenetic activation of CeA^{SOM} neurons by IP injection of CNO into CeA^{SOM}::hM3Dq mice did not affect food consumption in satiated mice (n= 6 mCherry, n= 8 hM3Dq).

Box–whisker plots indicate median, interquartile range and 5^{th}-95^{th} percentiles of the distribution. Two-way ANOVA with Bonerroni post-hoc test. * $p<0.05$,** $p<0.01$.

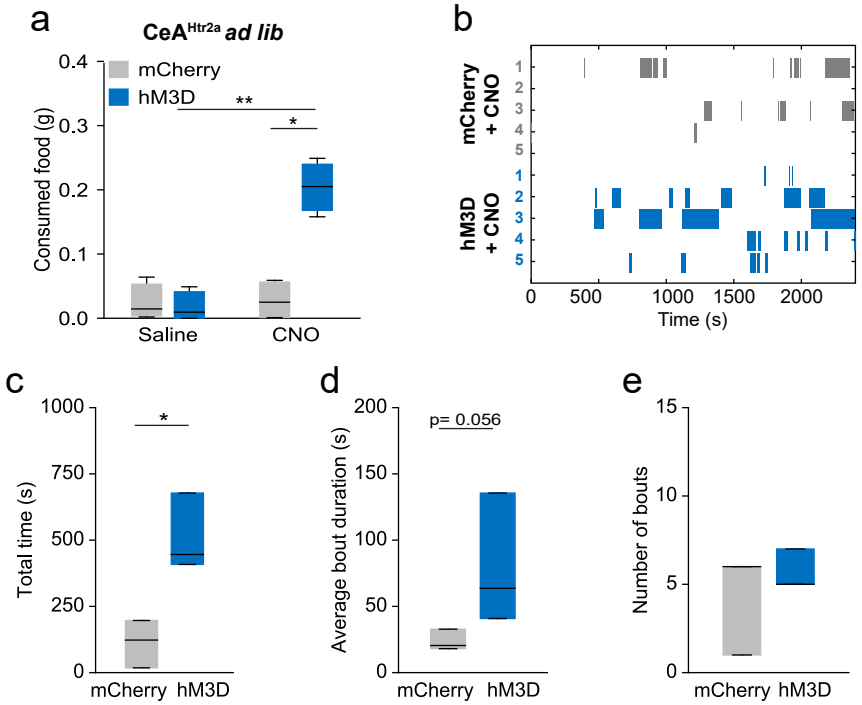

Figure 4.4: Chemogenetic activation of CeA^{Htr2a} neurons evokes food consumption. a) Chemogenetic activation of CeA^{Htr2a} neurons by IP injection of CNO into CeA^{Htr2a}::hM3Dq mice significantly increased food consumption in satiated mice compared to when the same mice were injected with saline and compared to CNO-treated CeA^{Htr2a}::mCherry mice (n= 6 mCherry, n= 6 hM3Dq). **b)** Ethogram depicting the feeding bouts of individual CeA^{Htr2a}::hM3Dq and CeA^{Htr2a}::mCherry CNO-treated mice throughout the 40min session. Each row is an individual animal. **c)** Chemogenetic activation of CeA^{Htr2a} neurons increased the total time the animals spent eating compared to CNO-treated CeA^{Htr2a}::mCherry controls (n= 5 mcherry, n= 5 hM3Dq). **d)** Chemogenetic activation of CeA^{Htr2a} neurons did not significantly increase the average duration of the feeding bouts (n= 5 mcherry, n= 5 hM3Dq). **e)** The number of feeding bouts of CeA^{Htr2a}::hM3Dq mice was not significantly different to CeA^{Htr2a}::mCherry controls (n= 5 mcherry, n= 5 hM3Dq).

Box–whisker plots indicate median, interquartile range and 5th-95th percentiles of the distribution. Two-way ANOVA with Bonerroni post-hoc test (Figure 4.4a). Two-way unpaired t-test (Figure 4.4c-e). * $p<0.05$,** $p<0.01$.

4.2.3 Activation of CeA$^{PKC\delta-}$ neurons rescues CeA$^{PKC\delta}$ neuron-mediated anorexia

I next determined whether there may be a functional interaction between CeA^{Htr2a} and CeA$^{PKC\delta}$ neurons by investigating whether activation of CeA^{Htr2a} neurons can overcome appetite suppression under conditions where CeA$^{PKC\delta}$ neurons are active. Thus, hM3Dq and mCherry-expressing *Htr2a-cre* or *SOM-cre* mice were fasted overnight and injected IP with different compounds that strongly suppress feeding in hungry mice (Figure 4.5a-c). Lithium chloride (LiCl) was used to mimic illness caused by toxic food ingestion[152] while lipopolysaccharide (LPS), a bacterial wall protein, was used to emulate bacterial infection[153]. I found that DREADD-mediated activation of CeA^{Htr2a} neurons blunted the anorexic effect of both compounds (Figure 4.5d). Conversely, activation of CeA^{SOM} neurons did not evoke such an effect, with hM3Dq-expressing animals treated with CNO eating comparable quantities of food to mCherry-expressing controls (Figure 4.5e). I also tested whether activation of these neuronal populations could rescue the feeding suppressant effect of bitter foods, previously shown to be mediated by CeA$^{PKC\delta}$ neurons[66]. To test this, normal food pellets were soaked in a concentrated quinine solution and dried before testing. I found that hungry mice ate more of the bitter food when their CeA^{SOM} or CeA^{Htr2a} neurons were activated than control mCherry-expressing animals (Figure 4.5f,g). These mice were still sensitive to bitter tastes, as quinine solution was still aversive compared to water, tested in a two-bottle choice assay (Figure 4.5h,i). Together these data show a dissociation between CeA^{Htr2a} and CeA^{SOM} neurons as to the conditions under which they evoke food intake, with CeA^{Htr2a} neurons more potently promoting consumption under *ad lib* fed and anorexigenic conditions.

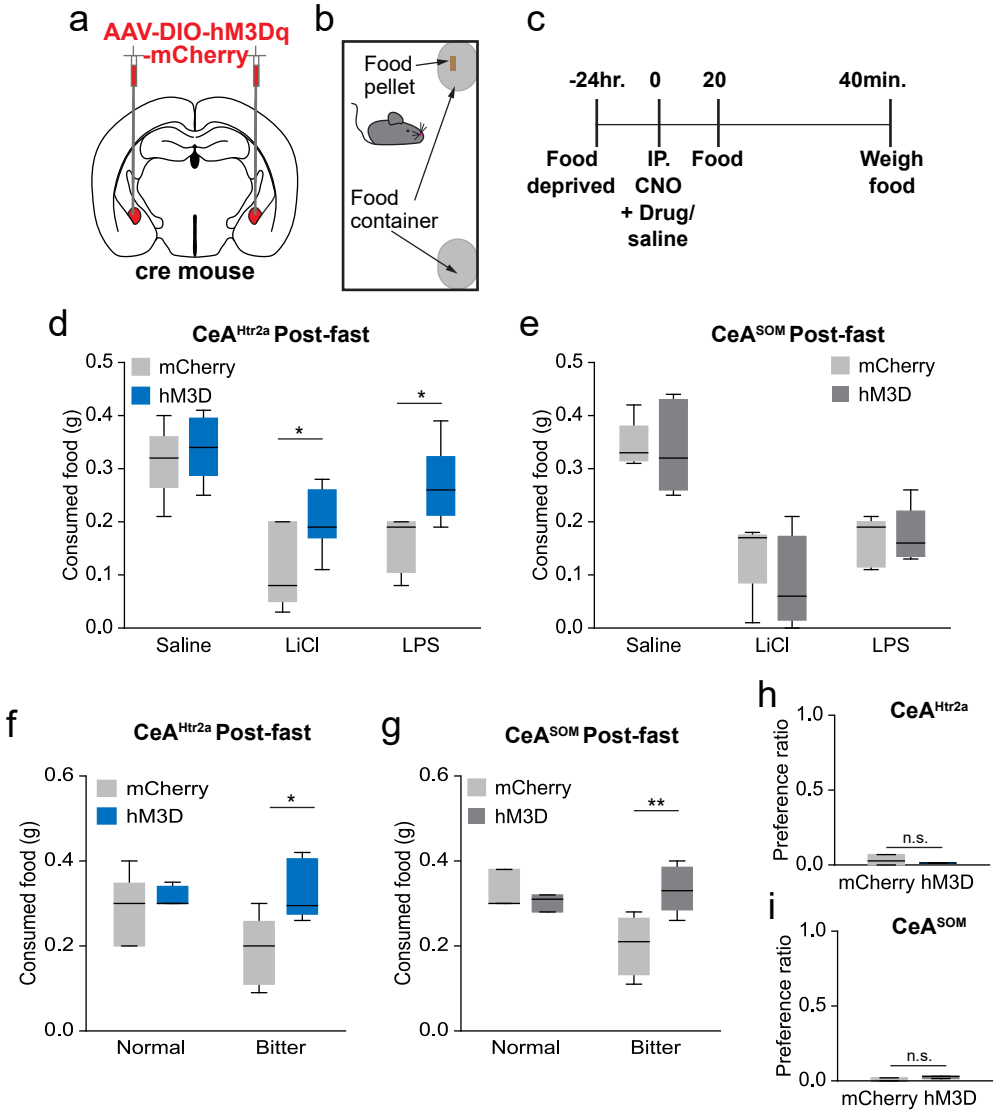

Figure 4.5: Chemogenetic activation of CeA^{Htr2a} and CeA^{SOM} neurons modulates the effects of anorectic drugs and food. a) Scheme depicting transduction of cre-dependent AAV-hM3dq-mCherry bilaterally into the CeA of *Htr2a-cre* mice by stereotaxic injection. **b)** Scheme depicting behaviour setup. Mice were free to explore an arena in which two plastic food cups were located, with one containing a pre-weighed food pellet. **c)** Experimental timeline. Mice were food deprived 24hrs prior to the experiment and tested during the light period in the light cycle. **d)** Chemogenetic activation of CeA^{Htr2a} neurons partially reduced the appetite-suppressant effect of LiCl and LPS (n= 7 mCherry, n= 8 hM3Dq (Saline); n= 9 mCherry, n= 11 hM3Dq (LiCl); n= 8 mCherry, n = 8 hM3Dq (LPS)). **e)** Chemogenetic activation of CeA^{SOM} neurons did not modulate the appetite-suppressant effect of LiCl and LPS. (n= 7 mCherry, n= 7 hM3Dq (Saline); n= 7 mCherry, n= 8 hM3Dq (LiCl); n= 7 mCherry, n = 7 hM3Dq (LPS)). **f)** Chemogenetic activation of CeA^{Htr2a} neurons rescued the appetite-suppressant effect of quinine-laced bitter food (n= 8 mCherry, n= 9 hM3Dq (Normal); n= 10 mCherry, n= 8 hM3Dq (Bitter). **g)** Chemogenetic activation of CeA^{SOM} neurons rescued the appetite-suppressant effect of quinine-laced bitter food (n= 5 mCherry, n= 5 hM3Dq (Normal); n= 6 mCherry, n= 7 hM3Dq (Bitter). **h)** CeA^{Htr2a}::hM3Dq mice avoided licking a spout containing 1mM quinine solution comparably to controls (n= 5 mCherry, n= 5 hM3Dq). **i)** CeA^{SOM}::hM3Dq mice avoided licking a spout containing 1mM quinine solution comparably to controls (n= 3 mCherry, n= 3 hM3Dq).

LiCl; Lithium chloride, LPS; lipopolysaccharide. Box–whisker plots indicate median, interquartile range and 5th-95th percentiles of the distribution. Two-way ANOVA with Bonerroni post-hoc test (Figure 4.5d-g). Two-way unpaired t-test (Figure 4.5h,i). * $p<0.05$,** $p<0.01$.

4.2.4 Chemogenetic activation of CeA^{Htr2a} neurons increases consumption based on edibility

Previous work has demonstrated that neural modulators of food consumption that reside in the lateral hypothalamus (LH) promote food consumption but also consummatory behavior directed at proximal stimuli irrespective of edibility or biological relevance[154]. I thus investigated whether, when their CeA^{Htr2a} neurons are active, mice would choose to ingest food items in preference to engaging with a non-food item. In a modified version of the free-feeding assay, CeA^{Htr2a}::hM3Dq mice and mCherry controls (Figure 4.6a) were allowed to explore an arena containing a pre-weighed food pellet and a piece of clay of similar size and color to the food pellet (Figure 4.6b). Prior to the experiment, mice were injected IP with CNO. After 30 minutes, the remaining food and clay pellets were weighed (Figure 4.6c). This revealed, that again, CeA^{Htr2a}::hM3D mice consumed more of the food pellet than controls and compared to their consumption of the clay pellet (Figure 4.6d). CeA^{Htr2a}::hM3D mice also spent more time engaging with the food pellet than the clay. Interaction with the food pellet was also increased compared to the CeA^{Htr2a}::mCherry controls (Figure 4.6e), while the average length of pellet bouts was longer than that of clay bouts (Figure 4.6f). The number of bouts of any type were unchanged (Figure 4.6g).

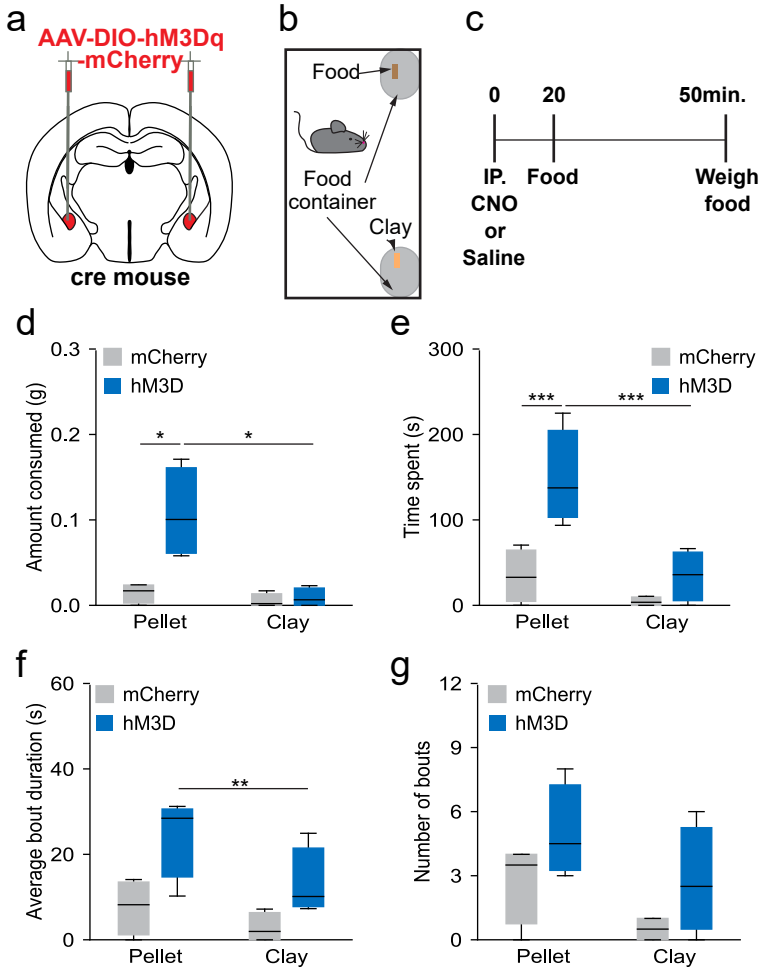

Figure 4.6: Chemogenetic activation of CeA^{Htr2a} neurons directs consumption towards edible items. **a)** Scheme depicting transduction of cre-dependent AAV-hM3Dq-mCherry bilaterally into the CeA of *Htr2a-cre* mice by stereotaxic injection. **b)** Scheme depicting behaviour setup. Mice were free to explore an arena in which two plastic food cups were located, with one containing a pre-weighed food pellet, the other a pre-weighed clay pellet. **c)** Experimental timeline. Mice had *ad libitum* access to food prior to the experiment and were tested during the light period in the light cycle. **d)** Chemogenetic activation of CeA^{Htr2a} neurons increased consumption of the food pellet compared to controls and compared to consumption of the clay pellet (n= 6 mCherry, n= 6 hM3Dq). **e)** Chemogenetic activation of CeA^{Htr2a} neurons increased the time spent eating the food pellet compared to controls and compared the time spent consuming the clay pellet (n= 6 mCherry, n= 6 hM3D). **f)** The average bout length of food-directed eating bouts was increased in CeA^{Htr2a}::hM3Dq mice compared to clay-directed eating bouts (n= 6 mCherry, n= 6 hM3Dq). **g)** The number of feeding bouts of both food types was not significantly different for either of the animal groups (n= 6 mCherry, n= 6 hM3Dq).

Box–whisker plots indicate median, interquartile range and 5th-95th percentiles of the distribution. Two-way ANOVA with Bonerroni post-hoc test. * $p<0.05$,** $p<0.01$,*** $p<0.001$.

4.2.5 Chemogenetic activation of CeA^{Htr2a} neurons does not increase motivation to work for food

Since activation of CeA^{Htr2a} neurons increased food consumption, I investigated whether the same manipulation would increase the effort made to obtain food. CeA^{Htr2a}::hM3D mice and mCherry controls were trained to nose-poke at a two-port apparatus for single 20mg food pellets (Figure 4.7a, b). Nose-pokes in the designated 'active' port lead to delivery of a food pellet in addition to reinforcing light and tone cues (see Materials and Methods). 'Inactive' nose-pokes did not lead to pellet delivery, but a different light and cue reinforcer was triggered (see Materials and Methods) (Figure 4.7b). Mice food restricted to 85-90% of their free-feeding body weight were trained on a fixed ratio 1 schedule (FR1) (one active poke delivers one pellet), followed by a FR5 (five active pokes are required to obtain one pellet) and finally a PR2 schedule, where the poke requirement for a single pellet increased by an additional two pellets (see Materials and Methods) (Figure 4.7c). The mice were tested for their motivation to obtain pellets in the *ad lib* fed state in two consecutive sessions after IP injection of CNO or saline (counterbalanced) (Figure 4.7d). CeA^{Htr2a}::hM3D mice did not increase their number of active pokes (Figure 4.7e) nor their breakpoint (number of consecutive nose-pokes made to obtain a single pellet) (Figure 4.7f) when treated with CNO prior to the session compared to when they received saline. This suggests that although activation of CeA^{Htr2a} neurons increases food consumption it does not increase the motivation to work for food.

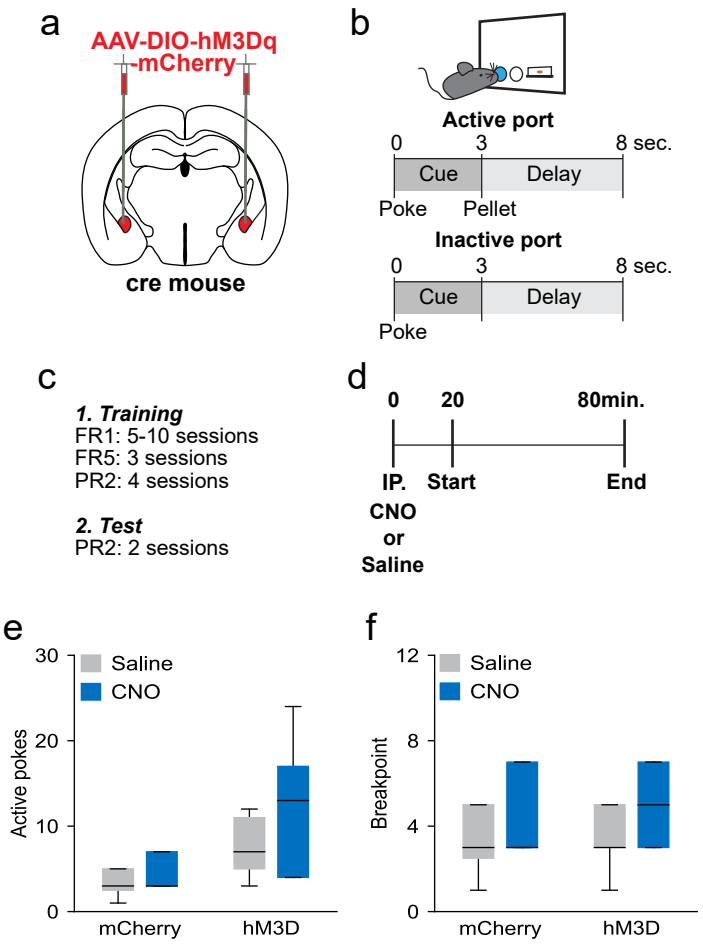

Figure 4.7: Chemogenetic activation of CeA^{Htr2a} neurons does not increase food seeking. a) Scheme depicting transduction of cre-dependent AAV-hM3Dq-mCherry bilaterally into the CeA of *Htr2a-cre* mice by stereotaxic injection. **b)** Scheme depicting behaviour setup. Mice were trained to nosepoke at a two-poke apparatus. The active poke (indicated in blue) triggered release of a 20 mg food pellet. Both active and inactive pokes were coupled to reinforcer light and tone cues. **c)** Outline of the training regime. **d)** Experimental timeline of the test sessions. Mice had *ad libitum* access to food prior to the experiment and were tested during the light period in the light cycle. **e)** There was no difference in the number of active pokes made by CeA^{Htr2a}::hM3Dq mice comparing the different treatment sessions. **f)** There was no difference in the breakpoint attained by CeA^{Htr2a}::hM3Dq mice comparing the different treatment sessions.

Box–whisker plots indicate median, interquartile range and 5th-95th percentiles of the distribution. Two-tailed paired t-test.

4.3 Control of feeding and related behaviours by CeA^{Htr2a} neurons.

4.3.1 Validation of optogenetic tools

Given the observed effects of artificial activation of CeA^{Htr2a} neurons, I further investigated this finding using optogenetic methods. I used the light-gated opsin channelrhodopsin (ChR2) to control neuron activity in order to perform more temporally-precise manipulations and investigate the threshold of activation necessary for the induction of feeding behaviour. To achieve this, I stereotaxically injected cre-dependent AAV-ChR2-eYFP into the CeA of *Htr2a-cre* mice

(Figure 4.8a), and implanted optical fibres bilaterally above the CeA to deliver light into the brain. Expression of the ChR2-eYFP was localized to neural processes in both the CeL and CeM (Figure 4.8b). In acute brain slices, ChR2 activation by 473nm light was found to induce high fidelity action potentials up to 20Hz frequency (Figure 4.8c). I verified the functionality of ChR2 *in vivo* by coupling the implanted fibres to optical fibre patch cables connected to a 473nm laser. ChR2 and eYFP-expressing animals were subjected to a 20 minute session of optical stimulation of CeA^{Htr2a} neurons (20Hz, ∼10mW 473nm) after which the brains were immunostained for the neural activity marker cfos. Cfos expression was strongly induced in the CeA of CeA^{Htr2a}::ChR2 mice but not in eYFP-expressing controls (Figure 4.8d,e).

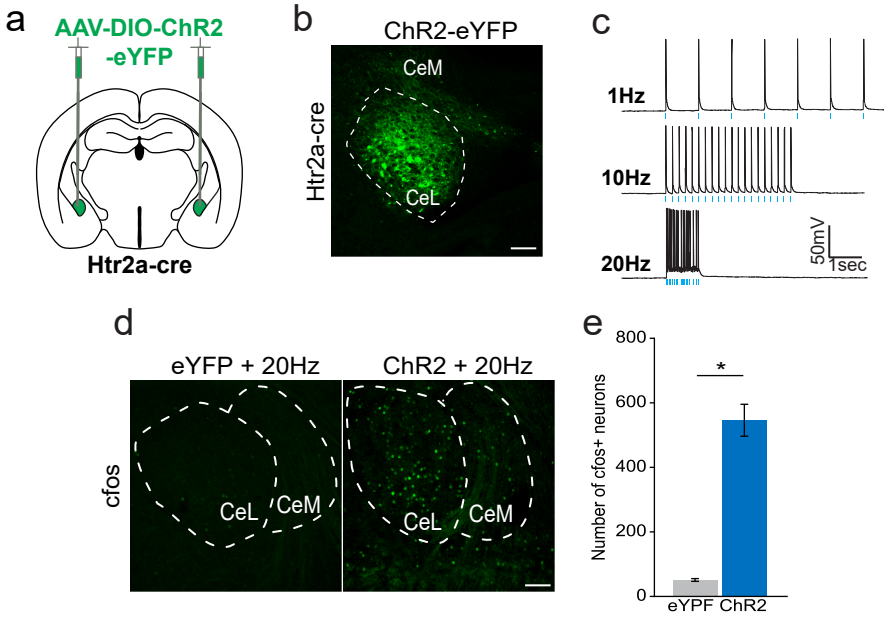

Figure 4.8: Validation of ChR2 for activation of CeA^{Htr2a} neurons. a) Scheme depicting expression of cre-dependent AAV-ChR2-eYFP bilaterally in the CeA of *Htr2a-cre* mice. **b)** Representative image of ChR2-eYFP expression in the CeA of an *Htr2a-cre* mouse. **c)** Representative photocurrents from a CeA^{Htr2a}::ChR2 cell recorded from an *ex vivo* brain slice. Blue bars represent delivery of 470 nm LED light pulses at the indicated photostimulation frequencies. **d)** Representative images of the CeA from mice expressing eYFP in the CeA (Left) or ChR2-eYFP (Right) immunostained for cfos (the cfos channel only is shown) after 20 mins 20Hz intracranial 473 nm light pulses. **e)** Quantification of the number of cfos positive neurons in the CeA after 20 mins 20Hz intracranial 473 nm light pulses. Cfos express is strongly induced only in ChR2-eYFP expressing mice (n= 3 brain sections/3 mice).

CeL, central lateral amygdala; CeM, central medial amygdala. Scale bar = 100 µm. Bar plots indicate mean ±SEM. Two-tailed unpaired t-test. * $p<0.05$.

4.3.2 Optogenetic activation of CeA^{Htr2a} neurons promotes feeding in fed mice

To confirm the finding that activation of CeA^{Htr2a} neurons evokes feeding behavior I allowed CeA^{Htr2a}::ChR2 and eYFP control mice to explore a behavior arena that contained a pre-weighed food pellet (Figure 4.9a,b, Figure Aa). The animals were exposed to a 20 minute epoch of photostimulation followed by a 20 minute period of no stimulation (Figure 4.9c). Each animal was subjected to three sessions where they received 5Hz, 10Hz or 20Hz photostimulation (473nm, $\sim$10mW). 20Hz photostimulation was found to elicit increased food consumption by CeA^{Htr2a}::ChR2 mice compared to eYFP controls (Figure 4.9d,e). This elevated food consumption was specific to the activation of CeA^{Htr2a} neurons as it did not continue into the subsequent 'laser OFF' epoch (Figure 4.9d). Photostimulation at 10Hz also elicited increased food intake above controls but this was not significantly increased above consumption during the 'laser OFF' period (Figure 4.9d).

Post-hoc video analysis of the microstructure of feeding behavior during 20Hz stimulation revealed that this phenotype was due to an increase in the total time spent feeding and a longer average bout length but not an increase in the number of bouts (Figure 4.10a-d). Additionally, the latency to the first eating bout after photostimulation onset was similar for both groups (Figure 4.10e).

4.3.3 Optogenetic activation promotes feeding-related motor behaviours

During the photostimulation experiments, I noted that the CeA^{Htr2a}::ChR2 mice would often engage in feeding-related motor sequences that were not directed at the food pellet. These included licking of surrounding structures such as the walls and floor of the arena, gnawing of the food container and motor sequences where the mouse would appear to be holding and eating a food pellet, in the absence of a pellet. The propensity of mice to engage in this behavior increased with the frequency of photostimulation (Figure 4.10f) and occurred in the presence

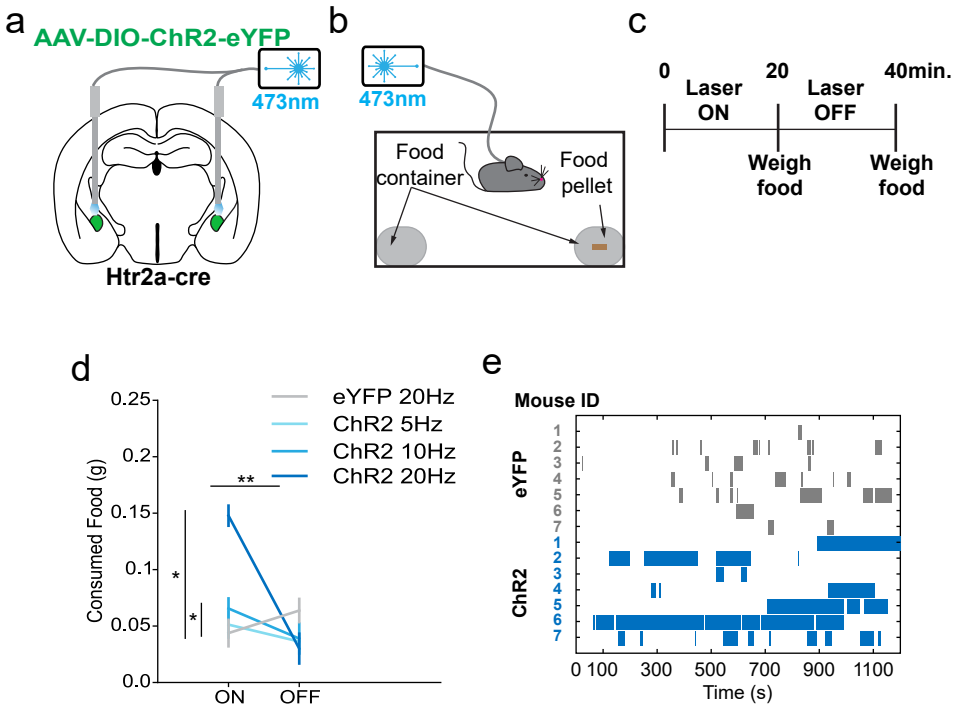

Figure 4.9: Optogenetic activation of CeA^{Htr2a} promotes food consumption. a) Scheme depicting expression of cre-dependent AAV-ChR2-eYFP bilaterally in the CeA of *Htr2a-cre* mice and bilateral placement of optic fibres. **b)** Scheme depicting behaviour setup. Optic fibre-tethered mice were free to explore an arena in which two plastic food cups were located, with one containing a pre-weighed food pellet. **c)** Experimental timeline. Mice were tested during the light period in the light cycle. **d)** Optogenetic activation of CeA^{Htr2a} neurons at 20Hz increased food consumption compared to the laser OFF epoch and eYFP-expressing control mice. Activation of CeA^{Htr2a} neurons at 10Hz increased consumption during the laser ON epoch compared to eYFP-expressing controls (n= 8 eYFP, n = 9 ChR2). **e)** Ethogram depicting the feeding bouts of individual CeA^{Htr2a}::ChR2 and CeA^{Htr2a}::eYFP mice during the 20min 20Hz laser ON epoch. Each row is an individual animal.

Line plotes indicate mean ±SEM. Two-tailed unpaired t-test or two-tailed paired t-test. * $p<0.05$,** $p<0.01$.

and absence of a food pellet.

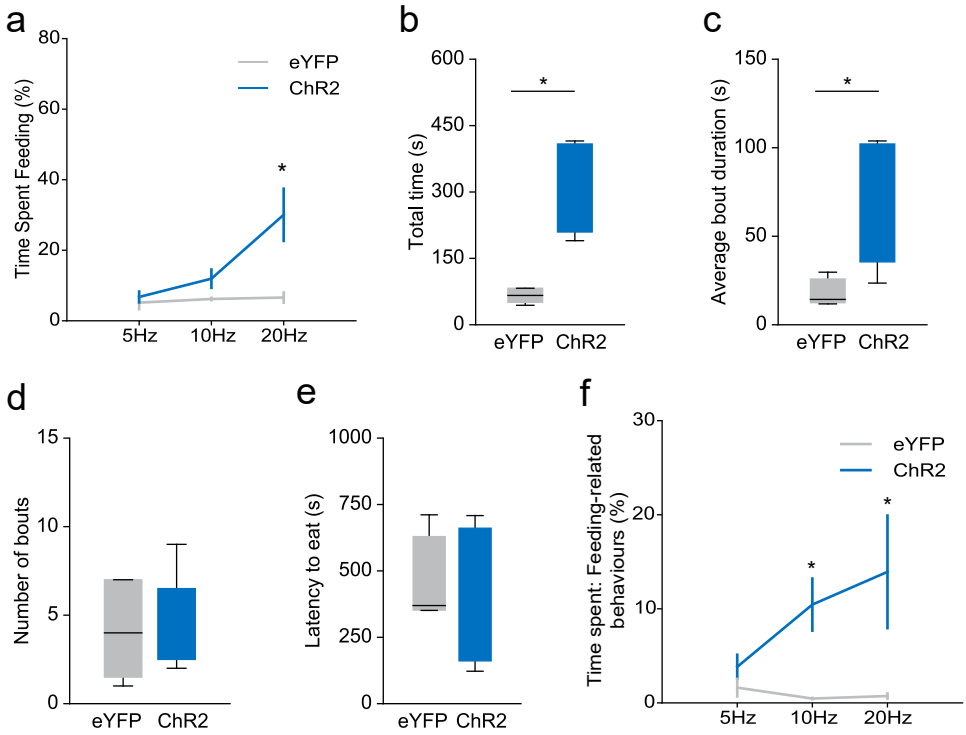

Figure 4.10: Optogenetic activation of CeA^{Htr2a} neurons increases feeding and elicits appetitive motor behavours. **a)** CeA^{Htr2a}::ChR2 animals spent a greater percentage of the laser ON epoch consuming food compared to CeA^{Htr2a}::eYFP control mice (n= 8 eYFP, n = 9 ChR2). **b)** Optogenetic activation of CeA^{Htr2a} neurons at 20Hz increased the total time the animals spent eating compared to CeA^{Htr2a}::eYFP controls (n= 6 eYFP, n = 5 ChR2). **c)** Optogenetic activation of CeA^{Htr2a} neurons increased the average duration of the feeding bouts (n= 6 eYFP, n = 5 ChR2). **d)** The number of feeding bouts of CeA^{Htr2a}::ChR2 mice was not significantly different to CeA^{Htr2a}::eYFP controls (n= 6 eYFP, n = 5 ChR2). **e)** Optogenetic activation of CeA^{Htr2a} neurons did not affect the latency of animals to eat after the laser was triggered (n= 6 eYFP, n = 5 ChR2). **f)** CeA^{Htr2a}::ChR2 mice engage in non-food directed appetitive motor behaviors during 10Hz and 20Hz laser ON epochs (n= 7 eYFP, n = 7 ChR2).

Box–whisker plots indicate median, interquartile range and 5th-95th percentiles of the distribution. Line plots indicate mean ±SEM. Two-tailed unpaired t-test (Figure 4.10a-e). Two-tailed unpaired t-test or Mann Whitney test (Figure 4.10f). * $p<0.05$.

4.4 CeA^{Htr2a} neurons are not necessary for long-term body weight homeostasis but for feeding after a fast

4.4.1 Virus-mediated ablation of CeA^{Htr2a} neurons does not affect long term body weight or food intake

I next determined the consequences of removing CeA^{Htr2a} neurons from the circuit on food intake. I reasoned that any effects on body weight or food consumption after ablation of these neurons would highlight their necessity for homeostatic control of feeding. A cre-dependent AAV carrying the A-subunit of the diphtheria toxin (dtA) was delivered into the CeA of *Htr2a-cre;tdTomato* mice (Figure 4.11a). After a month of recovery, the brains were examined for cell loss in the CeA. The number of tdTomato neurons in the CeA of dtA-expressing mice was reduced by approximately 70% compared to controls (Figure 4.11b,c) while the number of adjacent CeA$^{PKC\delta}$ neurons was not affected (Figure 4.11d,e). After surgery, the daily food intake and body weight of the animals was monitored while they were maintained on a regular chow diet. I found that over a 25-day period after surgery, the daily food intake and body weight was comparable to eYFP-expressing control mice (Figure 4.12a-c). Together these data suggest that CeA^{Htr2a} neurons are not required for long-term maintenance of body weight.

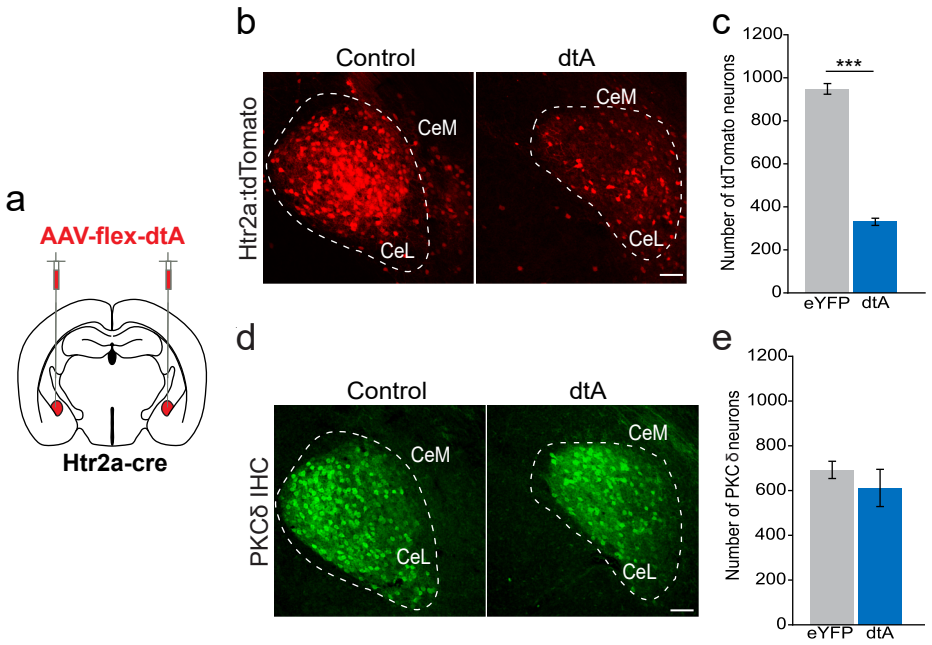

Figure 4.11: Virus-mediated ablation of CeA^{Htr2a} neurons. **a)** Scheme depicting transduction of cre-dependent AAV-dtA bilaterally into the CeA of *Htr2a-cre;tdTomato* mice by stereotaxic injection. **b)** Representative image of tdTomato expression in the CeA of an *Htr2a-cre;tdTomato* mouse expressing eYFP (left) or dtA (right) in the CeA (tdTomato channel only is shown). **c)** Quantification of the number of tdTomato neurons in CeA^{Htr2a}::eYFP and dtA mice. The number of tdTomato CeA neurons was significantly reduced in CeA^{Htr2a}::dtA mice (n= 3 brain sections from 3 mice). **d)** Representative image of PKCδ expression in the CeA of an *Htr2a-cre;tdTomato* mouse expressing eYFP (left) or dtA (right) in the CeA (PKCδ channel only is shown). **e)** Quantification of the number of PKCδ neurons in CeA^{Htr2a}::eYFP and dtA mice. The number of CeA^{PKCδ} neurons was unchanged in CeA^{Htr2a}::dtA mice (n= 3 brain sections from 3 mice).

CeL, central lateral amygdala; CeM, central medial amygdala. Scale bar = 100 µm. Bar plots indicate mean ±SEM. Two-tailed unpaired t-test. *** $p<0.001$.

4.4.2 Virus-mediated ablation of CeA^{Htr2a} neurons reduces short term feeding

I next examined the effect of CeA^{Htr2a} neuron ablation on short term feeding when mice were motivated to eat. First, I food deprived the mice overnight and measured food intake when the mice were hungry and therefore in a highly motivated state (Figure 4.12d,e). This revealed that CeA^{Htr2a}::dtA mice ate less than controls in a short refeeding period even though in the hungry state they should be highly motivated to do so (Figure 4.12f).

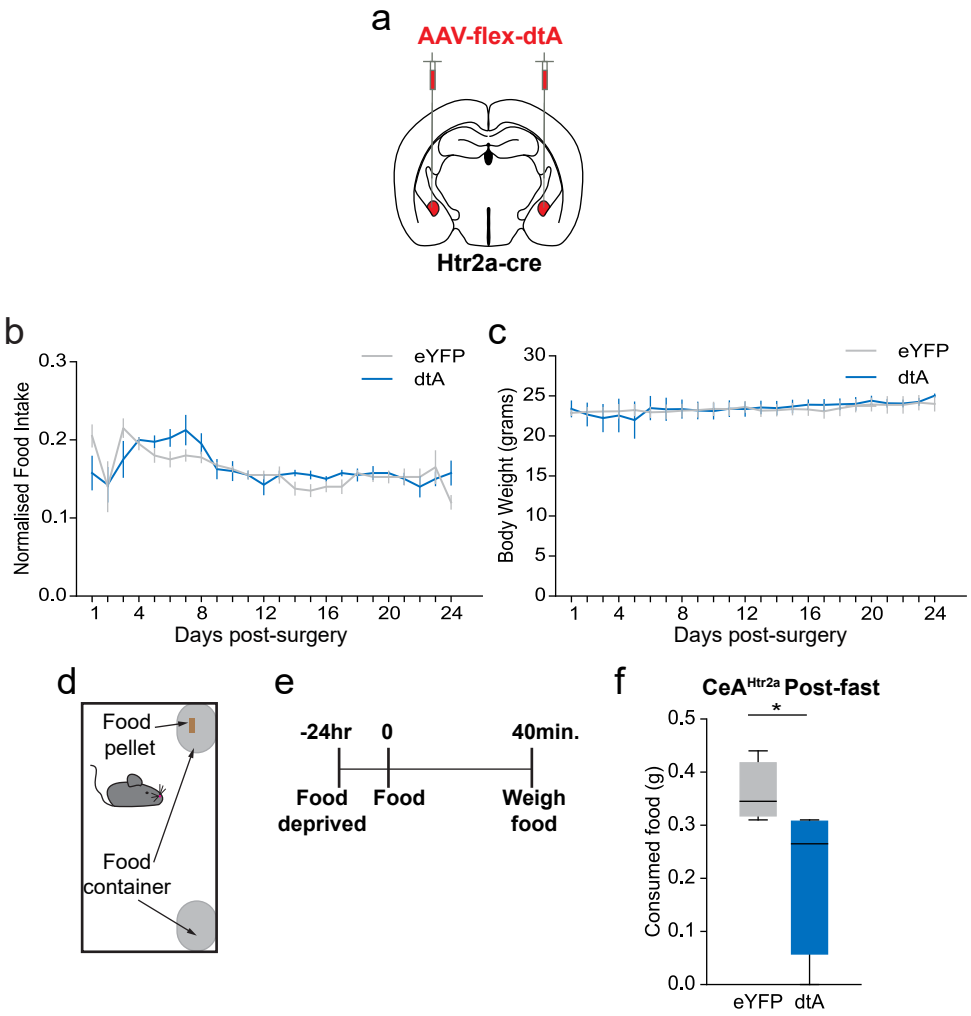

Figure 4.12: Virus-mediated ablation of CeA^{Htr2a} neurons reduces food consumption in the hungry but not *ad lib* fed state. **a)** Scheme depicting transduction of cre-dependent AAV-dtA bilaterally into the CeA of *Htr2a-cre;tdTomato* mice by stereotaxic injection. **b)** Ablation of CeA^{Htr2a} neurons did not affect food intake for 25 days after surgery (n= 4 eYFP, n = 4 dtA). **c)** Ablation of CeA^{Htr2a} neurons did not affect body weight for 25 days after surgery (n= 4 eYFP, n = 4 dtA). **d)** Scheme depicting behaviour setup. Mice were free to explore an arena in which two plastic food cups were located, with one containing a pre-weighed food pellet. **e)** Experimental timeline for refeeding assay. Mice were food deprived 24hrs prior to the experiment and tested during the light period in the light cycle. **f)** CeA^{Htr2a}::dtA mice consumed significantly less food than CeA^{Htr2a}::eYFP control mice during the 40min refeeding period after an overnight fast (n = 7 eYFP, n= 7 dtA).

Box–whisker plots indicate median, interquartile range and 5th-95th percentiles of the distribution. Line plots indicate mean ±SEM. Two-way ANOVA with Bonerroni post-hoc test (Figure 4.12b,c). Two-tailed unpaired t-test (Figure 4.12f). * $p<0.05$.

4.4.3 Optogenetic silencing of CeA^{Htr2a} neurons reduces food intake in the hungry state

I confirmed my finding that ablation of CeA^{Htr2a} neurons are necessary for post-fast refeeding by using the optogenetic silencer halorhodopsin to acutely silence CeA^{Htr2a} neurons. I injected cre-dependent AAV-NpHR-mCherry into the CeA of *Htr2a-cre* mice and bilaterally implanted optical fibres above the CeA (Figure 4.13a,b, Figure Ab). To ensure efficient silencing, I used constant 561nm laser light to silence the neurons, since CeA$^{PKC\delta-}$ neurons have been reported to exhibit rebound firing after silencing[67]. The animals were fasted overnight and allowed to explore the arena that contained a pre-weighed food pellet (Figure 4.13c). I exposed the animals to 10 minutes photoinhibition to minimize local tissue heating created by focal illumination. This was followed by a 10 minute of 'Light OFF' epoch. The remaining food was weighed at the end of each epoch (Figure 4.13d). The amount of food eaten by CeA^{Htr2a}::NpHR mice was significantly reduced during the photoinhibition period but was comparable to control CeA^{Htr2a}::mCherry mice in the subsequent 'Light OFF' epoch (Figure 4.13e,f). This corroborates my findings that CeA^{Htr2a} neurons are necessary for food consumption during a highly motivated, hungry state. Further analysis of the feeding bouts revealed that CeA^{Htr2a}::NpHR mice spent more time eating (Figure 4.13g) while the average bout duration, number of bouts and latency to eat were not significantly affected compared to CeA^{Htr2a}::mCherry controls (Figure 4.13h-j).

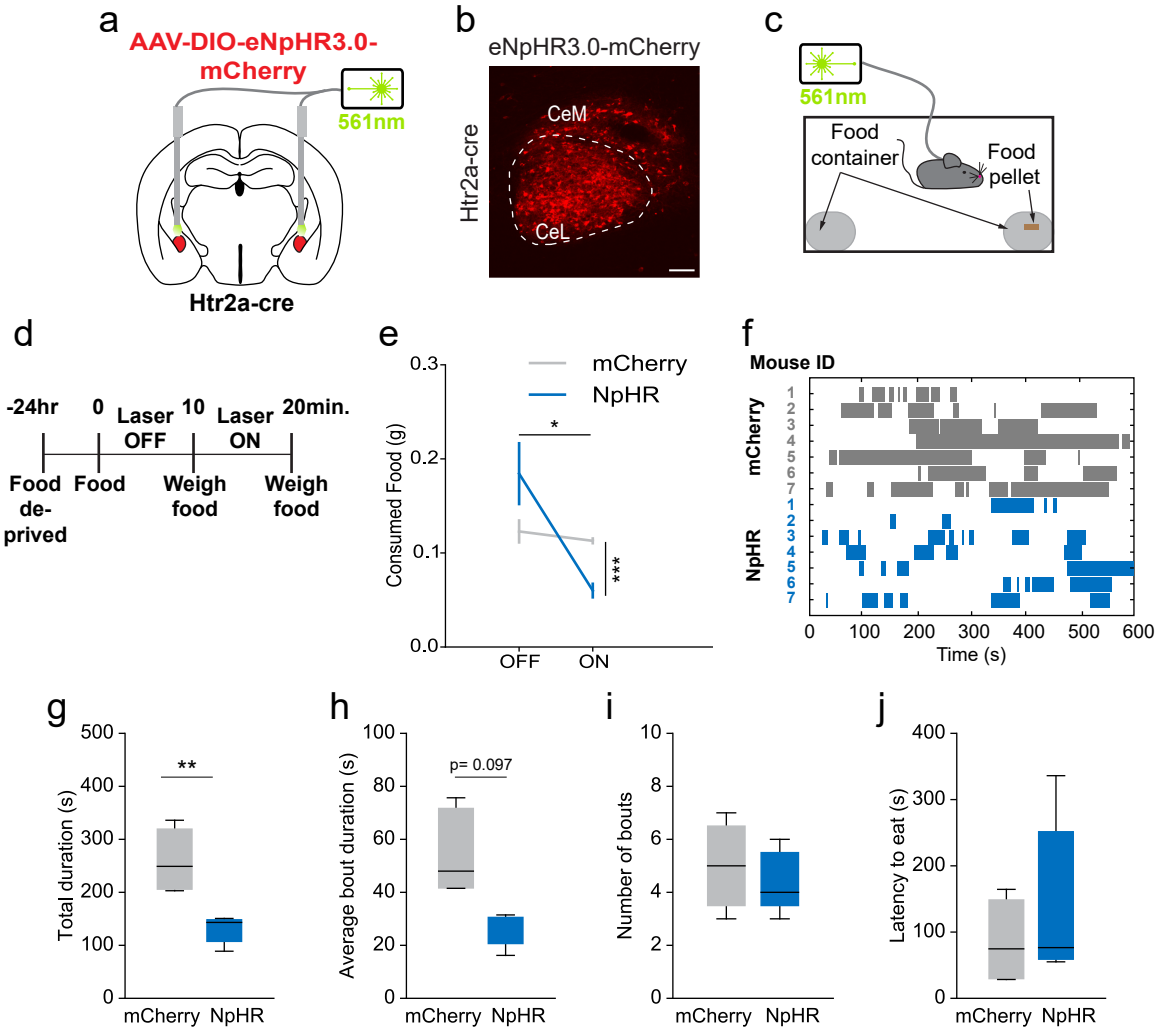

Figure 4.13: Optogenetic silencing of CeA^{Htr2a} neurons reduces food consumption. a) Scheme depicting expression of cre-dependent AAV-NpHR-mCherry bilaterally in the CeA of *Htr2a-cre* mice and bilateral placement of optic fibres. **b)** Representative image of NpHR-mCherry expression in the CeA of an *Htr2a-cre* mouse. **c)** Scheme depicting behaviour setup. Optic fibre-tethered mice were free to explore an arena in which two plastic food cups were located, with one containing a pre-weighed food pellet. **d)** Experimental timeline. Mice were food deprived 24hrs prior to the experiment and tested during the light period in the light cycle. **e)** Optogenetic silencing of CeA^{Htr2a} neurons reduced food consumption compared to the laser OFF epoch and eYFP-expressing control mice. **f)** Ethogram depicting the feeding bouts of individual CeA^{Htr2a}::NpHR and CeA^{Htr2a}::mCherry mice during the 10min laser ON epoch. Each row is an individual animal. **g)** Optogenetic silencing of CeA^{Htr2a} neurons decreased the total time the animals spent eating compared to CeA^{Htr2a}::mCherry controls (n= 7 mCherry, n = 7 NpHR). **h)** Optogenetic silencing of CeA^{Htr2a} neurons moderately reduced the average duration of the feeding bouts (n= 7 mCherry, n = 7 NpHR). **i)** The number of feeding bouts of CeA^{Htr2a}::NpHR mice was not significantly different to CeA^{Htr2a}::mCherry controls (n= 7 mCherry, n = 7 NpHR). **j)** Optogenetic silencing of CeA^{Htr2a} neurons did not affect the latency of animals to eat after the laser was triggered (n= 7 mCherry, n = 7 NpHR).

CeL, central lateral amygdala; CeM, central medial amygdala. Scale bar = 100 µm. Box–whisker plots indicate median, interquartile range and 5th-95th percentiles of the distribution. Line plots indicate mean ±SEM. Two-tailed unpaired t-test or two-tailed paired t-test (Figure 4.13e). Two-tailed unpaired t-test (Figure 4.13g-j). * $p<0.05$, ** $p<0.01$, *** $p<0.001$.

4.5 CeA^{Htr2a} neurons do not gate anxiety-like behaviour

Given that the CeA has been most notably implicated in fear and anxiety behavior, I assessed whether activation or ablation of the neurons would lead to anxiety-like phenotypes in a common paradigm used to access such behaviours (open field test) (Figure 4.14a,b). If so, this could suggest an interaction between anxiety-related behaviours and the effects on feeding that I observed. However, I found that in CNO-treated CeA^{Htr2a}::hM3Dq mice, mice displayed similar anxiety-like behavior to controls (number of entries to the center of the arena) (Figure 4.14c,d). Additional the distance travelled and velocity of the animals were comparable to controls (Figure 4.14e, f). Likewise, when CeA^{Htr2a} neurons were ablated, anxiety-like and locomotor behaviors were unaffected compared to controls (Figure 4.14g-j). These data thus suggest that the modulation of consummatory behaviour I observed is unlikely to result from altered anxiety-like or locomotor behaviours.

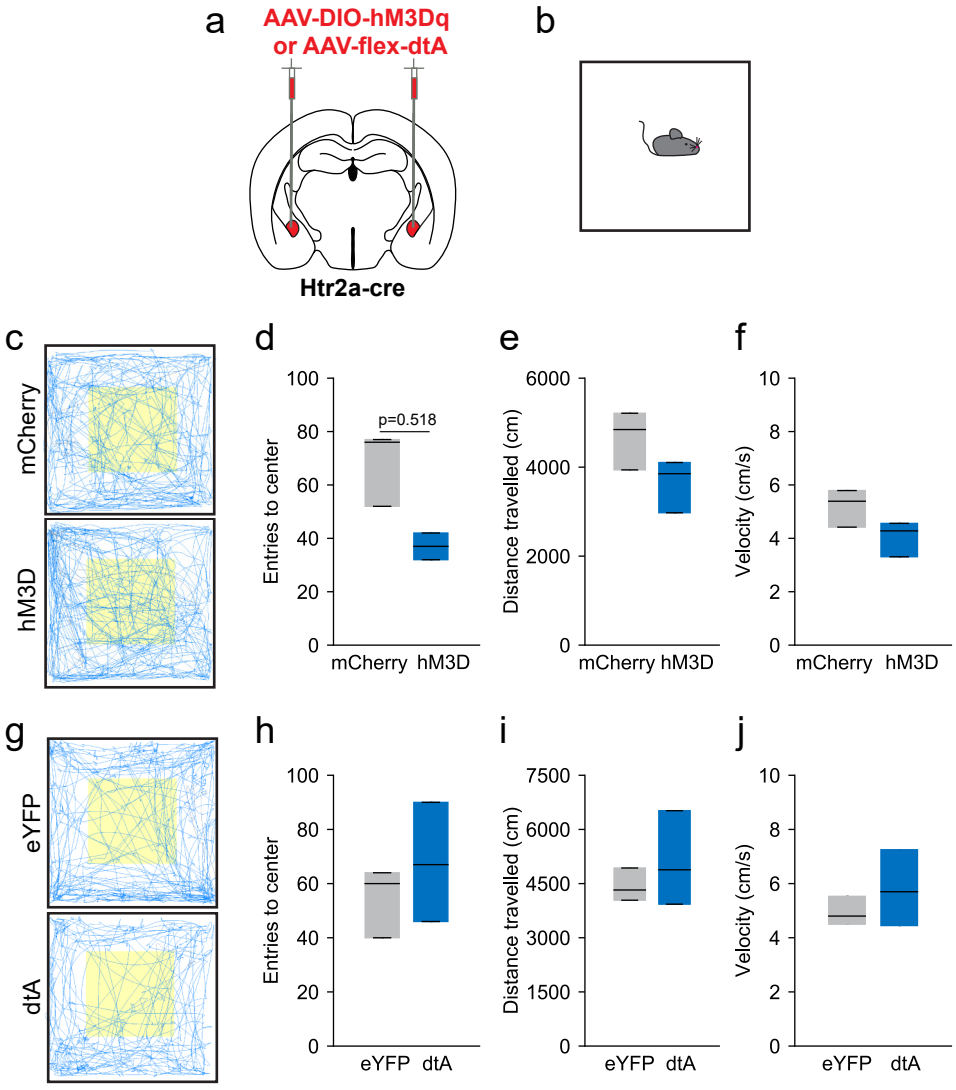

Figure 4.14: CeA^{Htr2a} neurons do not gate anxiety-like behaviour. a) Scheme depicting expression of cre-dependent AAV-hM3Dq-mCherry (for panel c-f) or AAV-dtA (for panel g-j) bilaterally in the CeA of *Htr2a-cre* mice. **b)** Scheme depicting open field apparatus. **c)** Locomotor traces of representative CeA^{Htr2a}::mCherry and CeA^{Htr2a}::hM3Dq mice in the open field experiment. Shading is the designated 'centre' zone. **d)** CeA^{Htr2a}::hM3Dq mice did not display a difference in anxiety-like behavior compared to controls. **e)** CeA^{Htr2a}::hM3Dq mice travelled a similar distance to the control animals in the open field arena. **f)** The velocity of CeA^{Htr2a}::hM3Dq mice was comparable to controls. **g)** Locomotor traces of representative CeA^{Htr2a}::eYFP and CeA^{Htr2a}::dtA mice in the open field experiment. Shading is the designated 'centre' zone. **h)** CeA^{Htr2a}::dtA mice travelled a similar distance to the control animals in the open field arena. **j)** The velocity of CeA^{Htr2a}::dtA mice was comparable to controls

Box–whisker plots indicate median, interquartile range and 5th-95th percentiles of the distribution. Two-tailed unpaired t-test.

4.6 CeA^{Htr2a} neurons increase activity during food consumption

Although my activity manipulations and ablation experiments reveal a role for CeA^{Htr2a} neurons in food consumption, they do not permit an appreciation of the endogenous activity of these neurons during consummatory behaviour which is essential to understanding the *in vivo* function of these neurons. To address this caveat and understand further how CeA^{Htr2a} neurons modulate food consumption, we examined the natural activity dynamics of CeA^{Htr2a} neurons during hunger and eating using *in vivo* Ca^{2+} imaging. This was achieved by expressing the cre-dependent genetically-encoded Ca^{2+} indicator, GCaMP6s in CeA^{Htr2a} neurons, delivered stereotaxically into the CeA of the left hemisphere by AAV, and a GRIN lense was implanted above the CeA (Figure 4.15a). Expression of the GCaMP was restricted to *Htr2a-cre* cells (Figure 4.15b). After approximately two weeks of recovery, mice in which fluorescent cells were observed through the head-mounted microscope were habituated to the behaviour protocol (Figure 4.15c). The animals were food deprived overnight so that they would be motivated to consume food. We first recorded GCaMP signals from CeA^{Htr2a} neurons before and during the first eating bout after the fast when food is a very salient stimulus. After post-processing of the acquired data, we identified 69 cells from 4 mice (example field-of-view and ROIs in Figure 4.15d,e).

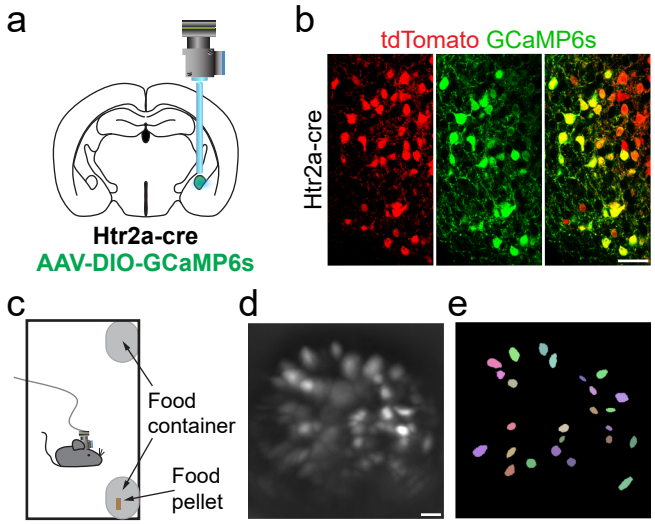

Figure 4.15: Ca^{2+} imaging in freely behaving mice. a) Scheme depicting expression of cre-dependent AAV-GCaMP6s unilaterally in the CeA of *Htr2a-cre;tdTomato* mice and placement of a GRIN lens above the structure. The fluorescent signal is capture using a miniaturized microscope head-mounted above the GRIN lens. **b)** Representative image of GCaMP6s expression in the CeA of an *Htr2a-cre;tdTomato* mouse. **c)** Scheme depicting behaviour setup. Mice with the head-mounted miniscope were free to explore an arena in which two plastic food cups were located, with one containing a food pellet. **d)** Maximum projection image of a representative imaging plane of CeA^{Htr2a}::GCaMP6s neurons. **e)** Corresponding region of interest (ROI) cell masks from imaging movie in (d).

Scale bar = 100 µm.

We found that Ca^{2+} activity rapidly increased upon the start of eating in all animals (Figure 4.16a) and across the population of all identified neurons (Figure 4.16b,d,e). The average activity of all neurons not only increased upon eating onset but also when the mice picked up the food pellet immediately prior to consumption (Figure 4.16c). Although, at the population level the activity of CeA^{Htr2a} neurons increased upon the start of eating, the responses of individual neurons were heterogeneous (Figure 4.16f).

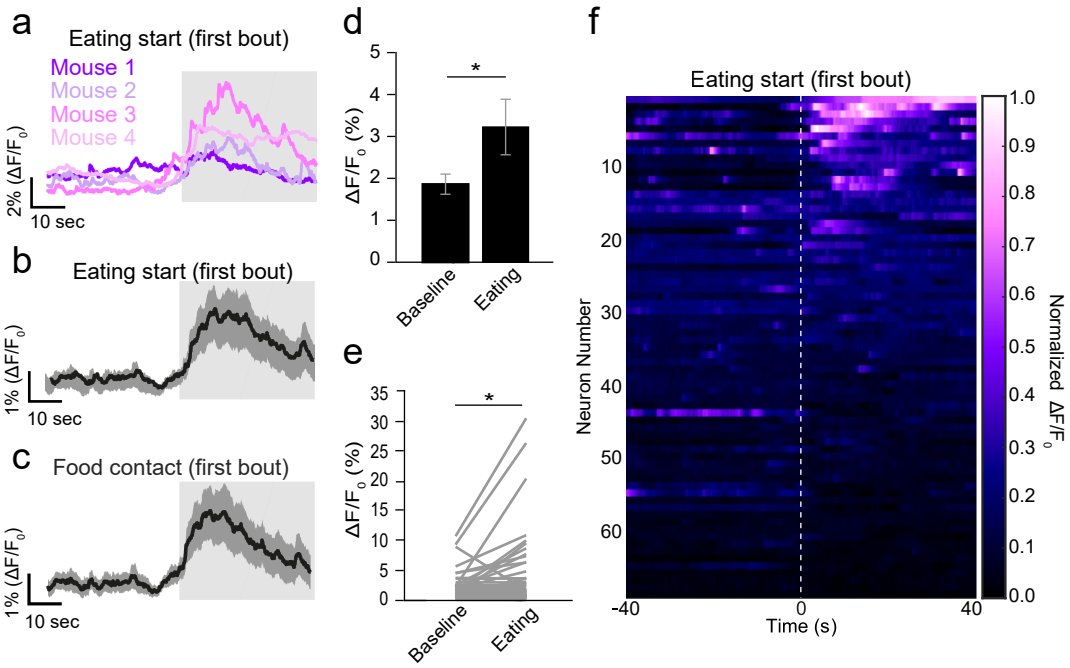

Figure 4.16: The CeA^{Htr2a} neuron population increases activity upon food consumption. a) Mean Ca^{2+} responses of neurons from individual animals aligned to onset of first eating bout in the imaging session (n= 4 mice). Grey box = eating. **b)** Mean Ca^{2+} responses of all neurons aligned to onset of first eating bout (n= 69 cells from 4 mice). Shading = SEM. Grey box = eating. **c)** Mean Ca^{2+} responses of all neurons aligned to contact with food prior to the first eating bout (n= 69 cells from 4 mice). Shading = SEM. Grey box = eating. **d)** Ca^{2+} responses of all neurons before and during the first eating bout. **e)** Same as (d) with individual neurons depicted as connected points. **f)** Normalized Ca^{2+} responses of individual CeA^{Htr2a}::GCaMP6s neurons prior to and during the first eating bout. Vertical stippled line= eating onset.

Bar plots indicate mean ±SEM. Two-tailed paired t-test. * $p<0.05$.

To examine this further, the response profiles of each cell was classified by comparing their activity prior to the feeding bouts to activity during each bout (see Materials and Methods). This revealed that 35% of the neurons with significant changes in activity were responsive to eating.

Next, a preference index to eating was calculated for each cell (Figure 4.17a).Of all the cells that were imaged, 22% of the neurons consistently increased activity during eating (Figure 4.17b-f) while a smaller subset reduced activity during eating (Figure 4.17b-d, g,h). These data demonstrate that a substantial fraction of CeA^{Htr2a} neurons are active during consumption of food.

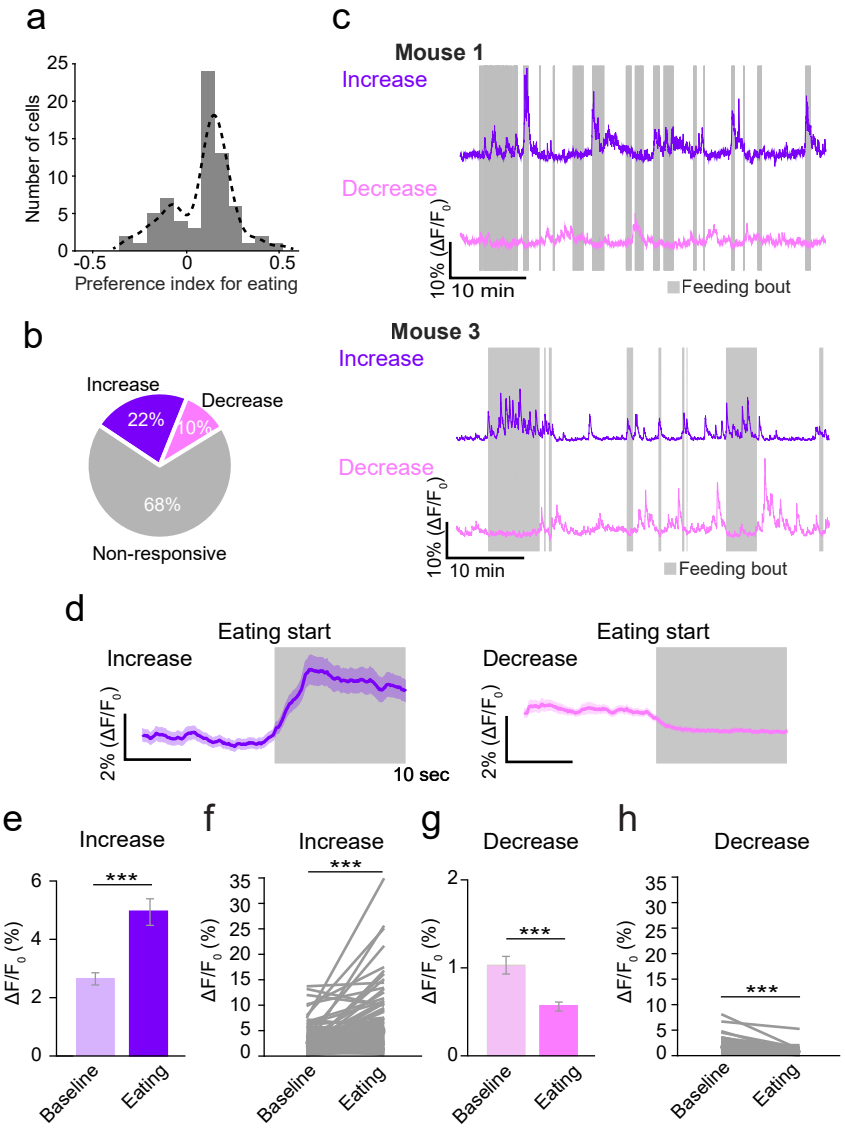

Figure 4.17: A subset of CeA^{Htr2a} neurons increase activity upon food consumption. a) Histogram of preference indices of individual neurons for eating from all eating bouts during the imaging sessions. **b)** Classification of all significantly responsive neurons based on preference index. **c)** Example neurons that consistently increased activity during eating (upper) and consistently reduced activity during eating (lower) from two mice. Grey bars = feeding bouts. **d)** Mean Ca^{2+} responses of neurons classified as increasing activity (15/69 neurons) (left) and decreasing activity (9/69 neurons) (right) across all feeding bout during the imaging session aligned to eating onset. Shading = SEM. Grey box = eating. **e)** Ca^{2+} responses of neurons that increased activity, before and during all eating bouts during the imaging session. **f)** Same as (e) with individual neurons depicted as connected points. **g)** Ca^{2+} responses of neurons that reduced activity, before and during all eating bouts during the imaging session. **h)** Same as (g) with individual neurons depicted as connected points.

Bar plots indicate mean ±SEM. Two-tailed paired t-test. *** $p<0.001$.

Despite the finding that CeA^{Htr2a} neurons increase activity during eating, this experiment left several questions open. From this experiment, it was not clear if CeA^{Htr2a} neurons are only active during consumption but also during food seeking. Additionally, since the mice were not actively engaged in food seeking and consumption behaviour during the free-feeding task, we next explored how activity of the neurons is modulated when mice are engaged in a food seeking task. To do so, GCaMP6s-expressing *Htr2a-cre* mice were trained to nose-poke at a two-poke apparatus (Figure 4.18a). Pokes in the designated 'active' port led to delivery of a single food pellet. Pellet delivery was proceeded by a 3 second light and tone cue. Ca^{2+} signal was recorded from 39 neurons from three CeA^{Htr2a} mice that performed 12 active pokes and 1-2 inactive pokes (Figure 4.18b).

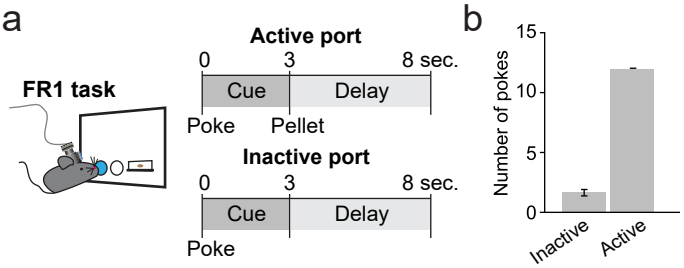

Figure 4.18: Assessing CeA^{Htr2a} neuronal activity during an operant feeding task. a) Scheme depicting behaviour setup. Mice were trained to nosepoke at a two-poke apparatus. The active poke (indicated in blue) triggered release of a 20 mg food pellet. Both active and inactive pokes were coupled to reinforcer light and tone cues. **b)** Quantification of poking behavior during the imaging sessions (3 mice). Imaging was performed from 12 active poke trials.

Bar plots indicate mean $\pm$SEM.

We first examined the Ca^{2+} activity during the 'active' nose-pokes that triggered food delivery and associated cues that signalled reward delivery. By examining the average response of all cells across the 12 trials, we found that most cells did not change activity during this 'appetitive' phase of food seeking (Figure 4.19a). We then examined the average response of the cells during the eating bout. As with the free-feeding experiment, activity of CeA^{Htr2a} neurons increased during the eating bout (Figure 4.19b). To investigate the response of individual neurons, the cells were classified according to whether their activity significantly changed activity

by comparing the area under the curve of the Ca^{2+} traces for each cell during the cue or eating bout to a baseline period of equivalent length. Only a small percentage of cells significantly increased activity during the 'appetitive' phase (Figure 4.19c). In contrast, many neurons increased activity during eating, while a smaller percentage decreased activity (Figure 4.19d). Interestingly, the peak of the Ca^{2+} signal occurred after the end of the eating bout (Figure 4.18e). Although there were very few trials, we also examined the activity of the neurons during the 'inactive' poke and associated cues. Here, there was no appreciable change in Ca^{2+} activity during this phase of behaviour (Figure 4.19f).

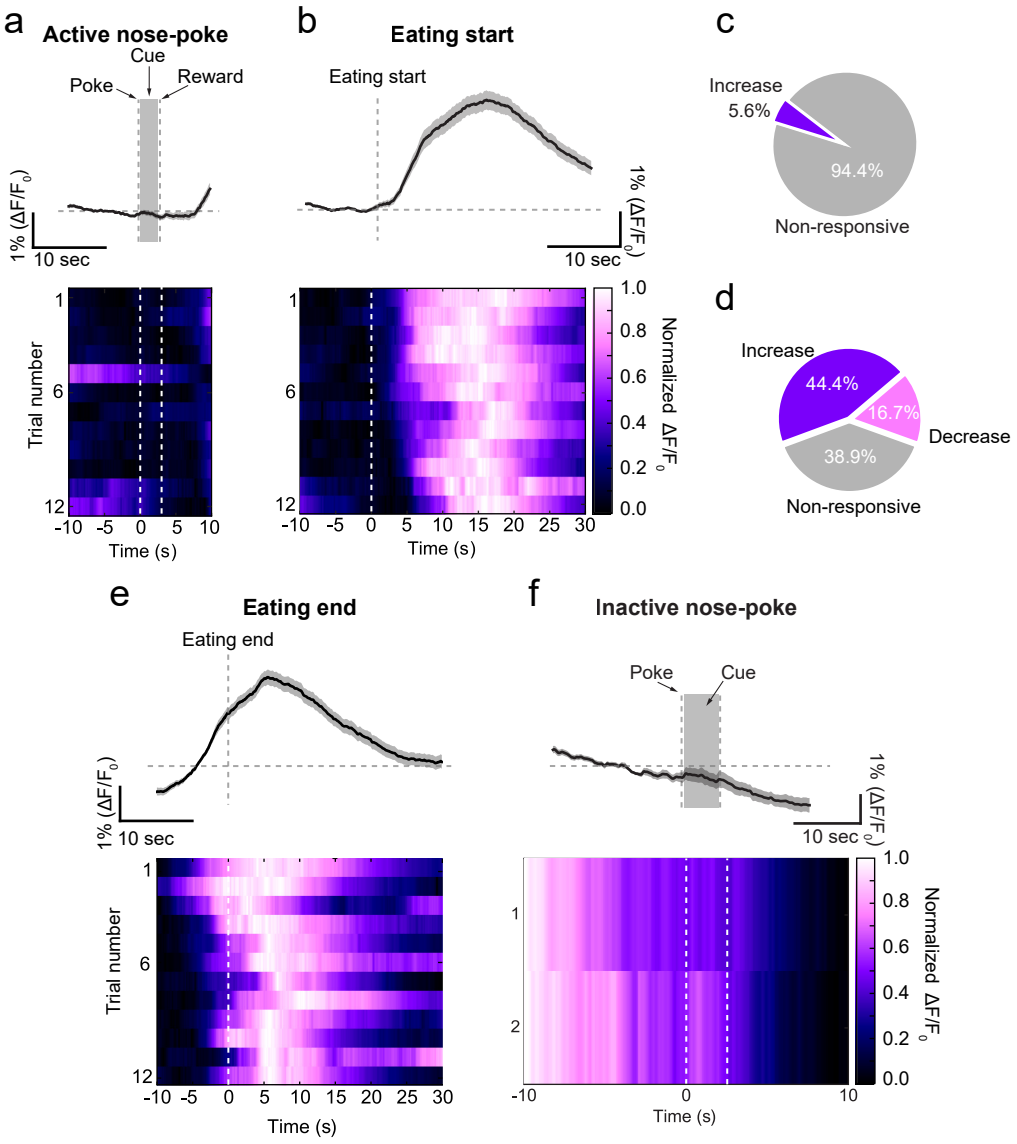

Figure 4.19: CeA^{Htr2a} neurons increase activity upon food consumption and not-food during food seeking. **a)** Mean Ca^{2+} responses from all neurons (36 cells from 3 mice) averaged across 12 trials aligned to the active nosepokes (upper). Shading = SEM. Normalized Ca^{2+} response from all neurons from 12 trials (lower). Each line is one trial. **b)** Mean Ca^{2+} responses from all neurons (36 cells from 3 mice) averaged across 12 trials aligned to eating onset (upper). Shading = SEM. Normalized Ca^{2+}response from all neurons from 12 trials (lower). Each line is one trial. **c)** Classification of all neurons during the active nosepoke. **d)** Classification of all neurons during the eating bout. **e)** Mean Ca^{2+} responses from all neurons (36 cells from 3 mice) averaged across 12 trials aligned to eating end (upper). Shading = SEM. Normalized Ca^{2+} response from all neurons from 12 trials (lower). Each line is one trial. **f)** Mean Ca^{2+} responses from all neurons (36 cells from 3 mice) averaged across 1-2 trials aligned to the inactive nosepokes (upper). Shading = SEM. Normalized Ca^{2+} response from all neurons from 1-2 trials (lower). Each line is one trial.

The consistent increase in activity of CeA^{Htr2a} neurons during eating was also consistent across cells. However, there was heterogeneity in the population. Some cells increased activity time-locked to eating onset (example cells 1,2; Figure 4.20a) while others increased with longer latency after eating start (example cells 3,4; Figure 4.20a). To examine how CeA^{Htr2a} neuron activity changed during the eating bout, the bouts were divided in half and the area under the curve of Ca^{2+} signal for each cell during each half was compared to a baseline of equivalent length. The cells were then classified according to whether there was a significant change in signal during each half of the eating bouts compared to the baseline period. This revealed that some cells that were initially classified as 'non-responders' increased activity during the second half of the eating bout (Figure 4.20b). Thus, CeA^{Htr2a} neurons are continually recruited to the circuit during eating as the average area under the curve of all 'increaser' cells significantly increased during the second half of the eating bouts (Figure 4.20c).

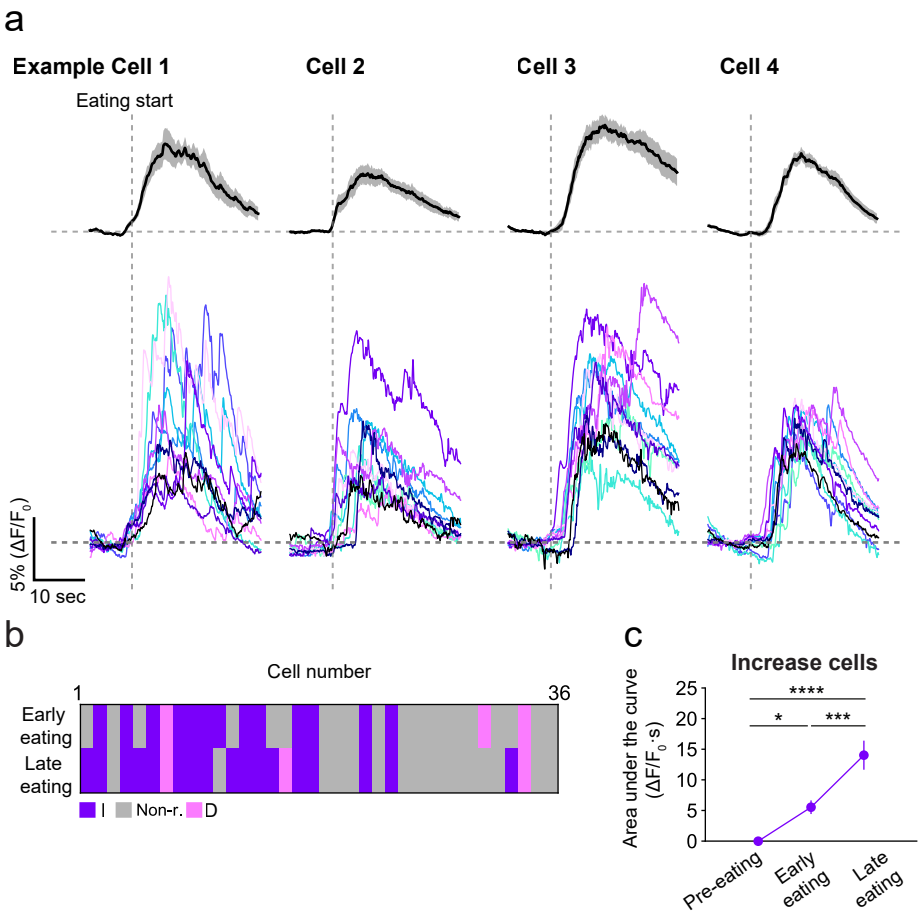

Figure 4.20: CeA^{Htr2a} neurons are recruited to the ensemble during eating. **a)** Mean Ca^{2+} responses of example CeA^{Htr2a}::GCaMP6s neurons from 12 trials aligned to eating start (upper). Shaing = SEM. Ca^{2+} traces of individual trials for each cell (lower). **b)** Classification of each cell during the two halves of the eating bouts (early vs late). 36% of neurons increased activity during the early phase of eating, compared to 47% during the late phase. **c)** Mean activity of up cells that increase activity, before eating onset and during each half of the eating bout.

Line graphs indicate mean ±SEM. One-way repeated measures ANOVA with Bonferroni post-hoc test. * $p<0.05$. *** $p<0.001$. **** $p<0.0001$.

4.7 CeA^{Htr2a} neurons promote positive reinforcement

4.7.1 Activation of CeA^{Htr2a} neurons supports place preference and self-stimulation

My experiments have revealed that CeA^{Htr2a} neurons promote food consumption but not food seeking and are active during eating behaviour. Additionally, activation of the neurons promotes consumption by extending feeding bouts rather than increasing the number of feeding incidences. Together, these data suggest that activity of CeA^{Htr2a} neurons during eating may increase consumption by prolonging eating behaviour.

Food is consumed not only because it is an energy source but because it is intrinsically rewarding. The rewarding properties of food, such as taste, smell, palatability and texture, not only make it desired, but reinforce its consumption one it is attained[147,155]. I hypothesized that because CeA^{Htr2a} neurons are active during eating and prolong consumption that activity of these neurons may contribute to food's rewarding properties and thus, reinforce ongoing consumption. If this is the case, mice will engage in behaviours that continually leads to activation of CeA^{Htr2a} neurons, such as feeding in this case. To test this, I asked if mice would engage in behaviours that leads to artificial activation of their CeA^{Htr2a} neurons. First, I tested if mice would choose to spend time where they received CeA^{Htr2a} neuron activation. Here, *Htr2a-cre* mice expressing ChR2 or eYFP were run through a real-time place preference (RTPP) assay where mice were free to explore a two-compartment arena with one side randomly paired with photostimulation of CeA^{Htr2a} neurons (Figure 4.21a, b). CeA^{Htr2a}::ChR2 mice consistently spent more time in the photostimulated side of the arena over the range of tested photostimulation frequencies (Figure 4.21c, d). The CeA^{Htr2a}::ChR2 mice displayed similar locomotor behaviour to the controls in the stimulated side of the area (Figure 4.21e, f). I further tested whether the seeking of CeA^{Htr2a} neuron activation was motivated, by testing whether mice would per-

form instrumental nose-pokes for 473nm intracranial light pulses (intracranial self-stimulation (ICSS)).

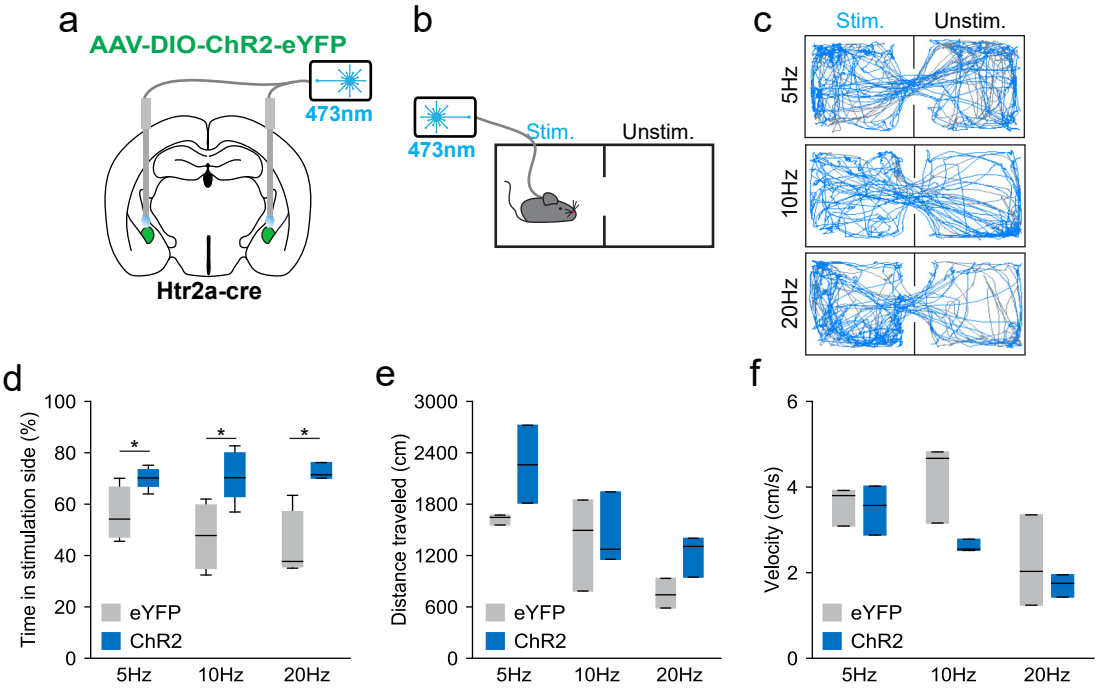

Figure 4.21: Activation of CeA^{Htr2a} neurons promotes place preference. **a)** Scheme depicting expression of cre-dependent AAV-ChR2-eYFP bilaterally in the CeA of *Htr2a-cre* mice and bilateral placement of optic fibres. **b)** Scheme depicting RTPP behaviour setup. Optic fibre-tethered mice were allowed to explore a two-chambered arena. One side (Stim.) was paired with pulse 473 nm intracranial stimulation. **c)** Representative locomotor traces of CeA^{Htr2a}::ChR2 mice where 473 nm light was received on the (Stim.) side at the indicated frequencies. **d)** CeA^{Htr2a}::ChR2 mice spent significantly more time in the photostimulated side of the arena at all frequencies tested. **e)** The distance travelled in the photostimulated side by CeA^{Htr2a}::ChR2 mice was not different from that of CeA^{Htr2a}::eYFP mice. **f)** The velocity of CeA^{Htr2a}::ChR2 mice in the photostimulated side was not different from that of CeA^{Htr2a}::eYFP mice.

Box–whisker plots indicate median, interquartile range and 5th-95th percentiles of the distribution. Two-tailed unpaired t-test. * $p<0.05$.

ChR2 and eYFP-expressing *Htr2a-cre* mice were trained to nosepoke at a two-port apparatus. Intracranial light pulses were triggered upon a nose-poke in the 'active' port while 'inactive' nose-pokes had no consequence (Figure 4.22a, b). CeA^{Htr2a}::ChR2 mice strongly nose-poked at the active port for CeA^{Htr2a} neuron activation compared to the inactive port and compared to the self-stimulation behaviour of control animals (Figure 4.22c, d). Together these data demonstrate that activation of CeA^{Htr2a} neurons is positively reinforcing, as animals are motivated

to seek out places where stimulation is encountered and perform instrumental responses for CeA^{Htr2a} neuron activation.

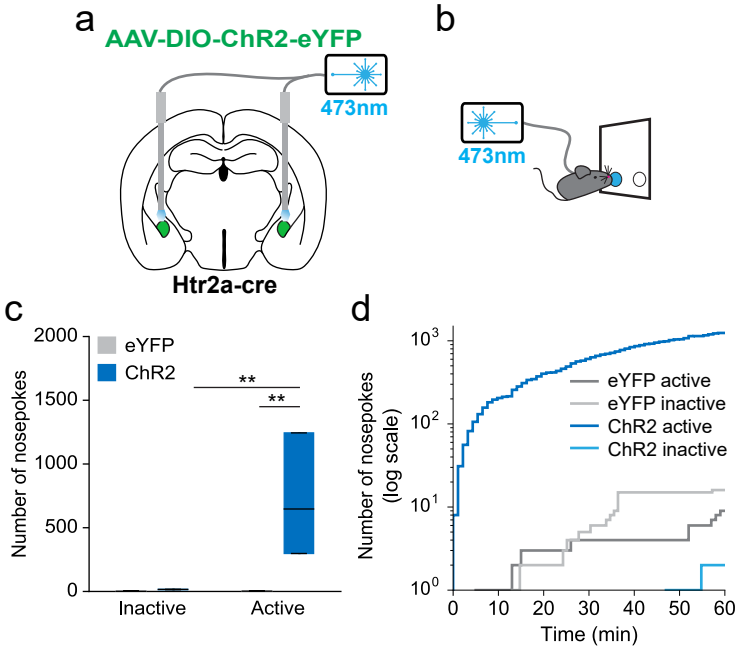

Figure 4.22: CeA^{Htr2a} neurons support self-stimulation behaviour. a) Scheme depicting expression of cre-dependent AAV-ChR2-eYFP bilaterally in the CeA of *Htr2a-cre* mice and bilateral placement of optic fibres. **b)** Scheme depicting ICSS behaviour setup. Optic fibre-tethered mice were trained to nose-poke at a two-port apparatus. One port (designated blue) was paired with intracranial 473 nm light pulses. **c)** CeA^{Htr2a}::ChR2 mice strongly nose-poked at the active port, compared to the inactive port and compared to the behaviour of CeA^{Htr2a}::eYFP controls. **d)** Cumulative nose-pokes made by representative ChR2 and eYFP-expressing mice throughout the 1hr session.

Box–whisker plots indicate median, interquartile range and 5th-95th percentiles of the distribution. Two-way ANOVA with Bonerroni post-hoc test. ** $p<0.01$.

4.7.2 CeA^{Htr2a} neurons condition flavour preference

Food consumption is reinforced by food's intrinsically rewarding properties such as taste and palatability. Therefore, since CeA^{Htr2a} neurons elicit a positive reinforcement signal, I next asked whether activity of CeA^{Htr2a} neurons could modulate specific rewarding properties of food to promote consumption. To test this, I investigated whether mice would learn to prefer specific flavours that are paired with activation of CeA^{Htr2a} neurons. Here, CeA^{Htr2a}::ChR2 mice were exposed to two differently flavoured non-nutritional gels (Figure 4.23a, b). First, the baseline

preference of each individual mouse was established. Then, the mice underwent alternating conditioning sessions where exposure to the less-preferred gel was paired with photostimulation of CeA^{Htr2a} neurons and the more-preferred with no photostimulation (Figure 4.23b). Following conditioning, the preference of the mice were tested. Strikingly, after conditioning, the less-preferred flavour was more-preferred (Figure 4.23c). This suggests that activity of CeA^{Htr2a} neurons can reinforce specific rewarding properties of foods to make them more consumed.

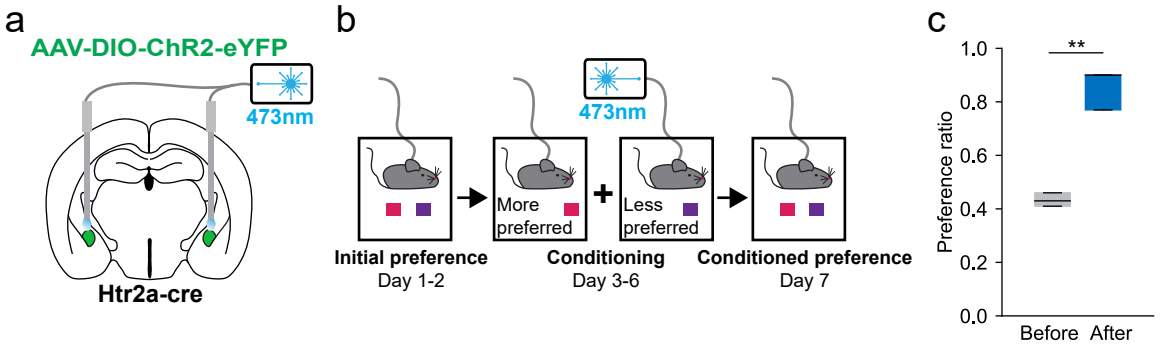

Figure 4.23: CeA^{Htr2a} neurons condition flavour preference. **a)** Scheme depicting expression of cre-dependent AAV-ChR2-eYFP bilaterally in the CeA of *Htr2a-cre* mice and bilateral placement of optic fibres. **b)** Scheme depicting conditioned flavour preference experiment. **c)** Photostimulation of CeA^{Htr2a} neurons reversed flavor preference of the initially less-preferred flavor.

Box–whisker plots indicate median, interquartile range and 5th-95th percentiles of the distribution. Two-tailed paired t-test. ** $p<0.01$.

4.7.3 Inhibition of CeA^{Htr2a} neurons reduces reward consumption

The modulation of food reward by CeA^{Htr2a} neuron activity suggests that under conditions where CeA^{Htr2a} neurons are inhibited, food's rewarding properties are no longer reinforced and less food will be consumed. Although I found that acute silencing of CeA^{Htr2a} neurons reduced food intake in hungry mice, it is unclear whether this occurred because food consumption food is less reinforced. To further explore this idea, I investigated whether silencing of CeA^{Htr2a} neurons would reduce consumption when food intake is driven by food's rewarding properties alone. To do so, I trained food restricted CeA^{Htr2a}::NpHR to freely lick a spout for a palatable liquid reward (Figure 4.24a, b). Once, stable licking was achieved, I tested the licking responses in *ad libitum*

fed mice during a photoinhibition session to ensure that licking behaviour was based on the palatability of the solution rather than homeostatic need. I found that CeA^{Htr2a}::NpHR mice licked at the spout less than control animals (Figure 4.24c, d), which suggests that silencing of CeA^{Htr2a} neurons reduces food intake when palatability is the driver of consumption.

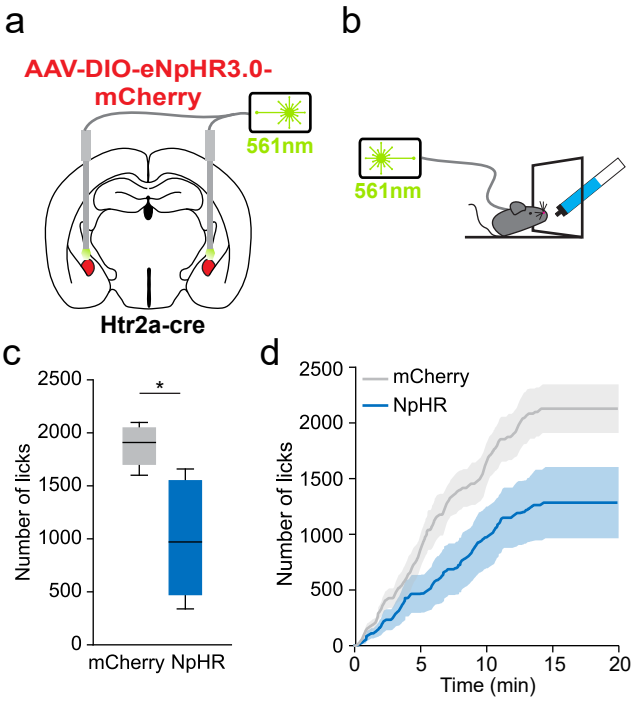

Figure 4.24: Silencing of CeA^{Htr2a} neurons decrease reward consumption. a) Scheme depicting expression of cre-dependent AAV-NpHR-mCherry bilaterally in the CeA of *Htr2a-cre* mice and bilateral placement of optic fibres. **b)** Scheme depicting behaviour setup. *Ad libitum* fed optic fibre-tethered mice were allowed to freely consume palatable reward from a spout. Intracranial constant 561nm light was delivered during the assay. **c)** CeA^{Htr2a}::NpHR licked less of the palatable solution than controls. **d)** Cumulative licks of reward solution during the photoinhibition session. Shading = SEM.

Box–whisker plots indicate median, interquartile range and 5th-95th percentiles of the distribution. Two-tailed unpaired t-test. * $p<0.05$.

Importantly, control experiments (Figure 4.25a, b) also revealed that CeA^{Htr2a}::NpHR mice did not avoid the side of the RTPP chamber in which they received photoinhibition of CeA^{Htr2a} neurons (Figure 4.25c), nor did they exhibit locomotor defects (Figure 4.25d, e). This indicates that silencing of CeA^{Htr2a} neurons does not elicit an intrinsically aversive state but instead modulates food consumption based on rewarding properties of the food. Together these data support my hypothesis that CeA^{Htr2a} neurons positively reinforce eating behaviour by modulating the rewarding properties of food.

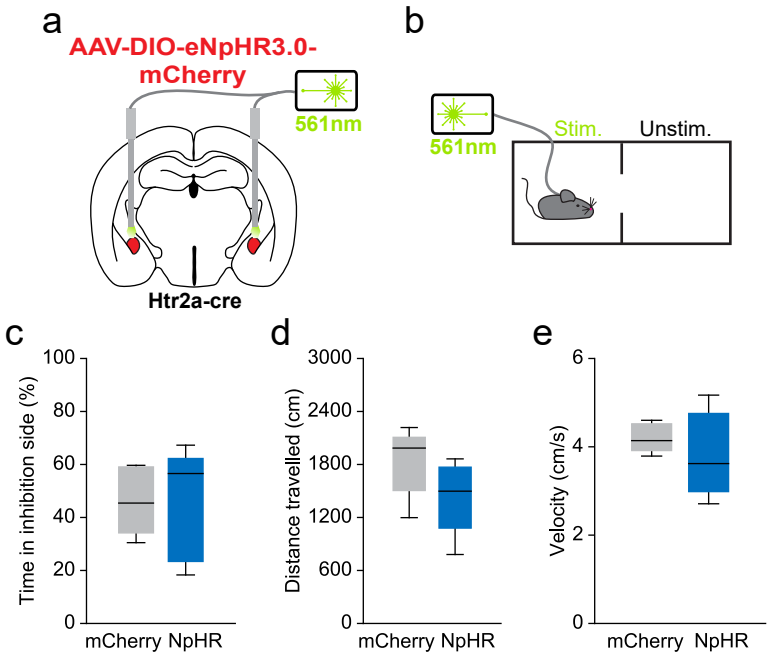

Figure 4.25: Silencing of CeA^{Htr2a} neurons does not promote place avoidance. **a)** Scheme depicting expression of cre-dependent AAV-NpHR-mCherry bilaterally in the CeA of *Htr2a-cre* mice and bilateral placement of optic fibres. **b)** Scheme depicting RTPP behaviour setup. Optic fibre-tethered mice were allowed to explore a two-chambered arena. One side (Stim.) was paired with constant 561 nm intracranial light. **c)** CeA^{Htr2a}::NpHR mice spent comparable time in the photoinhibited side of the arena as CeA^{Htr2a}::mCherry mice. **d)** The distance travelled in the photoinhibited side by CeA^{Htr2a}::NpHR mice was not different from that of CeA^{Htr2a}::mCherry mice. **e)** The velocity of CeA^{Htr2a}::NpHR mice in the photoinhibited side was not different from that of CeA^{Htr2a}::mCherry mice.

Box–whisker plots indicate median, interquartile range and 5th-95th percentiles of the distribution. Two-tailed unpaired t-test.

4.8 Efferent projections from CeA^{Htr2a} neurons to the PBN promote food consumption and reward

To explore the circuits by which CeA^{Htr2a} neurons exert effects on consumption and reward, we mapped the efferent projections of these neurons by expressing cre-dependent AAV-ChR2 into the CeA and examining the brains of these animals of ChR2-eYFP terminals (Figure 4.26a). Dense ChR2-eYFP terminals were observed in the PBN (Figure 4.26b). Given that this region is known to play an integral role in feeding behaviour, I accessed the functionality of the CeA^{Htr2a}-PBN projection in feeding behaviour. *Htr2a-cre* mice were bilaterally injected with ChR2 in the CeA and optic fibres above the PBN (Figure 4.26c, Figure Ac).

CeA^{Htr2a-}PBN::ChR2 and control mice were allowed to explore a behavior arena that contained a pre-weighed food pellet (Figure 4.26d). The animals were exposed to a 20 minute epoch of photostimulation (473nm 20Hz ∼10mW) followed by a 20 minute period of no stimulation (Figure 4.26e). Stimulation of CeA^{Htr2a-}PBN terminals evoked a modest but significant increase in food consumption compared to the laser OFF epoch (Figure 4.26f).

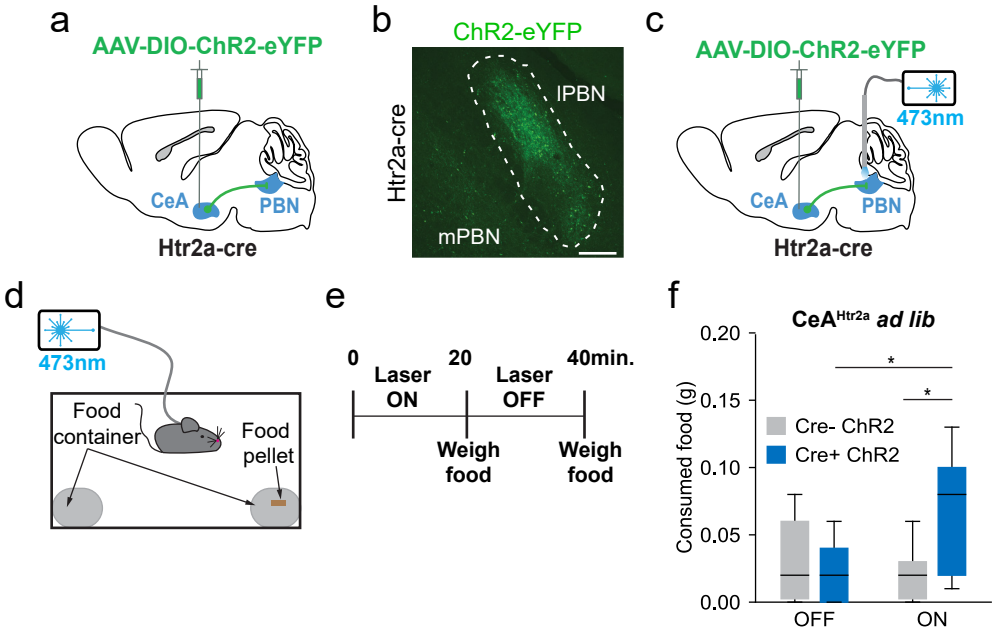

Figure 4.26: Activation of CeA^{Htr2a}-PBN terminals promotes food consumption. **a)** Scheme depicting transduction of cre-dependent AAV-ChR2-eYFP in the CeA of *Htr2a-cre* mice (only unilateral injection is shown). **b)** Representative image of CeA^{Htr2a} neuron fibres in the PBN (only one side of the brain is shown). **c)** Scheme depicting expression of cre-dependent AAV-ChR2-eYFP in the CeA of *Htr2a-cre* mice and placement of optic fibres above the PBN (only one side of the brain is shown). **d)** Scheme depicting behaviour setup. Optic fibre-tethered mice were free to explore an arena in which two plastic food cups were located, with one containing a pre-weighed food pellet. **e)** Experimental timeline. Mice were tested during the light period in the light cycle. **f)** Optogenetic activation of CeA^{Htr2a}-PBN projections at 20Hz increased food consumption compared to the laser OFF epoch and eYFP-expressing control mice.

lPBN, lateral parabrachial nucleus; mPBN, medial parabrachial nucleus. Scale bar = 100 µm. Box–whisker plots indicate median, interquartile range and 5th-95th percentiles of the distribution. Two-tailed unpaired t-test or two-tailed paired t-test. * $p<0.05$.

Analysis of the feeding bouts revealed that the total duration of eating was not increased in CeA^{Htr2a-}PBN::ChR2 animals (Figure 4.27a, b) with the average bout duration increased (Figure 4.27c). The number of feeding bouts and the latency to feeding was comparable between CeA^{Htr2a}::ChR2 animals and controls (Figure 4.27d, e).

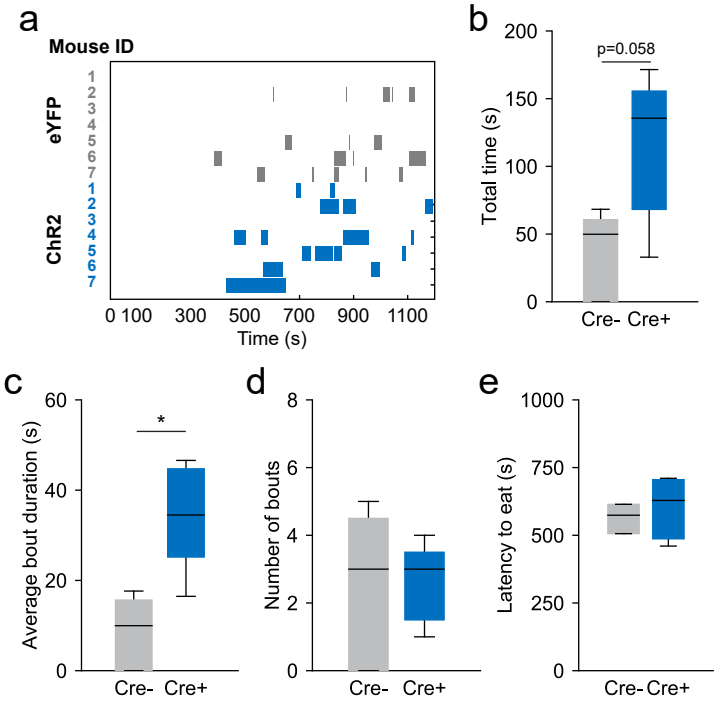

Figure 4.27: Activation of CeA^{Htr2a}-PBN terminals increases feeding. a) Ethogram depicting the feeding bouts of individual CeA^{Htr2a}::ChR2 and CeA^{Htr2a}::eYFP mice during the 20min 20Hz laser ON epoch. Each row is an individual animal. **b)** Optogenetic activation of CeA^{Htr2a}-PBN projections did not significantly increase the total time the animals spent eating compared to controls. **c)** Optogenetic activation of CeA^{Htr2a}-PBN projections increased the average duration of the feeding bouts. **d)** The number of feeding bouts of CeA^{Htr2a}-PBN::ChR2 mice was not significantly different to controls. **e)** Optogenetic activation of CeA^{Htr2a}-PBN projections did not affect the latency of animals to eat after the laser was triggered.

Box–whisker plots indicate median, interquartile range and 5th-95th percentiles of the distribution. Two-tailed unpaired t-test (Figure 4.27b,d,e). Mann Whitney test (Figure 4.26c). * $p<0.05$.

I also tested whether activation of the CeA^{Htr2a-}PBN terminals recapitulated the positive reinforcement effects of CeA^{Htr2a} neuron cell body stimulation. CeA^{Htr2a-}PBN::ChR2 mice and controls were run through the real-time place preference experiment (Figure 4.28a, b). CeA^{Htr2a-}PBN::ChR2 mice spent significantly more time on the side of the arena where intracranial 20Hz 473nm laser stimulation was received (Figure 4.28c, d). The self-stimulation behaviour of CeA^{Htr2a-}PBN::ChR2 mice was also tested (Figure 4.28e) which revealed that CeA^{Htr2a-}PBN::ChR2 mice strongly nose-poked for activation of the CeAHt2a-PBN projection (Figure 4.28f). Together these data reveal that the food intake and positive reinforcement properties of CeA^{Htr2a} neurons are mediated through projections to the PBN.

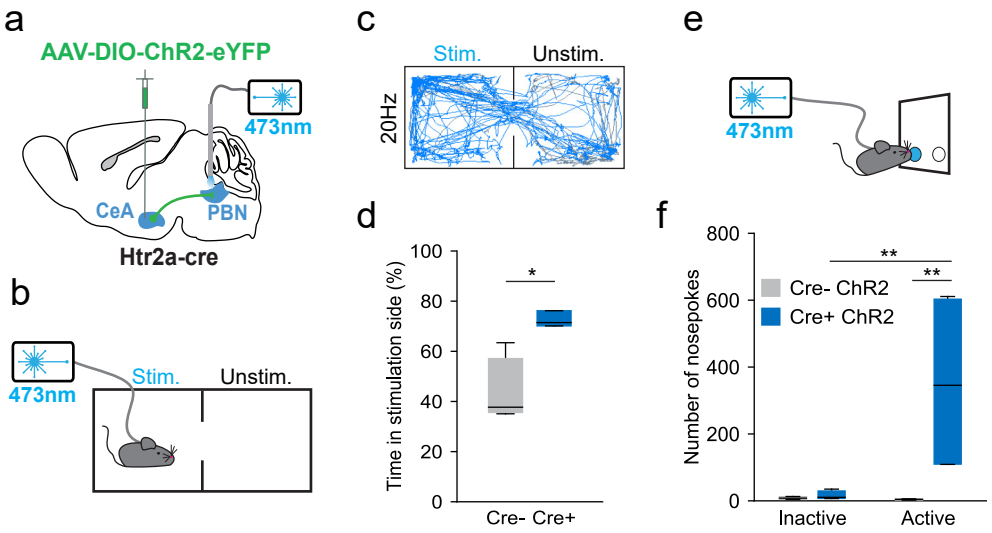

Figure 4.28: Activation of CeA^{Htr2a}-PBN terminals is rewarding. a) Scheme depicting transduction of cre-dependent AAV-ChR2-eYFP in the CeA of *Htr2a-cre* mice and placement of optic fibres above the PBN (only one side of the brain is shown). **b)** Scheme depicting RTPP behaviour setup. Optic fibre-tethered mice were allowed to explore a two-chambered arena. One side (Stim.) was randomly paired with 20Hz 473 nm intracranial stimulation. **c)** Representative locomotor trace of a CeA^{Htr2a}-PBN::ChR2 mouse where 20Hz 473 nm light was received on the (Stim.) side. **d)** CeA^{Htr2a}-PBN::ChR2 mice spent significantly more time in the photostimulated side of the arena. **e)** Scheme depicting ICSS behaviour setup. Optic fibre-tethered mice were trained to nose-poke at a two-port apparatus. One port (designated blue) was paired with intracranial 473 nm light pulses. **f)** CeA^{Htr2a}-PBN::ChR2 mice strongly nose-poked at the active port, compared to the inactive port and compared to the behaviour of CeA^{Htr2a}-PBN::eYFP controls.

Box–whisker plots indicate median, interquartile range and 5th-95th percentiles of the distribution. Two-tailed unpaired t-test (Figure 4.28d). Two-way ANOVA with Bonerroni post-hoc test (Figure 4.28f). * $p<0.05$, ** $p<0.01$.

Chapter 5

Discussion

5.1 Summary of thesis findings

In my thesis work, I have identified a molecularly-defined population of CeA neurons expressing Htr2a, that positively regulate food intake. Neural activation, inhibition and ablation experiments *in vivo* revealed a role for these neurons in increasing food intake in *ad libitum* fed mice and under conditions where eating is unfavourable and where the motivation to find and consume food is low. Further, in comparison to another population of CeA neurons that express SOM, most of these effects were specific to the Htr2a neuron population. Additional experiments demonstrated that CeA^{Htr2a} neurons do not increase the motivation to work for food, suggesting these neurons specifically modulate food consumption. Accordingly, *in vivo* Ca^{2+} imaging revealed that these neurons increase activity during eating but not during food seeking and that CeA^{Htr2a} neurons are recruited to the active ensemble during eating. Further exploration of the mechanism by which CeA^{Htr2a} neurons modulate eating revealed that these neurons promote positive reinforcement as mice continually engage in behaviours that activate the neurons. This suggested that activity of the neurons positively reinforces eating behaviour. Further experiments demonstrated that this positive valence signal modulates

the rewarding properties of food, promoting its consumption. Investigation into the long-range neural circuits in which CeA^{Htr2a} neurons function revealed that efferent projections to the PBN promote food consumption and positive reinforcement. Together, these findings reveal specific neurons, associated circuits and mechanisms through which the CeA positively regulates food consumption.

5.2 Identification of central amygdala neural modulators of feeding

This study has revealed the neural mechanism by which the CeA positively regulates food consumption. A role for the CeA in promoting food intake has long been postulated, but the neural players involved and the underlying circuit mechanisms have not been definitively shown. Cai et al., (2014) showed that CeA neurons expressing PKCδ, when active, rapidly suppress food consumption and proposed that the mechanism is through local inhibition of $CeA^{PKC\delta\text{-}}$ neurons, suggesting these neurons promote food intake. My data suggest that CeA^{Htr2a} neurons likely fulfil this role. Not only did activation of CeA^{Htr2a} neurons increase food consumption in *ad lib* fed mice, but increased intake under conditions where $CeA^{PKC\delta}$ neurons are reportedly active- during exposure to malaise-inducing compounds and unpalatable foods[66]. These data suggest that functional antagonism between CeA^{Htr2a} and $CeA^{PKC\delta}$ neurons modulates eating behaviour, likely depending on the internal state of the animal and the sensory environment.

For my behavioural studies using chemogenetics, I compared the effect of activating CeA^{Htr2a} neurons and another population of $CeA^{PKC\delta\text{-}}$ neurons- those expressing SOM. Molecular characterization of CeA^{Htr2a} neurons revealed that approximately 60% of CeA^{Htr2a} neurons express SOM. However, the majority of the effects on eating observed by activation of CeA^{Htr2a} neurons were not observed upon CeA^{SOM} neuron activation. The exception was that activation of both CeA^{Htr2a} and CeA^{SOM} neuron populations elicited increased consumption of bitter foods

compared to control groups. A recent report has also shown that CeA^{SOM} neurons in the CeA, as well as other genetically-defined $CeA^{PKC\delta-}$ neurons, elicit self-stimulation behaviour[156]. However, silencing of these neurons did not affect food consumption but reduced drinking behaviour[156]. These data together suggest that in general, $CeA^{PKC\delta-}$ neurons encode positive valence but that the positive modulation of consummatory behaviours such as eating and drinking are influenced by defined CeA subpopulations. Additionally, although food consumption appears specific to the broad CeA^{Htr2a} neuron population, CeA^{Htr2a} subsets that express additional markers such as SOM, corticotrophin-releasing hormone (CRH) and tachykinin 2 (Tac2) may in turn influence specific aspects of consumption such as palatability.

Recent studies that describe a role for molecularly-defined CeA neurons in appetitive and aversive behaviours have used genetic markers to classify neurons into functional cell types. One caveat of this approach is that expression of a cellular marker is only a single attribute with which to define a cell population. Since many of these markers overlap, the classification of neurons into functional cell populations based on expression of a single marker has its caveats. My analysis of the CeA^{Htr2a} neuron population revealed that approximately 60% of these cells also express SOM. This suggests that Htr2a+/SOM+ neurons may be functionally distinct from Htr2a+/SOM- neurons, however, the existence of other molecular markers (eg. Tac2, CRH, neurotensin, dynorphin)[67,130,156] that likely overlap to various degrees with both populations complicates this simplistic interpretation. Additionally, neural subpopulations can be classified based on other features such as projection target, inputs or activity pattern during a given behaviour. Nevertheless, it is becoming clear that classification of functional neural subpopulations should take into account multiple anatomical, cellular and functional features.

5.3 Mechanisms of feeding modulation by the central amygdala

The discovery and ingestion of nutrients in the form of food is integral to the maintenance of physiological balance of an organism and ultimately its survival. Food intake consists of multiple behaviour sequences that constitute the conscious detection of hunger signals, the decision to forage for food, foraging, food discovery, the decision to eat and the act of chewing and ingestion of food. Distributed neural circuits control food intake and modulate specific aspects of this behaviour. Broadly, appetite is regulated by three interacting sets of neural circuits that drive food seeking and consumption (arcuate nucleus of the hypothalamus), modulate food intake by influencing food reward (LH) and suppress intake under unfavourable conditions (PBN)[33]. Within this framework of appetite control, my work has revealed a role for the CeA in modulating food consumption.

Behavioural experiments revealed that Htr2a-expressing CeA neurons are important for potentiating food consumption. Specifically, chemogenetic and optogenetic activation of these neurons elicited increased food consumption while acute silencing and ablation of the neurons decreased food intake in hungry animals. Interestingly, increased food intake was manifested as a lengthening of individual feeding bouts rather than in the number of bouts, indicating that these neurons may sustain eating behaviour. Importantly, ablation of the neurons did not affect long-term body weight or daily food intake and specifically decreased consumption when mice were hungry and motivated to eat. This suggests that these neurons do not play a role in long-term energy balance, but may play a more nuanced role in eating behaviour. Further experiments revealed that these neurons do not drive food-seeking behaviour, as their chemogenetic activation did not increase effort to work for food pellets. Thus, CeA^{Htr2a} neurons appear to modulate food consumption specifically. This model was supported by *in vivo* imaging of the neurons, which revealed that they increase activity during eating but not dur-

ing foraging. Together, behavioural and imaging data suggest that activity of CeA^{Htr2a} neurons sustains ongoing eating behaviour.

Further insight into how CeA^{Htr2a} neurons modulate food consumption came from behaviour experiments showing that activity of CeA^{Htr2a} neurons is intrinsically rewarding. Specifically, mice will perform operant responses for CeA^{Htr2a} neuron stimulation and prefer locations where CeA^{Htr2a} neurons are photostimulated. This suggests that because mice continue to engage in behaviours where CeA^{Htr2a} neurons are active, that activity of CeA^{Htr2a} neurons positively reinforces ongoing behaviour. These data support a model where activity of CeA^{Htr2a} neurons during eating, positively reinforces and therefore sustains this behaviour.

Food consumption is driven by signals of energy deficit that manifest as a physiological hunger state. Food itself is a naturally rewarding stimulus as its ingestion is necessary to sustain life as well as alleviate the negative valence nature of hunger[29]. Thus, food intake must be positively reinforced in order to ensure that body weight and energy homeostasis are maintained. The specific properties of food, including sensory attributes (eg. sight, smell, taste, flavour) and post-ingestive effects (eg. nutrient absorption), constitute what are considered 'rewarding properties of food'[147]. These properties, when associated with food consumption, attain rewarding properties themselves and together positively reinforce food intake. In addition, these rewarding properties reinforce eating at different stages of food intake. Those cues that predict food availability such as sight and smell influence food intake prior to eating onset, while other factors such as taste and palatability come into effect once eating has commenced. Additionally, post-ingestive food reward is modulated by metabolic changes and nutrient absorption[147]. Our finding that CeA^{Htr2a} neurons increase activity proximal to eating onset suggests that activity of the neurons modulates the rewarding properties of food in the early stages of eating such as taste, palatability and texture. Indeed, some of these properties are modulated by CeA^{Htr2a} neural activity since mice learned to prefer flavours paired with activity of these neurons. Fur-

ther, food intake driven exclusively by palatability was reduced when CeA^{Htr2a} neurons were silenced. Together these findings suggest that the positive valence signal encoded by these neurons influences the rewarding properties of food to modulate consumption.

The *in vivo* dynamics of CeA^{Htr2a} neural activity revealed further insight into the coding of appetitive behaviour within the CeA. Although at the population level, the activity of CeA^{Htr2a} neurons increased proximal to eating onset, the onset of Ca^{2+} activity varied across individual cells with many cells exhibiting an increase during the later phases of eating. One hypothesis to explain this finding is that different neurons within the CeA^{Htr2a} neurons may regulate distinct aspects of eating behaviour that are temporally distinct. For example, motor actions necessary for physical ingestion of food (discussed further below), taste and palatability may be modulated by different components of the ensemble. Thus, as eating progresses, the accumulation of this activity leads to positive reinforcement of the behaviour. Interestingly, the Ca^{2+} signal recorded from CeA^{Htr2a} neurons was found to outlast the end of the eating bouts (Fig. 19e). This may reflect an accumulation of Ca^{2+} in the cell given that CeA^{Htr2a} neurons are continually recruited to the active ensemble throughout eating. This is consistent with the slow decay time of GCaMP6s signal which does not recapitulate the spiking activity of neurons[138]. Alternatively, early activity of CeA^{Htr2a} neurons may lead to an increase in GCaMP signal to the upper threshold of detection such that subsequent firing of the cells after eating has ended may be undetectable. Therefore, the precise activity dynamics of CeA^{Htr2a} neurons throughout and beyond the cessation of eating would be impossible to resolve with the use of GCaMP6s and would require Ca^{2+} sensors that better conform to neuron spike rates (eg. GCaMP6f) or the use of *in vivo* electrophysiology experiments.

These findings reveal a role for the CeA in modulating the rewarding properties of food to control food intake. The attributes of these neurons parallel those of GABAergic neurons in the LH, which are well documented to promote food intake and support positive reinforcement[55,157].

These LH neurons appear to modulate food consumption as their bulk activation promotes consumption and not food seeking[157]. Within the functional ensemble, many GABA LH neurons increase activity during eating behaviour[157]. Additionally, activity of the neurons modulates food palatability, suggesting that like CeA^{Htr2a} neurons, consumption is promoted by a positive valence mechanism. The similarities between CeA^{Htr2a} neurons and LH neurons contrasts the control of appetite by AgRP-expressing 'hunger' neurons in the hypothalamic arcuate nucleus that are activated by energy deficit and strongly drive food seeking and consumption[24,25,29,30]. Additionally activity of the neurons modulates food incentive value prior to consumption, rather than modulating the rewarding properties during consumption[158]. These different neural players in the control of feeding, although mechanistically distinct, are by no means mutually exclusive and act in concert to control appetite. Specifically, modulation of food's rewarding properties is likely under homeostatic control and may be negatively regulated in unfavourable conditions.

5.4 Nuanced modulation of appetite-related behaviours by the central amygdala

This study has revealed a mechanism by which neurons in the CeA positively modulate eating behaviour. A recent study revealed a role for the CeA in the hunting and biting of prey and in feeding-related motor behaviours[159]. Importantly, these effects on appetitive related-behaviours were independent of increased food consumption. In contrast, my work revealed that neurons within the CeA promote food intake but also induce feeding-related motor behaviours. There are several important points to consider when corroborating the findings of these studies. First, Han et al.,(2017)[159] use a broad cre-driver (VGat-cre) that targets all CeA neurons. This would lead to simultaneous activation of neurons that both increase and suppress eating, thus masking effects on food intake. Secondly, hunting and biting of prey were shown to

be mediated by CeA projections to the PAG and reticular formation, respectively[159]. This contrasts my data, which show that CeA^{Htr2a} neurons modulate food consumption via projections to the PBN. In addition, the fictive motor sequences observed by CeA^{Htr2a} neuron cell body stimulation were not observed by PBN projection photostimulation. Together these studies suggest that multiple aspects of appetite-related behaviours, pursuit, attack and eating of prey, are modulated through the CeA and that they are delineated at the level of efferent projections. Finally, Han et al showed that activation of the whole CeA drives attack and biting of prey in addition to fictive motor sequences. This consummatory behaviour does not appear to be based on edibility as false prey items and wood pieces are often 'attacked' and ingested[159]. In contrast, I found that activation of CeA^{Htr2a} neurons biases consumption towards food over an inedible item, suggesting that consumption is specific to food. Thus, although the CeA controls many aspects of appetitive behaviour, processing of edibility signals and execution of behavioural actions appear to be separable.

5.5 Central amygdala-associated circuits for feeding-related behaviours

The data discussed above together reveal new roles for CeA neurons in the modulation of food intake whereby a molecularly-defined population of CeA neurons expressing Htr2a positively regulates eating behaviour in a manner opposed to CeA$^{PKC\delta}$ neurons. Additionally, activity of CeA^{Htr2a} neurons can antagonize the feeding suppression mediated by CeA$^{PKC\delta}$ neurons in multiple contexts ie. satiety, malaise and when unpalatable foods are encountered. However, these findings not only suggest that CeA^{Htr2a} neurons antagonize the anorexigenic function of PKCδ neurons but that these cells can counteract reduced feeding that occurs when motivation to obtain and consume food is low. This notion is in line with the model that CeA^{Htr2a} neurons positively reinforce eating behaviour and thus enhance the rewarding properties of food even

under conditions where food saliency is reduced.

The control of food intake by the CeA appears to be executed by two functionally opposing cell types, CeA^{Htr2a} and $CeA^{PKC\delta}$ neurons, that promote and suppress feeding, respectively. Previously, ChR2-assisted circuit mapping revealed that $CeA^{PKC\delta}$ neurons locally inhibit other neurons with the CeA[66]. Data from our lab revealed that CeA^{Htr2a} neurons also locally inhibit other CeA neurons, some of which are PKCδ+ (data not shown- experiments conducted by Hakan Kucukdereli). This suggests that activation of one population and thus inhibition of the other ultimately dictates how feeding is controlled by the CeA. Whether CeA^{Htr2a} or $CeA^{PKC\delta}$ neurons control the output of the CeA likely depends on the nature of the inputs to the CeA, which would reflect the internal state of the animal and cues within the environment. Monosynaptic rabies tracing from $CeA^{PKC\delta}$ neurons has shown that a suite of brain regions provide input to these neurons, including components of the gustatory and limbic systems, cortices and thalamus[66]. The same approach targeting CeA^{Htr2a} neurons in our lab has revealed that these neurons receive inputs from similar regions (data not shown- experiments conducted by Marion Ponserre). However, this approach does not reveal the nature of these inputs nor their temporal coding and so although the same regions target these neurons, their functional effects may differ markedly. Nevertheless, based on their functions, CeA^{Htr2a} and $CeA^{PKC\delta}$ neurons are likely to be differentially activated by appetitive and aversive signals, respectively, allowing flexible, context-dependent modulation of feeding by the CeA. Thus, the CeA is a site of integration of salient appetite-related stimuli. Our *in vivo* imaging of CeA^{Htr2a} neural activity support this notion. The heterogeneity in activity dynamics within this population during eating suggests that neurons are excited by different inputs and that integration of a combination of appetitive signals within the CeA^{Htr2a} neuron population may drive feeding related behaviours.

The mechanism by which the CeA controls feeding appears to also occur at the level of long-range CeA efferents. Interestingly, $CeA^{PKC\delta}$ neurons were shown to project to a small

number of brain regions, none of which were sufficient to inhibit food intake[66]. Thus, the authors concluded that CeA$^{PKC\delta}$ neurons locally inhibit, likely orexigenic, CeA neurons to inhibit consumption. My work has indeed shown that CeA$^{PKC\delta-}$ neurons expressing Htr2a account for this effect, however I have also revealed that the long-range modulation of feeding behaviour by the CeA is through CeA^{Htr2a} neurons. Projections to the PBN, which are inhibitory in nature (data not shown- experiments conducted by Hakan Kucukdereli), promote both the feeding and positive reinforcement properties of CeA^{Htr2a} neurons. This suggests that when activity of CeA^{Htr2a} neurons predominates at the level of the CeA, long-range circuits are also engaged. Importantly, the identity of the cells in the PBN that receive this input as well as the nature of the signals they convey are unknown. However, since the PBN is a primary relay from the periphery of taste, malaise and satiety signals[37,160,161] , inhibition of this region by the CeA may serve to modulate gustatory input to the forebrain thereby influencing feeding. CeA^{Htr2a} neurons project to multiple other brain regions in addition to the PBN. Predominant sites of innervation include the BNST, PAG, NTS and LH (data not shown- experiments conducted by Marion Ponserre). The function of these projections in feeding behaviour remains an interesting direction for future research into understanding the long-range circuits through which CeA^{Htr2a} neurons modulate eating behaviour.

5.6 The central amygdala as a flexible modulator of context-specific behaviours

The CeA has long been considered a key site where negative valence signals are processed and anxiety and fear-related behaviour are modulated. However, the role of the CeA in processing appetitive signals has recently come to light. Both appetitive and aversive behaviours have been ascribed to molecularly-defined CeA subpopulations, however it is also clear that the functional circuits within the CeA are highly flexible depending on behavioural con-

text. CeA subpopulations defined by expression of SOM or CRH have well described roles in aversive and defensive behaviours[76,84,162] but have been recently shown to promote appetitive behaviours[156], demonstrating that behaviour modulated by the specific CeA subpopulations is clearly context-depended. Although most studies do not consider the *in vivo* firing rate of CeA neurons, differences in the parameters used for neural activity manipulations (ie. frequency of photostimulation) likely account for the different behaviours observed. This suggests that appetitive and aversive signals may be encoded at different firing rates within the CeA, reflective of differential input signals that converge on the CeA depending on the behavioural context. The complexity of appetite and aversive coding within the CeA may also lead to flexible engagement of neurons that themselves receive CeA input, as the profile of neurotransmitters/peptides released is strongly dependent on neural firing rate[163,164]. The complex connectivity between CeA neurons further suggests that CeA neurons are not specialized mediators of specific behaviours, but through local circuit interactions are likely involved in many different behaviours.

Considering the behavioural flexibility of CeA circuits, the absence of anxiety-related behaviours upon chemogenetic activation or ablation of CeA^{Htr2a} neurons do not preclude a role for these neurons in aversive behaviours. Indeed, the population activity of these same neurons was shown to be reduced upon exposure to innately fear-inducing stimuli[86]. This implicates CeA^{Htr2a} neurons in both appetitive and aversive behaviours and further supports the idea that coding of appetitive and aversive behaviours in the CeA is flexible, intricate and depends on the behavioural context.

The positive valence property of CeA^{Htr2a} neural activity also suggests that these neurons may positively reinforce other behaviours in addition to feeding. Indeed, GABAergic LH neurons also promote positive reinforcement and when these neurons are stimulated, mice will engage in consummatory behaviour directed towards proximal salient stimuli such as food, water, a mate or a conspecific depending on the stimuli in the environment[55,154,157]. Although I did not

examine whether activation of CeA^{Htr2a} neurons modulates other consummatory behaviours, the positive valence signal transmitted by these neurons may play a generalizable role in positively reinforcing appetitive behaviours. This raises the possibility that these neurons flexibly modulate behaviours towards appetitive stimuli depending on the behavioural context and the internal state of the animal and suggests that a broad suite of appetitive signals converge on the CeA.

5.7 Conclusion and outlook

The CeA has long been considered a site where primarily aversive signals are integrated and from which anxiety and fear-related behaviours are executed. Despite this, it is now becoming clear that this region is also involved in appetitive behaviours. My work has revealed that a molecularly defined CeA neural subpopulation expressing Htr2a positively regulates food consumption by modulating food's intrinsically rewarding properties and thereby reinforcing ongoing eating behaviour. The circuit mechanisms underlying these effects are likely to be both through local inhibition of anorexigenic CeA$^{PKC\delta}$ neurons and long-range inhibition of the PBN. Further, behaviour and *in vivo* imaging experiments revealed that these cells modulate food consumption rather that food-seeking behaviour, suggesting these neurons and associated circuits lie downstream of those that detect hunger signals and promote foraging behaviour.

These findings lay the groundwork for further investigation into how appetitive signals are routed in the brain. To do so, it will be important to determine the nature of the appetitive signal that leads to CeA^{Htr2a} neuron activation. Since CeA^{Htr2a} neurons promote food consumption and modulate food reward, appetitive signals that excite these neurons are likely to convey information about hunger, internal and motivational state as well as food-predictive cues that inform about the upcoming meal. Considering the diversity of these signals it is likely that they converge on CeA^{Htr2a} neurons from multiple input sources. For example, hunger-related

information may originate from the hypothalamus while food predictive cue signals may arise from sensory cortical areas. Furthermore, the extremely high degree of connectivity within the CeA suggests that signals are not linearly processed in the CeA (ie. one input signal relayed to one output pathway) but is indicative of intricate computation of converging inputs. This is also supported by the relative sparsity of regions innervated by CeA^{Htr2a} neurons compared to regions which provide input regions which again suggests that CeA^{Htr2a} neurons are excited by diverse appetitive inputs. Along these same lines, further analysis of the coding of consummatory responses within the CeA^{Htr2a} neuron population using *in vivo* Ca^{2+} imaging based on the inputs or outputs of these neurons will be important to understanding the circuitry that underlies the processing of appetitive signals and behavioural execution.

Given that CeA^{Htr2a} neurons promote intrinsic positive reinforcement, the functional interactions between the CeA and the dopaminergic reward system is an important area for future research. Dopaminergic neurons of the VTA and SN are important neural components of motivated behaviours as their activity promotes positive reinforcement and enhances saliency of food predictive cues[55,59–61]. The rewarding nature of CeA^{Htr2a} neuron stimulation suggests that CeA may act in concert with the dopaminergic reward system to modulate food's rewarding properties and elicit positive reinforcement. Anatomical reciprocal connections between these regions have been described[98,99,101] and CeA neurons are also known to express dopamine receptors[165,166]. Therefore this area will be an exciting avenue for future research.

A complete investigation of the neural circuits in which these CeA^{Htr2a} neurons function will also be critical for understanding how these neurons modulate appetitive behaviour. In my study, I found that long-range inputs to the PBN from CeA^{Htr2a} neurons also promote positive reinforcement and food consumption. It will be important to determine the identity of PBN neurons, through immunostaining or RNA-seq, that receive CeA^{Htr2a} neuron input and the nature of the signals they convey in order to fully understand the function of this descending projection.

The PBN is a key relay site for satiety and malaise signals to the forebrain, which suggests that CeA^{Htr2a} neurons may inhibit these signals to promote food consumption. However, given that my data suggest that CeA^{Htr2a} neurons modulate the rewarding properties of food, CeA^{Htr2a} neurons may modulate palatability and taste signals. Indeed, descending projections from the CeA have been shown to modulate the taste responsive profiles of PBN neurons[160], suggesting that this long-range projection may influence food's rewarding properties.

In summary, my work has revealed a mechanism by which neurons in the CeA promote positive reinforcement to modulate food consumption and influence the positively rewarding properties of food. These findings not only reveal that the role of the CeA is more complex than previously considered, but also set the groundwork for a thorough investigation of interactions between positive and negative emotional states, food intake and reward processing and implicate the CeA in human disorders in which these aspects of behaviour and physiology are affected.

Appendix A

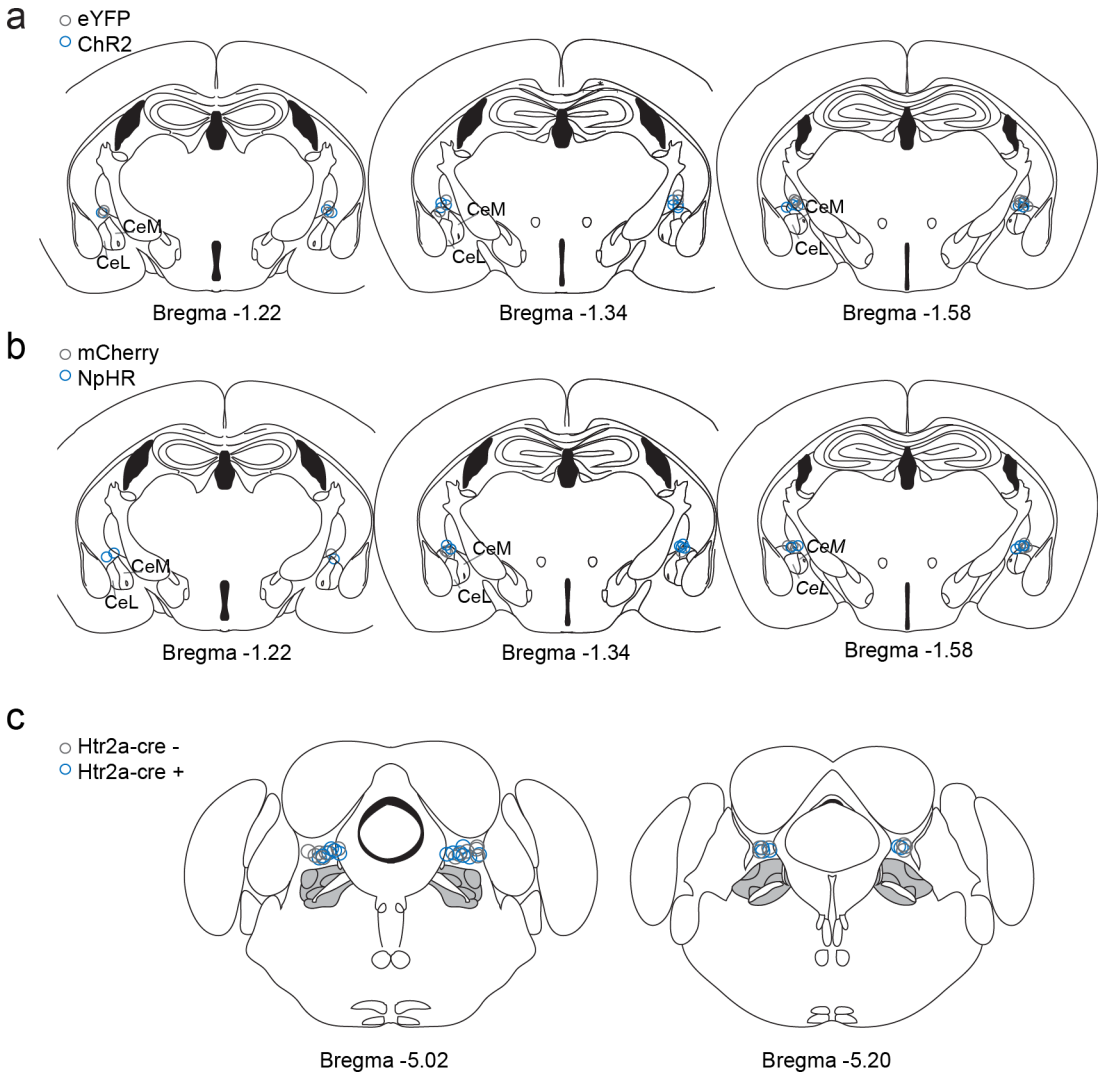

Appendix A: Fibre placements. **a)** Approximate anatomical locations of optic fibre tips implanted about the CeA for activation experiments in the Figure 4.8, Figure 4.10, Figure 4.20 ,Figure 4.21 and Figure 4.22. **b)** Approximate anatomical locations of optic fibre tips implanted about the CeA for silencing experiments in the Figure 4.13, Figure 4.23 and Figure 4.24. **c)** Approximate anatomical locations of optic fibre tips implanted about the PBN for experiments in Figure 4.25, Figure 4.26 and Figure 4.27.

Abbreviations

AAV	Adenoassociated viruse
aCSF	Articial cerebrospinal fluid
AgRP	agouti-related protein
AP	area postrema
Arch	Archaerhodopsin
BA	Basal amygdala
BAC	Bacterial artificial chromosome
BLA	Basolateral amygdala
BMA	Basomedial amygdala
BNST	Bed nucleus of the stria terminalis
Ca^{2+}	Calcium
CCK	cholecystokinin
CeA	Central amygdala
CeL	Central lateral amygdala
CeM	Central medial amygdala
CGRP	Calcitonin gene-relted peptide
ChR2	Channelrhodophsin-2
CNO	chlozapine-N-oxide
CRH	Corticotrophin-releasing hormone
CS	Conditioned stimulus
DA	dopamine
DIO	Double floxed inverted open reading frame
DR	Dorsal Raphe
DREADDs	designer receptors exclusively activated by designer drugs
dtA	diphtheria toxin receptor A subunit

DVC	Dorsal vagal complex
eYFP	Enhanced yellow fluorescent protein
FR1	Fixed ratio 1
FR5	Fixed ratio 5
GABA	gamma-Aminobutyric acid
$GABA_A$	gamma-Aminobutyric acid receptor A
GCaMP	Genetically-encoded Ca^{2+} indicator
GLP1	glucagon-like-peptide 1
GPCR	G-protein coupled receptor
GRIN	Gradient refractive index
Htr2a	Serotonin receptor 2a
ICA	Independent component analysis
ICSS	Intracranial self-stimulation
InsCtx	Insular cortex
IP	intraperitoneal
IR-DIC	Intrared differential interference contrast
LA	Lateral amygdala
LED	Light emitting diode
LH	Lateral hypothalamus
LiCl	Lithium chloride
LPS	Lipopolysaccharide
ME	Medial amygdala
NA	numerical appeture
NAc	Nucleus accumbens
NpHR	Halorhodopsin
NPY	neuropeptide Y
NTS	Nucleus of the solitary tract
PAG	Periaqueductual gray
PBN	parabrachial nucleus
PBS	Phosphate buffered saline
PCA	Principal component analysis

PFA	Paraformaldehyde
PKCδ	protein kinase C δ
POMC	pro-opiomelanocortin
PR2	Progressive ratio 2
PVH	Paraventricular hypothalamus
PVT	Paraventricular thalamus
ROI	region of interest
RTPP	Real-time place preference
SN	Substantia nigra
SOM	Somatostatin
Tac2	Tachykinin 2
US	Unconditioned stimulus
VLP	ventral posterior lateral thalamic nucleus
VTA	Ventral tegmental area
βgal	Beta-galactosidase

Bibliography

1. Morton, G. J., Meek, T. H. & Schwartz, M. W. Neurobiology of food intake in health and disease. *Nature Reviews Neuroscience* **15,** 367–378 (May 2014).
2. Vaisse, C., Clement, K., Guy-Grand, B. & Froguel, P. *Nature Genetics* **20,** 113–114 (Oct. 1998).
3. Bell, C. G., Walley, A. J. & Froguel, P. The genetics of human obesity. *Nature Reviews Genetics* **6,** 221–234 (Feb. 2005).
4. Farooqi, I. S. *et al.* Heterozygosity for aPOMC-Null Mutation and Increased Obesity Risk in Humans. *Diabetes* **55,** 2549–2553 (Aug. 2006).
5. Ferrario, C. R. *et al.* Homeostasis Meets Motivation in the Battle to Control Food Intake. *J Neurosci* **36,** 11469–11481. ISSN: 0270-6474 (2016).
6. Bagdade, J. D., Bierman, E. L. & Porte D., J. The significance of basal insulin levels in the evaluation of the insulin response to glucose in diabetic and nondiabetic subjects. *J Clin Invest* **46,** 1549–57. ISSN: 0021-9738 (Print) 0021-9738 (1967).
7. Considine, R. V. *et al.* Serum immunoreactive-leptin concentrations in normal-weight and obese humans. *N Engl J Med* **334,** 292–5. ISSN: 0028-4793 (Print) 0028-4793 (1996).
8. Elmquist, J. K., Bjorbaek, C., Ahima, R. S., Flier, J. S. & Saper, C. B. Distributions of leptin receptor mRNA isoforms in the rat brain. *J Comp Neurol* **395,** 535–47. ISSN: 0021-9967 (Print) 0021-9967 (1998).
9. Grill, H. J. *et al.* Evidence that the caudal brainstem is a target for the inhibitory effect of leptin on food intake. *Endocrinology* **143,** 239–46. ISSN: 0013-7227 (Print) 0013-7227 (2002).
10. Zhang, Y. *et al.* Positional cloning of the mouse obese gene and its human homologue. *Nature* **372,** 425–32. ISSN: 0028-0836 (Print) 0028-0836 (1994).
11. Woods, S. C., Lotter, E. C., McKay, L. D. & Porte D., J. Chronic intracerebroventricular infusion of insulin reduces food intake and body weight of baboons. *Nature* **282,** 503–5. ISSN: 0028-0836 (Print) 0028-0836 (1979).
12. Bruning, J. C. *et al.* Role of brain insulin receptor in control of body weight and reproduction. *Science* **289,** 2122–5. ISSN: 0036-8075 (Print) 0036-8075 (2000).
13. Lee, G. H. *et al.* Abnormal splicing of the leptin receptor in diabetic mice. *Nature* **379,** 632–5. ISSN: 0028-0836 (Print) 0028-0836 (1996).
14. Cowley, M. A. *et al.* The distribution and mechanism of action of ghrelin in the CNS demonstrates a novel hypothalamic circuit regulating energy homeostasis. *Neuron* **37,** 649–61. ISSN: 0896-6273 (Print) 0896-6273 (2003).
15. Nakazato, M. *et al.* A role for ghrelin in the central regulation of feeding. *Nature* **409,** 194–8. ISSN: 0028-0836 (Print) 0028-0836 (2001).

16. Gibbs, J., Young, R. C. & Smith, G. P. Cholecystokinin decreases food intake in rats. *J Comp Physiol Psychol* **84,** 488–95. ISSN: 0021-9940 (Print) 0021-9940 (1973).
17. Turton, M. D. *et al.* A role for glucagon-like peptide-1 in the central regulation of feeding. *Nature* **379,** 69–72. ISSN: 0028-0836 (Print) 0028-0836 (1996).
18. Faipoux, R., Tome, D., Gougis, S., Darcel, N. & Fromentin, G. Proteins activate satiety-related neuronal pathways in the brainstem and hypothalamus of rats. *J Nutr* **138,** 1172–8. ISSN: 0022-3166 (2008).
19. Pappas, T. N., Melendez, R. L. & Debas, H. T. Gastric distension is a physiologic satiety signal in the dog. *Dig Dis Sci* **34,** 1489–93. ISSN: 0163-2116 (Print) 0163-2116 (1989).
20. Broberger, C. & Hokfelt, T. Hypothalamic and vagal neuropeptide circuitries regulating food intake. *Physiol Behav* **74,** 669–82. ISSN: 0031-9384 (Print) 0031-9384 (2001).
21. Morton, G. J. *et al.* Leptin action in the forebrain regulates the hindbrain response to satiety signals. *J Clin Invest* **115,** 703–10. ISSN: 0021-9738 (Print) 0021-9738 (2005).
22. Aponte, Y., Atasoy, D. & Sternson, S. M. AGRP neurons are sufficient to orchestrate feeding behavior rapidly and without training. *Nat Neurosci* **14,** 351–5. ISSN: 1097-6256 (2011).
23. Atasoy, D., Betley, J. N., Su, H. H. & Sternson, S. M. Deconstruction of a neural circuit for hunger. *Nature* **488,** 172–7. ISSN: 1476-4687 (Electronic) 0028-0836 (Linking) (2012).
24. Krashes, M. J. *et al.* Rapid, reversible activation of AgRP neurons drives feeding behavior in mice. *J Clin Invest* **121,** 1424–8. ISSN: 0021-9738 (2011).
25. Chen, Y., Lin, Y. C., Kuo, T. W. & Knight, Z. A. Sensory detection of food rapidly modulates arcuate feeding circuits. *Cell* **160,** 829–41. ISSN: 0092-8674 (2015).
26. Zhan, C. *et al.* Acute and long-term suppression of feeding behavior by POMC neurons in the brainstem and hypothalamus, respectively. *J Neurosci* **33,** 3624–32. ISSN: 0270-6474 (2013).
27. Cowley, M. A. *et al.* Leptin activates anorexigenic POMC neurons through a neural network in the arcuate nucleus. *Nature* **411,** 480–4. ISSN: 0028-0836 (Print) 0028-0836 (2001).
28. Takahashi, K. A. & Cone, R. D. Fasting induces a large, leptin-dependent increase in the intrinsic action potential frequency of orexigenic arcuate nucleus neuropeptide Y/Agouti-related protein neurons. *Endocrinology* **146,** 1043–7. ISSN: 0013-7227 (Print) 0013-7227 (2005).
29. Betley, J. N. *et al.* Neurons for hunger and thirst transmit a negative-valence teaching signal. *Nature* **521,** 180–5. ISSN: 0028-0836 (2015).
30. Mandelblat-Cerf, Y. *et al.* Arcuate hypothalamic AgRP and putative POMC neurons show opposite changes in spiking across multiple timescales. *Elife* **4.** ISSN: 2050-084x. doi:10.7554/eLife.07122 (2015).
31. Chen, Y. & Knight, Z. A. Making sense of the sensory regulation of hunger neurons. *Bioessays* **38,** 316–24. ISSN: 0265-9247 (2016).
32. Andermann, M. L. & Lowell, B. B. Toward a Wiring Diagram Understanding of Appetite Control. *Neuron* **95,** 757–778 (Aug. 2017).
33. Sternson, S. M. & Eiselt, A. K. Three Pillars for the Neural Control of Appetite. *Annu Rev Physiol* **79,** 401–423. ISSN: 0066-4278 (2017).
34. Betley, J. N., Cao, Z. F., Ritola, K. D. & Sternson, S. M. Parallel, redundant circuit organization for homeostatic control of feeding behavior. *Cell* **155,** 1337–50. ISSN: 0092-8674 (2013).

35. Luquet, S., Perez, F. A., Hnasko, T. S. & Palmiter, R. D. NPY/AgRP neurons are essential for feeding in adult mice but can be ablated in neonates. *Science* **310,** 683–5. ISSN: 0036-8075 (2005).

36. Carter, M. E., Han, S. & Palmiter, R. D. Parabrachial calcitonin gene-related peptide neurons mediate conditioned taste aversion. *J Neurosci* **35,** 4582–6. ISSN: 0270-6474 (2015).

37. Carter, M. E., Soden, M. E., Zweifel, L. S. & Palmiter, R. D. Genetic identification of a neural circuit that suppresses appetite. *Nature* **503,** 111–4. ISSN: 0028-0836 (2013).

38. Wu, Q., Clark, M. S. & Palmiter, R. D. Deciphering a neuronal circuit that mediates appetite. *Nature* **483,** 594–7. ISSN: 0028-0836 (2012).

39. Cabanac, M. Physiological role of pleasure. *Science* **173,** 1103–7. ISSN: 0036-8075 (Print) 0036-8075 (1971).

40. Dossat, A. M., Lilly, N., Kay, K. & Williams, D. L. Glucagon-like peptide 1 receptors in nucleus accumbens affect food intake. *J Neurosci* **31,** 14453–7. ISSN: 0270-6474 (2011).

41. Mehta, S. *et al.* Regional brain response to visual food cues is a marker of satiety that predicts food choice. *Am J Clin Nutr* **96,** 989–99. ISSN: 0002-9165 (2012).

42. Cameron, J. D., Goldfield, G. S., Finlayson, G., Blundell, J. E. & Doucet, E. Fasting for 24 hours heightens reward from food and food-related cues. *PLoS One* **9,** e85970. ISSN: 1932-6203 (2014).

43. Sharma, S., Hryhorczuk, C. & Fulton, S. Progressive-ratio responding for palatable high-fat and high-sugar food in mice. *J Vis Exp,* e3754. ISSN: 1940-087x (2012).

44. Berthoud, H. R., Lenard, N. R. & Shin, A. C. Food reward, hyperphagia, and obesity. *Am J Physiol Regul Integr Comp Physiol* **300,** R1266–77. ISSN: 0363-6119 (2011).

45. Stice, E., Figlewicz, D. P., Gosnell, B. A., Levine, A. S. & Pratt, W. E. The contribution of brain reward circuits to the obesity epidemic. *Neurosci Biobehav Rev* **37,** 2047–58. ISSN: 0149-7634 (2013).

46. Delgado, J. M. & Anand, B. K. Increase of food intake induced by electrical stimulation of the lateral hypothalamus. *Am J Physiol* **172,** 162–8. ISSN: 0002-9513 (Print) 0002-9513 (1953).

47. Olds, J. & Milner, P. Positive reinforcement produced by electrical stimulation of septal area and other regions of rat brain. *J Comp Physiol Psychol* **47,** 419–27. ISSN: 0021-9940 (Print) 0021-9940 (1954).

48. Heimer, L., Zahm, D. S., Churchill, L., Kalivas, P. W. & Wohltmann, C. Specificity in the projection patterns of accumbal core and shell in the rat. *Neuroscience* **41,** 89–125. ISSN: 0306-4522 (Print) 0306-4522 (1991).

49. Jennings, J. H., Rizzi, G., Stamatakis, A. M., Ung, R. L. & Stuber, G. D. The inhibitory circuit architecture of the lateral hypothalamus orchestrates feeding. *Science* **341,** 1517–21. ISSN: 0036-8075 (2013).

50. Root, D. H., Melendez, R. I., Zaborszky, L. & Napier, T. C. The ventral pallidum: Subregion-specific functional anatomy and roles in motivated behaviors. *Prog Neurobiol* **130,** 29–70. ISSN: 0301-0082 (2015).

51. O'Connor, E. C. *et al.* Accumbal D1R Neurons Projecting to Lateral Hypothalamus Authorize Feeding. *Neuron* **88,** 553–64. ISSN: 0896-6273 (2015).

52. Wu, Z. *et al.* GABAergic projections from lateral hypothalamus to paraventricular hypothalamic nucleus promote feeding. *J Neurosci* **35,** 3312–8. ISSN: 0270-6474 (2015).

53. Barbano, M. F., Wang, H. L., Morales, M. & Wise, R. A. Feeding and Reward Are Differentially Induced by Activating GABAergic Lateral Hypothalamic Projections to VTA. *J Neurosci* **36,** 2975–85. ISSN: 0270-6474 (2016).

54. Nieh, E. H. *et al.* Decoding neural circuits that control compulsive sucrose seeking. *Cell* **160,** 528–41. ISSN: 0092-8674 (2015).

55. Nieh, E. H. *et al.* Inhibitory Input from the Lateral Hypothalamus to the Ventral Tegmental Area Disinhibits Dopamine Neurons and Promotes Behavioral Activation. *Neuron.* ISSN: 0896-6273. doi:10.1016/j.neuron.2016.04.035 (2016).

56. Stuber, G. D. & Wise, R. A. Lateral hypothalamic circuits for feeding and reward. *Nat Neurosci* **19,** 198–205. ISSN: 1097-6256 (2016).

57. Corbett, D. & Wise, R. A. Intracranial self-stimulation in relation to the ascending dopaminergic systems of the midbrain: a moveable electrode mapping study. *Brain Res* **185,** 1–15. ISSN: 0006-8993 (Print) 0006-8993 (1980).

58. Kim, K. M. *et al.* Optogenetic mimicry of the transient activation of dopamine neurons by natural reward is sufficient for operant reinforcement. *PLoS One* **7,** e33612. ISSN: 1932-6203 (2012).

59. Berridge, K. C. & Robinson, T. E. What is the role of dopamine in reward: hedonic impact, reward learning, or incentive salience? *Brain Res Brain Res Rev* **28,** 309–69 (1998).

60. Goto, Y. & Grace, A. A. Dopaminergic modulation of limbic and cortical drive of nucleus accumbens in goal-directed behavior. *Nat Neurosci* **8,** 805–12. ISSN: 1097-6256 (Print) 1097-6256 (2005).

61. Wise, R. A. Role of brain dopamine in food reward and reinforcement. *Philos Trans R Soc Lond B Biol Sci* **361,** 1149–58. ISSN: 0962-8436 (Print) 0962-8436 (2006).

62. Berridge, K. C. The debate over dopamine's role in reward: the case for incentive salience. *Psychopharmacology (Berl)* **191,** 391–431. ISSN: 0033-3158 (Print) 0033-3158 (2007).

63. Cohen, J. Y., Haesler, S., Vong, L., Lowell, B. B. & Uchida, N. Neuron-type-specific signals for reward and punishment in the ventral tegmental area. *Nature* **482,** 85–8. ISSN: 0028-0836 (2012).

64. Schultz, W., Dayan, P. & Montague, P. R. A neural substrate of prediction and reward. *Science* **275,** 1593–9. ISSN: 0036-8075 (Print) 0036-8075 (1997).

65. Bermudez-Rattoni, F. Molecular mechanisms of taste-recognition memory. *Nat Rev Neurosci* **5,** 209–17. ISSN: 1471-003X (Print) 1471-003x (2004).

66. Cai, H., Haubensak, W., Anthony, T. E. & Anderson, D. J. Central amygdala PKC-delta(+) neurons mediate the influence of multiple anorexigenic signals. *Nat Neurosci* **17,** 1240–8. ISSN: 1097-6256 (2014).

67. Haubensak, W. *et al.* Genetic dissection of an amygdala microcircuit that gates conditioned fear. *Nature* **468,** 270–6. ISSN: 0028-0836 (2010).

68. Brown, S. & Schafer, E. A. An Investigation into the Functions of the Occipital and Temporal Lobes of the Monkey's Brain. *Philosophical Transactions of the Royal Society of London. (B.)* **179,** 303–327 (1888).

69. Klüver, H. & Bucy, P. C. "Psychic blindness" and other symptoms following bilateral temporal lobectomy in Rhesus monkeys. *American Journal of Physiology* **119,** 352–353 (1937).

70. Weiskrantz, L. Behavioral changes associated with ablation of the amygdaloid complex in monkeys. *J Comp Physiol Psychol* **49,** 381–91. ISSN: 0021-9940 (Print) 0021-9940 (1956).

71. Adolphs, R., Tranel, D., Damasio, H. & Damasio, A. Impaired recognition of emotion in facial expressions following bilateral damage to the human amygdala. *Nature* **372,** 669–72. ISSN: 0028-0836 (Print) 0028-0836 (1994).

72. Anderson, A. K. & Phelps, E. A. Lesions of the human amygdala impair enhanced perception of emotionally salient events. *Nature* **411,** 305–9. ISSN: 0028-0836 (Print) 0028-0836 (2001).

73. Sah, P., Faber, E. S., Lopez De Armentia, M. & Power, J. The amygdaloid complex: anatomy and physiology. *Physiol Rev* **83,** 803–34. ISSN: 0031-9333 (Print) 0031-9333 (2003).

74. Pare, D. & Duvarci, S. Amygdala microcircuits mediating fear expression and extinction. *Curr Opin Neurobiol* **22,** 717–23. ISSN: 0959-4388 (2012).

75. Duvarci, S. & Pare, D. Amygdala microcircuits controlling learned fear. *Neuron* **82,** 966–80. ISSN: 0896-6273 (2014).

76. Fadok, J. P. *et al.* A competitive inhibitory circuit for selection of active and passive fear responses. *Nature* **542,** 96–100. ISSN: 0028-0836 (2017).

77. Penzo, M. A., Robert, V. & Li, B. Fear conditioning potentiates synaptic transmission onto long-range projection neurons in the lateral subdivision of central amygdala. *J Neurosci* **34,** 2432–7. ISSN: 0270-6474 (2014).

78. Cassell, M. D., Freedman, L. J. & Shi, C. The intrinsic organization of the central extended amygdala. *Ann N Y Acad Sci* **877,** 217–41. ISSN: 0077-8923 (Print) 0077-8923 (1999).

79. Cassell, M. D., Gray, T. S. & Kiss, J. Z. Neuronal architecture in the rat central nucleus of the amygdala: a cytological, hodological, and immunocytochemical study. *J Comp Neurol* **246,** 478–99. ISSN: 0021-9967 (Print) 0021-9967 (1986).

80. Hunt, S., Sun, Y., Kucukdereli, H., Klein, R. & Sah, P. Intrinsic Circuits in the Lateral Central Amygdala. *eNeuro* **4.** ISSN: 2373-2822. doi:10.1523/eneuro.0367-16.2017 (2017).

81. Hopkins, D. A. & Holstege, G. Amygdaloid projections to the mesencephalon, pons and medulla oblongata in the cat. *Exp Brain Res* **32,** 529–47. ISSN: 0014-4819 (Print) 0014-4819 (1978).

82. Viviani, D. *et al.* Oxytocin selectively gates fear responses through distinct outputs from the central amygdala. *Science* **333,** 104–7. ISSN: 0036-8075 (2011).

83. Ciocchi, S. *et al.* Encoding of conditioned fear in central amygdala inhibitory circuits. *Nature* **468,** 277–82. ISSN: 0028-0836 (2010).

84. Li, H. *et al.* Experience-dependent modification of a central amygdala fear circuit. *Nat Neurosci* **16,** 332–9. ISSN: 1097-6256 (2013).

85. Botta, P. *et al.* Regulating anxiety with extrasynaptic inhibition. *Nat Neurosci* **18,** 1493–500. ISSN: 1097-6256 (2015).

86. Isosaka, T. *et al.* Htr2a-Expressing Cells in the Central Amygdala Control the Hierarchy between Innate and Learned Fear. *Cell* **163,** 1153–64. ISSN: 1097-4172 (Electronic) 0092-8674 (Linking) (2015).

87. Gallagher, M., Graham, P. W. & Holland, P. C. The amygdala central nucleus and appetitive Pavlovian conditioning: lesions impair one class of conditioned behavior. *J Neurosci* **10,** 1906–11. ISSN: 0270-6474 (Print) 0270-6474 (1990).

88. Parkinson, J. A., Robbins, T. W. & Everitt, B. J. Dissociable roles of the central and basolateral amygdala in appetitive emotional learning. *Eur J Neurosci* **12,** 405–13. ISSN: 0953-816X (Print) 0953-816x (2000).

89. McBride, W. J. Central nucleus of the amygdala and the effects of alcohol and alcohol-drinking behavior in rodents. *Pharmacol Biochem Behav* **71,** 509–15. ISSN: 0091-3057 (Print) 0091-3057 (2002).

90. Zarrindast, M. R., Rezayof, A., Sahraei, H., Haeri-Rohani, A. & Rassouli, Y. Involvement of dopamine D1 receptors of the central amygdala on the acquisition and expression of morphine-induced place preference in rat. *Brain Res* **965,** 212–21. ISSN: 0006-8993 (Print) 0006-8993 (2003).

91. Zhu, W., Bie, B. & Pan, Z. Z. Involvement of non-NMDA glutamate receptors in central amygdala in synaptic actions of ethanol and ethanol-induced reward behavior. *J Neurosci* **27,** 289–98. ISSN: 0270-6474 (2007).

92. Robinson, M. J., Warlow, S. M. & Berridge, K. C. Optogenetic excitation of central amygdala amplifies and narrows incentive motivation to pursue one reward above another. *J Neurosci* **34,** 16567–80. ISSN: 0270-6474 (2014).

93. Mahler, S. V. & Berridge, K. C. Which cue to "want?" Central amygdala opioid activation enhances and focuses incentive salience on a prepotent reward cue. *J Neurosci* **29,** 6500–13. ISSN: 0270-6474 (2009).

94. Kaada, B. R. in *The Neurobiology of the Amygdala: The Proceedings of a Symposium on the Neurobiology of the Amygdala, Bar Harbor, Maine, June 6–17, 1971* 205–281 (Springer US, Boston, MA, 1972). ISBN: 978-1-4615-8987-7. doi:10.1007/978-1-4615-8987-7_8. http://dx.doi.org/10.1007/978-1-4615-8987-7_8.

95. Beyeler, A. *et al.* Divergent Routing of Positive and Negative Information from the Amygdala during Memory Retrieval. *Neuron* **90,** 348–61. ISSN: 0896-6273 (2016).

96. Namburi, P. *et al.* A circuit mechanism for differentiating positive and negative associations. *Nature* **520,** 675–8. ISSN: 0028-0836 (2015).

97. Kim, J., Pignatelli, M., Xu, S., Itohara, S. & Tonegawa, S. Antagonistic negative and positive neurons of the basolateral amygdala. *Nature Neuroscience* **19,** 1636–1646 (Oct. 2016).

98. Beier, K. T. *et al.* Circuit Architecture of VTA Dopamine Neurons Revealed by Systematic Input-Output Mapping. *Cell* **162,** 622–34. ISSN: 0092-8674 (2015).

99. Gonzales, C. & Chesselet, M. F. Amygdalonigral pathway: an anterograde study in the rat with Phaseolus vulgaris leucoagglutinin (PHA-L). *J Comp Neurol* **297,** 182–200. ISSN: 0021-9967 (Print) 0021-9967 (1990).

100. Mascaro, M. B., Prosdocimi, F. C., Bittencourt, J. C. & Elias, C. F. Forebrain projections to brainstem nuclei involved in the control of mandibular movements in rats. *Eur J Oral Sci* **117,** 676–84. ISSN: 0909-8836 (2009).

101. Watabe-Uchida, M., Zhu, L., Ogawa, S. K., Vamanrao, A. & Uchida, N. Whole-brain mapping of direct inputs to midbrain dopamine neurons. *Neuron* **74,** 858–73. ISSN: 0896-6273 (2012).

102. Esber, G. R., Torres-Tristani, K. & Holland, P. C. Amygdalo-striatal interaction in the enhancement of stimulus salience in associative learning. *Behav Neurosci* **129,** 87–95. ISSN: 0735-7044 (2015).

103. Lee, H. J., Gallagher, M. & Holland, P. C. The central amygdala projection to the substantia nigra reflects prediction error information in appetitive conditioning. *Learn Mem* **17,** 531–8. ISSN: 1072-0502 (2010).

104. Lee, H. J., Wheeler, D. S. & Holland, P. C. Interactions between amygdala central nucleus and the ventral tegmental area in the acquisition of conditioned cue-directed behavior in rats. *Eur J Neurosci* **33,** 1876–84. ISSN: 0953-816x (2011).

105. LeDoux, J. E., Iwata, J., Cicchetti, P. & Reis, D. J. Different projections of the central amygdaloid nucleus mediate autonomic and behavioral correlates of conditioned fear. *J Neurosci* **8,** 2517–29. ISSN: 0270-6474 (Print) 0270-6474 (1988).

106. Bovetto, S. & Richard, D. Lesion of central nucleus of amygdala promotes fat gain without preventing effect of exercise on energy balance. *Am J Physiol* **269,** R781–6. ISSN: 0002-9513 (Print) 0002-9513 (1995).

107. Lenard, L. & Hahn, Z. Amygdalar noradrenergic and dopaminergic mechanisms in the regulation of hunger and thirst-motivated behavior. *Brain Res* **233,** 115–32. ISSN: 0006-8993 (Print) 0006-8993 (1982).

108. Boghossian, S., Park, M. & York, D. A. Melanocortin activity in the amygdala controls appetite for dietary fat. *Am J Physiol Regul Integr Comp Physiol* **298,** R385–93. ISSN: 0363-6119 (2010).

109. Primeaux, S. D., York, D. A. & Bray, G. A. Neuropeptide Y administration into the amygdala alters high fat food intake. *Peptides* **27,** 1644–51. ISSN: 0196-9781 (Print) 0196-9781 (2006).

110. Ekstrand, M. I. *et al.* Molecular profiling of neurons based on connectivity. *Cell* **157,** 1230–42. ISSN: 0092-8674 (2014).

111. Huang, Z. J. & Zeng, H. Genetic approaches to neural circuits in the mouse. *Annu Rev Neurosci* **36,** 183–215. ISSN: 0147-006x (2013).

112. Knight, Z. A. *et al.* Molecular profiling of activated neurons by phosphorylated ribosome capture. *Cell* **151,** 1126–37. ISSN: 0092-8674 (2012).

113. Nagel, G. *et al.* Channelrhodopsin-2, a directly light-gated cation-selective membrane channel. *Proc Natl Acad Sci U S A* **100,** 13940–5. ISSN: 0027-8424 (Print) 0027-8424 (2003).

114. Boyden, E. S., Zhang, F., Bamberg, E., Nagel, G. & Deisseroth, K. Millisecond-timescale, genetically targeted optical control of neural activity. *Nat Neurosci* **8,** 1263–8. ISSN: 1097-6256 (Print) 1097-6256 (2005).

115. Zhang, F. *et al.* Multimodal fast optical interrogation of neural circuitry. *Nature* **446,** 633–9. ISSN: 0028-0836 (2007).

116. Chow, B. Y. *et al.* High-performance genetically targetable optical neural silencing by light-driven proton pumps. *Nature* **463,** 98–102. ISSN: 0028-0836 (2010).

117. Mattis, J. *et al.* Principles for applying optogenetic tools derived from direct comparative analysis of microbial opsins. *Nat Methods* **9,** 159–72. ISSN: 1548-7091 (2012).

118. Raimondo, J. V., Kay, L., Ellender, T. J. & Akerman, C. J. Optogenetic silencing strategies differ in their effects on inhibitory synaptic transmission. *Nat Neurosci* **15,** 1102–4. ISSN: 1097-6256 (2012).

119. Mahn, M., Prigge, M., Ron, S., Levy, R. & Yizhar, O. Biophysical constraints of optogenetic inhibition at presynaptic terminals. *Nat Neurosci* **19,** 554–6. ISSN: 1097-6256 (2016).

120. Petreanu, L., Huber, D., Sobczyk, A. & Svoboda, K. Channelrhodopsin-2-assisted circuit mapping of long-range callosal projections. *Nat Neurosci* **10,** 663–8. ISSN: 1097-6256 (Print) 1097-6256 (Linking) (2007).

121. Shin, G. *et al.* Flexible Near-Field Wireless Optoelectronics as Subdermal Implants for Broad Applications in Optogenetics. *Neuron* **93,** 509–521.e3. ISSN: 0896-6273 (2017).

122. Allen, B. D., Singer, A. C. & Boyden, E. S. Principles of designing interpretable optogenetic behavior experiments. *Learn Mem* **22,** 232–8. ISSN: 1072-0502 (2015).

123. Otchy, T. M. *et al.* Acute off-target effects of neural circuit manipulations. *Nature* **528,** 358–63. ISSN: 0028-0836 (2015).

124. Pisanello, F. *et al.* Dynamically controlled light delivery over large brain volumes through tapered optical fibers. *bioRxiv.* doi:10.1101/094524 (2016).

125. Rungta, R. L., Osmanski, B. F., Boido, D., Tanter, M. & Charpak, S. Light controls cerebral blood flow in naive animals. *Nat Commun* **8,** 14191. ISSN: 2041-1723 (2017).

126. Roth, B. L. DREADDs for Neuroscientists. *Neuron* **89,** 683–94. ISSN: 0896-6273 (2016).

127. Alexander, G. M. *et al.* Remote control of neuronal activity in transgenic mice expressing evolved G protein-coupled receptors. *Neuron* **63,** 27–39. ISSN: 1097-4199 (Electronic) 0896-6273 (Linking) (2009).

128. Armbruster, B. N., Li, X., Pausch, M. H., Herlitze, S. & Roth, B. L. Evolving the lock to fit the key to create a family of G protein-coupled receptors potently activated by an inert ligand. *Proc Natl Acad Sci U S A* **104,** 5163–8. ISSN: 0027-8424 (Print) 0027-8424 (2007).

129. Jarrard, L. E. On the use of ibotenic acid to lesion selectively different components of the hippocampal formation. *J Neurosci Methods* **29,** 251–9. ISSN: 0165-0270 (Print) 0165-0270 (1989).

130. Andero, R., Dias, B. G. & Ressler, K. J. A role for Tac2, NkB, and Nk3 receptor in normal and dysregulated fear memory consolidation. *Neuron* **83,** 444–54. ISSN: 0896-6273 (2014).

131. Ventura-Silva, A. P. *et al.* Excitotoxic lesions in the central nucleus of the amygdala attenuate stress-induced anxiety behavior. *Frontiers in Behavioral Neuroscience* **7.** ISSN: 1662-5153. doi:10.3389/fnbeh.2013.00032. http://journal.frontiersin.org/article/10.3389/fnbeh.2013.00032 (2013).

132. Wu, Z., Autry, A. E., Bergan, J. F., Watabe-Uchida, M. & Dulac, C. G. Galanin neurons in the medial preoptic area govern parental behaviour. *Nature* **509,** 325–30. ISSN: 0028-0836 (2014).

133. Yang, C. F. *et al.* Sexually Dimorphic Neurons in the Ventromedial Hypothalamus Govern Mating in Both Sexes and Aggression in Males. *Cell* **153,** 896–909. ISSN: 0092-8674.

134. Nakai, J., Ohkura, M. & Imoto, K. A high signal-to-noise Ca(2+) probe composed of a single green fluorescent protein. *Nat Biotechnol* **19,** 137–41. ISSN: 1087-0156 (Print) 1087-0156 (2001).

135. Tian, L. *et al.* Imaging neural activity in worms, flies and mice with improved GCaMP calcium indicators. *Nat Methods* **6,** 875–81. ISSN: 1548-7091 (2009).

136. Helmchen, F., Imoto, K. & Sakmann, B. Ca2+ buffering and action potential-evoked Ca2+ signaling in dendrites of pyramidal neurons. *Biophys J* **70,** 1069–81. ISSN: 0006-3495 (Print) 0006-3495 (1996).

137. Sun, X. R. *et al.* Fast GCaMPs for improved tracking of neuronal activity. *Nat Commun* **4,** 2170. ISSN: 2041-1723 (2013).

138. Chen, T. W. *et al.* Ultrasensitive fluorescent proteins for imaging neuronal activity. *Nature* **499,** 295–300. ISSN: 0028-0836 (2013).

139. Hamel, E. J., Grewe, B. F., Parker, J. G. & Schnitzer, M. J. Cellular level brain imaging in behaving mammals: an engineering approach. *Neuron* **86,** 140–59. ISSN: 0896-6273 (2015).

140. Denk, W. *et al.* Anatomical and functional imaging of neurons using 2-photon laser scanning microscopy. *J Neurosci Methods* **54,** 151–62. ISSN: 0165-0270 (Print) 0165-0270 (1994).

141. Svoboda, K. & Yasuda, R. Principles of two-photon excitation microscopy and its applications to neuroscience. *Neuron* **50,** 823–39. ISSN: 0896-6273 (Print) 0896-6273 (2006).

142. Cui, G. *et al.* Deep brain optical measurements of cell type-specific neural activity in behaving mice. *Nat Protoc* **9,** 1213–28. ISSN: 1750-2799 (2014).

143. Gunaydin, L. A. *et al.* Natural neural projection dynamics underlying social behavior. *Cell* **157,** 1535–51. ISSN: 0092-8674 (2014).

144. Levene, M. J., Dombeck, D. A., Kasischke, K. A., Molloy, R. P. & Webb, W. W. In vivo multiphoton microscopy of deep brain tissue. *J Neurophysiol* **91,** 1908–12. ISSN: 0022-3077 (Print) 0022-3077 (2004).

145. Resendez, S. L. *et al.* Visualization of cortical, subcortical and deep brain neural circuit dynamics during naturalistic mammalian behavior with head-mounted microscopes and chronically implanted lenses. *Nat Protoc* **11,** 566–97. ISSN: 1750-2799 (2016).

146. McHenry, J. A. *et al.* Hormonal gain control of a medial preoptic area social reward circuit. *Nat Neurosci* **20,** 449–458. ISSN: 1097-6256 (2017).

147. De Araujo, I. E. in *Neurobiology of Sensation and Reward* (ed Gottfried, J. A.) (CRC Press/Taylor Francis Llc., Boca Raton (FL), 2011).

148. Madisen, L. *et al.* A toolbox of Cre-dependent optogenetic transgenic mice for light-induced activation and silencing. *Nat Neurosci* **15,** 793–802. ISSN: 1546-1726 (Electronic) 1097-6256 (Linking) (2012).

149. Soriano, P. Generalized lacZ expression with the ROSA26 Cre reporter strain. *Nat Genet* **21,** 70–1. ISSN: 1061-4036 (Print) 1061-4036 (Linking) (1999).

150. Lopes, G. *et al.* Bonsai: an event-based framework for processing and controlling data streams. *Front Neuroinform* **9,** 7. ISSN: 1662-5196 (2015).

151. Slotnick, B. A simple 2-transistor touch or lick detector circuit. *J Exp Anal Behav* **91,** 253–5. ISSN: 0022-5002 (2009).

152. McCann, M. J., Verbalis, J. G. & Stricker, E. M. LiCl and CCK inhibit gastric emptying and feeding and stimulate OT secretion in rats. *Am J Physiol* **256,** R463–8. ISSN: 0002-9513 (Print) 0002-9513 (1989).

153. Dantzer, R. Cytokine-induced sickness behavior: mechanisms and implications. *Ann N Y Acad Sci* **933,** 222–34. ISSN: 0077-8923 (Print) 0077-8923 (2001).

154. Navarro, M. *et al.* Lateral Hypothalamus GABAergic Neurons Modulate Consummatory Behaviors Regardless of the Caloric Content or Biological Relevance of the Consumed Stimuli. *Neuropsychopharmacology* **41,** 1505–12. ISSN: 0893-133x (2016).

155. Berridge, K. C. Food reward: brain substrates of wanting and liking. *Neurosci Biobehav Rev* **20,** 1–25. ISSN: 0149-7634 (Print) 0149-7634 (1996).

156. Kim, J., Zhang, X., Muralidhar, S., LeBlanc, S. A. & Tonegawa, S. Basolateral to Central Amygdala Neural Circuits for Appetitive Behaviors. *Neuron* **93,** 1464–1479.e5. ISSN: 0896-6273 (2017).

157. Jennings, J. H. *et al.* Visualizing hypothalamic network dynamics for appetitive and consummatory behaviors. *Cell* **160,** 516–27. ISSN: 0092-8674 (2015).

158. Chen, Y., Lin, Y. C., Zimmerman, C. A., Essner, R. A. & Knight, Z. A. Hunger neurons drive feeding through a sustained, positive reinforcement signal. *Elife* **5.** ISSN: 2050-084x. doi:10.7554/eLife.18640 (2016).

159. Han, W. *et al.* Integrated Control of Predatory Hunting by the Central Nucleus of the Amygdala. *Cell* **168,** 311–324.e18. ISSN: 0092-8674 (2017).

160. Lundy R. F., J. & Norgren, R. Pontine gustatory activity is altered by electrical stimulation in the central nucleus of the amygdala. *J Neurophysiol* **85,** 770–83. ISSN: 0022-3077 (Print) 0022-3077 (2001).

161. Scott, T. R. & Small, D. M. The role of the parabrachial nucleus in taste processing and feeding. *Ann N Y Acad Sci* **1170,** 372–7. ISSN: 0077-8923 (2009).

162. McCall, J. G. *et al.* CRH Engagement of the Locus Coeruleus Noradrenergic System Mediates Stress-Induced Anxiety. *Neuron* **87,** 605–20. ISSN: 0896-6273 (2015).

163. Han, J. S. Acupuncture: neuropeptide release produced by electrical stimulation of different frequencies. *Trends Neurosci* **26,** 17–22. ISSN: 0166-2236 (Print) 0166-2236 (2003).

164. Whim, M. D. & Lloyd, P. E. Frequency-dependent release of peptide cotransmitters from identified cholinergic motor neurons in Aplysia. *Proc Natl Acad Sci U S A* **86,** 9034–8. ISSN: 0027-8424 (Print) 0027-8424 (1989).

165. Scibilia, R. J., Lachowicz, J. E. & Kilts, C. D. Topographic nonoverlapping distribution of D1 and D2 dopamine receptors in the amygdaloid nuclear complex of the rat brain. *Synapse* **11,** 146–54. ISSN: 0887-4476 (Print) 0887-4476 (1992).

166. Weiner, D. M. *et al.* D1 and D2 dopamine receptor mRNA in rat brain. *Proc Natl Acad Sci U S A* **88,** 1859–63. ISSN: 0027-8424 (Print) 0027-8424 (1991).

SIGILL. UNIVERSI TAT. LUDOVIC. MAXIM.

BIBLIOGRAPHY

Amelia Douglass

Am Klopferspitz 18, 82152 Martinsried, Germany

douglass@neuro.mpg.de

Education

Max Planck Institute of Neurobiology — *Martinsried, Germany*
PhD in Systemic Neurosciences — *2012 - 2017*

Ludwig-Maximilians-Universität München (LMU) — *Munich, Germany*
PhD in Systemic Neurosciences — *2012 - 2017*
- Graduate School of Systemic Neurosciences PhD Program.

The University of Queensland (UQ) — *Brisbane, Australia*
Bachelor of Biomedical Science with Honours Class I — *2008 - 2011*

Research Experience

Max Planck Institute of Neurobiology, Lab of Rüdiger Klein — *Martinsried, Germany*
PhD Candidate — *Oct. 2012 - Nov. 2017*
- Central amygdala circuits that modulate feeding and reward behaviors.

Max Planck Institute of Neurobiology, Lab of Rüdiger Klein — *Martinsried, Germany*
Visiting scientist — *Feb. 2012 - Mar. 2012*
- Analysis of guidance receptor interactions in corpus callosum development.

UQ- Queensland Brain Institute, Lab of Linda Richards — *Brisbane, Australia*
Research Assistant — *Nov. 2011 - Sept. 2012*
- The role of DCC and Robo guidance receptors in callosal axon guidance.

UQ- Queensland Brain Institute, Lab of Linda Richards — *Brisbane, Australia*
Honours Thesis Student — *Feb. 2011 - Nov. 2011*
- The role of DCC in corpus callosum development.

UQ- Institute for Molecular Biosciences, Lab of Carol Wicking — *Brisbane, Australia*
Undergraduate Research Scholar — *Mar. 2010 - Jul. 2010*
- The role of primary cilia in craniofacial development.

UQ- School of Biomedical Sciences, Lab of David Simmons — *Brisbane, Australia*
Summer Research Scholar — *Jan. 2010 - Feb. 2010*
- Regulation of Na+-K+-ATPase subunit expression in the murine uterine luminal epithelium by oestrogen and progesterone.

BIBLIOGRAPHY

Publications

- **Amelia M. Douglass***, Hakan Kucukdereli*, Marion Ponserre*, Milica Markovic, Jan Gründemann, Cornelia Strobel, Pilar L. Alcala Morales, Karl-Klaus Conzelmann, Andreas Lüthi, and Rüdiger Klein. Central amygdala circuits modulate food consumption through a positive valence mechanism (2017). *Nature Neuroscience. AOP*. *Co-authorship.
- Thomas Fothergill*, Amber-Lee S. Donahoo*, **Amelia M. Douglass**, Oressia Zalucki, Jiajia Yuan, Tianzhi Shu, Geoffery J. Goodhill, and Linda J. Richards. Netrin-DCC signaling regulates corpus callosum formation through attraction of pioneering axons and by modulating Slit2-mediated repulsion (2014). *Cerebral Cortex. 24(5):1138-1151*. *Co-authorship.

Presentations

Society for Neuroscience Annual Meeting 2016 — *San Diego, CA, USA*
POSTER PRESENTATION — *November 2016*
- Central amygdala circuits modulate reward and consummatory behavior.

GRC: Optogenetic Approaches to Understanding Neural Circuits & Behavior — *Newry, ME, USA*
POSTER PRESENTATION — *July 2016*
- Central amygdala circuits controlling feeding and reward.

EMBO Workshop: Neural control of metabolism and eating behavior — *Cascais, Portugal*
ORAL PRESENTATION — *May 2016*
- Central amygdala Htr2a-expressing neurons control feeding and appetitive behaviors.

<Interact> Life Sciences Symposium 6th Annual Meeting — *Munich, Germany*
POSTER PRESENTATION — *March 2013*
- The role of DCC in corpus callosum development.

QBI-MCN Systems Neuroscience Symposium 2nd Annual Meeting — *Martinsried, Germany*
POSTER PRESENTATION — *October 2012*
- The role of DCC in corpus callosum development.

The Australian Neuroscience Society 32nd Annual Meeting — *Gold Coast, Australia*
POSTER PRESENTATION — *February 2012*
- DCC functions in multiple aspects of corpus callosum development.

BIBLIOGRAPHY

Honors & Awards

Best Poster Prize — *Newry, ME, USA*
GRC: Optogenetic Approaches to Understanding Neural Circuits & Behavior — *July 2016*

Dean's Commendation for High Achievement — *Brisbane, Australia*
The University of Queensland — *2008-2011*

Bachelor of Biomedical Science 3rd Year Prize — *Brisbane, Australia*
The University of Queensland — *2010*
- Highest cumulative GPA over the Bachelor of Biomedical Science program.

Bachelor of Biomedical Science 3rd Year Developmental Biology Prize — *Brisbane, Australia*
The University of Queensland — *2010*
- Highest overall grade for 'Developmental Neurobiology' and 'Molecular Mechanisms of Development' courses.

Skills

Languages	English (native)
Programming	Python, MATLAB, Arduino, Bonsai
Technical Skills	Fundamental molecular biology and wet lab techniques (protein biochemistry, cloning, tissue culture, etc.)
	Histology (immunohistochemistry and *in situ* hybridization)
	Mouse genetics and husbandry
	Rodent stereotaxic surgery
	Rodent *in utero* electroporation
	Viral circuit tracing
	Mouse behavior (feeding, drinking and reward-related paradigms, appetitive & aversive learning)
	Behavioral set up design and fabrication (laser cutting, 3D printing, rapid prototyping with Arduino and basic PCB design)
	in vivo optogenetics and chemogenetics
	in vivo miniscope calcium imaging

Courses

CAJAL Course (FENS): Behavior and Neural Systems — *Lisbon, Portugal*
Champalimaud Centre for the Unknown — *July 2015*

Supervision

Supervising undergraduate student Tommaso Caudullo — *Martinsreid, Germany*
Max Planck Institute of Neurobiology — *June 2015 - May 2017*

Declaration

Eidesstattliche Versicherung/Affidavit

Hiermit versichere ich an Eides statt, dass ich die vorliegende Dissertation ”Neural circuit mechanisms underlying modulation of food consumption and reward by the central amygdala” selbstständig angefertigt habe, mich außer der angegebenen keiner weiteren Hilfsmittel bedient und alle Erkenntnisse, die aus dem Schrifttum ganz oder annähernd übernommen sind, als solche kenntlich gemacht und nach ihrer Herkunft unter Bezeichnung der Fundstelle einzeln nachgewiesen habe.

I hereby confirm that the dissertation ”Neural circuit mechanisms underlying modulation of food consumption and reward by the central amygdala” is the result of my own work and that I have only used sources or materials listed and specified in the dissertation.

München, 26th June 2017 Unterschrift/Signature

Author Contributions

List of Contributors: Amelia M. Douglass*, Hakan Kucukdereli*, Milica Markovic, Jan Gründemann, Cornelia Strobel

A.M.D designed, performed and analysed behaviour experiments using chemogenetics and cell ablations. A.M.D and H.K designed and analysed optogenetic behaviour experiments. A.M.D performed optogenetic behaviour experiments. H.K performed electrophysiology experiments for channelrhodopsin verification (Figure 8C). C.S performed electrophysiology experiments for hM3Dq verification (Figure 2C). A.M.D and H.K designed all the imaging experiments. A.M.D, H.K, M.M and J.G performed and analysed the free-feeding imaging experiments. A.M.D, and H.K performed the FR1 imaging experiment. H.K. and A.M.D analysed the FR1 imaging experiments with input from M.M and J.G. H.K wrote the code for analysis of imaging experiments with input from A.M.D, M.M and J.G.

(*) Equal contribution

München, 26th June 2017

Supervisor's Signature Author's Signature Co-contributor's Signature